Modulation of myofibroblast phenotype and function by c-Ski

by

Ryan H. Cunnington

A Thesis submitted to the Faculty of Graduate Studies of

The University of Manitoba

in partial fulfilment of the requirements of the degree of

Doctor of Philosophy

Department of Physiology

University of Manitoba

Winnipeg

Acknowledgements

I would like to start by acknowledging those who contributed vital reagents and data for my project: Dr. Shunsuke Ishii and Dr. Ed Stavnezer for providing Ski/pCMV and pBABEpurohuSki, respectively, which allowed for the cloning of c-Ski into retro- and adenoviruses. Dr. Michael P. Czubryt for providing pcDNA3.1-N-HA which allowed me to tag c-Ski for easier downstream detection. Dr. Jeffrey T. Wigle for providing pMxie retroviral plasmid and Eco-phoenix cells for retroviral construction and the Meox2 adenoviral vectors. Dr. Saeid Ghavami for performing and instructing me in how to perform different cell viability assays. Ms. Josette M. Douville for performing qPCR on RNA isolated by our lab to detect Meox1 and Meox2 mRNA expression in control, LacZ and c-Ski overexpressing cells. Dr. Mark Hnatowich for guidance in all techniques for successful molecular biology experiments.

I am grateful to have been funded by the St. Boniface General Hospital Research Foundation, the Institute of Cardiovascular Sciences at the St. Boniface Research Center and with a Canadian Institutes for Health Research/Manitoba Health Research Council Regional Partnership Program studentship. I also acknowledge the Heart and Stroke Foundation of Manitoba for laboratory funding for this project.

I would like to show my appreciation to my committee members, Dr. Newman L. Stephens, Dr. Michael P. Czubryt, Dr. Jeffrey T. Wigle and former committee member Dr. Nasrin Mesaeli, for the excellent insight, direction, and support they have provided through my many years as a PhD student.

I have had the great benefit of working with many talented students and researchers in my time with the Dixon lab which has made it a wonderful environment in which to work. I would like to thank Tatjana Angelovska, Vanja Drobic, and Dr. Bai Qiu Wang for getting me started in the laboratory by showing me great work ethic and technique. Stephen Jones, Kristen Bedosky, Joshua E.Raizman, Aran Dangerfield, and Sarah O'Connor for their friendship and camaraderie and for their assistance and always making the lab a great place to be. I would like to acknowledge Krista Bathe for her technical skill and invaluable assistance in my data collection. Thank you to Sunil Rattan for making sure the lab always ran smoothly, for being able to troubleshoot any problem, for challenging me and being a great friend.

I would like to acknowledge my supervisor, Dr. Ian M.C. Dixon, for his incredible patience, understanding and support in developing this project from the ground up. He is, and will always be, an exceptional mentor and friend.

Finally, I would like to thank my parents, Henley and Cheryl, my sister Lindsey and girlfriend Jasmine for their unfailing support in helping me realize this accomplishment.

Abstract

Cardiovascular disease is a leading cause of death and a major economic burden in the developed and developing world. Many heart diseases, including post-myocardial infarction, include a fibrotic component with remodeling of the extracellular matrix in the myocardium. Cardiac myofibroblasts are non-myocyte cells derived from relatively quiescent fibroblasts and are the main mediators of collagen remodeling in disease states. TGF-β is recognized as an important contributor to adverse cardiac remodeling in heart disease. In this study we have investigated the role of c-Ski, which is an endogenous TGF-β inhibitor, in controlling/regulating myofibroblast function and phenotype. We have developed an adenoviral overexpression system to study these endpoints using Western blot, immunofluorescence, MTT assay, flow cytometry, procollagen type I amino terminal peptide secretion and qPCR analysis. We observed that the 95 kDa c-Ski form is overexpressed upon virus infection with adenovirus encoding c-Ski and this form of c-Ski is localized to the nucleus. c-Ski expression inhibited cardiac myofibroblast collagen synthesis and secretion as well as contractility. Phosphorylation and translocation of Smad2 into the nucleus was not affected in the presence of c-Ski overexpression. We found that c-Ski overexpression was associated with diminution of the myofibroblastic phenotype with reduced α-smooth muscle actin and extra domain-A fibronectin expression (but not non-muscle myosin heavy chain B expression). c-Ski may reduce cell viability via the induction of apoptosis. Finally, we have elucidated a putative mechanism for c-Ski-mediated reduction of myofibroblast phenotype through the upregulation of the homeodomain protein Meox2. Adenoviral overexpression of Meox2 was associated with a significant reduction of α-smooth muscle actin and extra domain-A

fibronectin expression in a similar manner to that of c-Ski overexpression. Thus we have identified c-Ski as being an antifibrotic protein as well as a novel mechanism for modulation of cardiac myofibroblast phenotype, possibly through the induction of Meox2 expression.

Table of Contents **page**

List of Tables

List of Figures

List of Abbreviations

ACE – angiotensin converting enzyme

AT_1 – angiotensin 1

CVD – cardiovascular disease

CHD – coronary heart disease

Co-Smad4 – common Smad4

Cdc34 – cell division cycle 34

Cdk2 – cyclin dependent kinase 2

ECM – extracellular matrix

ED-A fibronectin – extra domain A fibronectin

EMT – epithelial to mesenchymal transition

FA – focal adhesion

Gax – growth arrest specific homeobox

gp-130 – glycoprotein 130

HA – hemagglutinin

HDAC – histone deacetylase

Hhex – hematopoietically expressed homeobox

Hsc70 – heat shock protein cognate 1

I-Smad7 – inhibitory Smad7

JNK – c-Jun N terminal kinase

LAP – latency associated peptide

LIFR – leukemia inhibitory factor receptor

LTBP – latent TGF-β-binding protein

N-CoR – nuclear corepressor

NF1 – nuclear factor 1

NF-κB – nuclear factor κB

MeCP2 – methyl CpG binding protein

Meox – mesenchyme homeobox

MI – myocardial infarction

MKK – mitogen activated protein kinase kinase

MMP – matrix metalloproteinase

MOI – multiplicity of infection

MTT – 3-(4,5-dimethylthiazol-2-yl)-2,5-diphenyltetrazolium bromide

PINP-EIA – procollagen type I amino terminal peptide enzyme immunoassay

Prox – prospero-related homeobox

Prx – paired-related homeobox

P-Smad – phosphorylated R-Smad

ROCK – Rho-associated kinase

R-Smad – receptor-regulated Smad

SBE – Smad binding element

α-SMA – α-smooth muscle actin

SMemb – non-muscle myosin heavy chain b

Smurf2 – smad ubiquitination regulatory factor 2

SMRT – silencing mediator of retinoic acid & thyroid hormone

SUMO-1 – small ubiquitin-like modifier-1

TAK1 – TGF-β associated kinase 1

TGF-β – transforming growth factor β

TβRI – transforming growth factor β receptor type I

TβRII – transforming growth factor β receptor type II

vp – viral particles

VSMC – vascular smooth muscle cells

I. Introduction/Statement of the problem

Cardiovascular disease is the most common cause of death in the world [1]. In 2007, cardiovascular disease accounted for one-third of deaths of Americans [2] and nearly 17% of all deaths were attributed to coronary heart disease (CHD) [2]. In Canada, cardiovascular disease accounts for ~30% of all deaths [3] and, of these, nearly 50% were due to ischemic heart disease and heart attack. While these numbers represent a decrease in overall deaths from CHD since 1950 [2], they still represent a major economic burden of almost $178 billion in healthcare costs in the United States [2], €169 billion in the countries of the European Union (2003) [4] and $22 billion in Canada [5]. The World Health Organization estimates that cardiovascular disease accounted for 17.1 million deaths in 2004 with the majority of death occuring in low and middle income countries [6]. Cardiovascular diseases encompass a broad spectrum of disease etiologies including hypertension, diabetic cardiomyopathy and myocardial infarction (MI), many involving inappropriate fibrotic remodeling of the heart. In the case of non-fatal myocardial infarction (MI), patients face increased risk of developing heart failure within five years of the initial injury [2]. After MI, cardiomyocyte loss is followed within days by the phenoconversion of quiescent interstitial fibroblasts to hypersynthetic contractile myofibroblasts [7]. These myofibroblasts are responsible for extracellular matrix (ECM) deposition leading to acute reparative fibrosis. Persistent presence of these cells also leads to extracellular matrix deposition in the remnant heart leading to overt cardiac fibrosis and congestive heart failure [7].

Acutely, myofibroblasts generate extracellular matrix (ECM) for reparative fibrosis of the injured myocardium [8, 9]. This ECM serves to reinforce the infarcted area thereby preventing cardiac rupture and also promoting the efficient pumping of blood by the remnant heart by preventing bulging of the scar [10]. Chronically, however, persistent myofibroblast activation and collagen synthesis results in pathologic hypertrophy. Collagen matrix synthesis spreads to the viable remnant heart contributing to increased stiffness of the active muscle thereby impairing cardiac beating efficiency [11]. Phenoconversion of cardiac fibroblasts to hypersynthetic myofibroblasts is an incompletely understood process. There are many factors that induce this phenoconversion with one of the most important being TGF-β. The recent recognition that myofibroblasts may play a primary role in disease pathology versus a secondary reactive role identifies these cells as being important therapeutic targets [12]. Despite this knowledge, the underlying mechanism behind fibroblast to myofibroblast conversion is unknown.

c-Ski is an evolutionarily conserved, phosphorylatable proto-oncoprotein that is implicated in the inhibition of TGF-β signalling [13-19]. While it is most commonly studied in cancer biology, transgenic models identify c-Ski as an important protein in both the nervous and muscular systems [20, 21]. Overexpression of c-Ski leads to skeletal muscle hypertrophy but is associated with muscle degeneration [22, 23]. While cardiac expression of c-Ski has been shown [24], further work on its expression in the major cells of the heart, eg fibroblasts/myofibroblasts, has not been examined. As TGF-β is an important cytokine in cardiac wound remodelling and in fibroblast to myofibroblast differentiation [25] and as c-Ski is able to inhibit TGF-β signalling via multiple mechanisms [26, 27], it is worth studying

the role of c-Ski in the function and phenotype of cardiac myofibroblasts within the context of post-MI cardiac remodelling. c-Ski may be an important endogenous inhibitor of TGF-β1 signalling and may modulate the progression of heart failure due to MI.

This thesis summarizes our studies wherein we examine the role of c-Ski in myofibroblast function and phenotype and provides a potential mechanism for its mode of action. We have developed a viral-mediated c-Ski overexpression system to assess the functional role of c-Ski in first passage cardiac myofibroblasts. Using this system we have tested the ability of c-Ski to inhibit TGF-β mediated collagen type I synthesis and secretion in primary cardiac myofibroblasts. Further, we have overexpressed c-Ski in these cells and assessed the effect on contractility through the use of two dimensional collagen gel contraction assays. Using Western blot, we have characterized the phenotypic changes in first passage myofibroblasts resulting from c-Ski overexpression. By using immunofluorescence, we have tracked the time course change in TGF-β1 induced localization of this protein. We have also assessed the effects of exogenous c-Ski expression on cell viability. Finally, we begin to piece together a possible mechanism for the actions of c-Ski through its up regulation of the Meox2 homeobox protein.

II. Literature Review

1. Cardiac fibrosis in cardiovascular disease

Cardiovascular disease encompasses a broad range of etiologies, many of them resulting in fibrosis of the myocardium. Hypertension, diabetic cardiomyopathy and

myocardial infarction (MI) and others may all lead to maladaptive collagen deposition [28, 29, 30]. Fibrotic remodeling may occur in response to large scale loss of cardiomyocytes as in the case of MI [31], in diabetes that is independent of body mass index and arterial pressure [28, 32] and in chronic pressure overload in patients with hypertension [33]. While these disease pathologies are heterogeneous, the fibrotic component serves a similar function – stiffening of the myocardium causing reduced cardiac efficiency, impedance of electrical activity leading to arrhythmia, and, ultimately, heart failure resulting in fatality. Despite differences in the causes of these cardiovascular diseases, the fundamental mechanisms for collagen synthesis and secretion may overlap.

2. Myocardial infarction and wound healing

Myocardial infarction (MI) due to coronary artery occlusion results in loss of myocardial tissue. The remnant heart must adapt with increased muscle mass (hypertrophy) due to chronic overload [34-39]. Large MI may induce the ventricular chamber to remodel with an increase in volume [40] and severe hypertrophy associated with increased myocyte size and decreased intrinsic cardiac performance [34]. Progressive cardiac dysfunction (prefailure, moderate and severe heart failure) is accompanied by chronically elevated fibrillar collagen expression in remnant heart and infarct scar ultimately leading to congestive heart failure, a leading cause of death in North America [41-44].

The post-MI heart provides a good setting to describe the activation and participation of cardiac fibroblasts and myofibroblasts in both acute and chronic cardiac

wound healing. The remodeling heart undergoes four main stages of wound healing. The first stage comprises the initial 24h following MI and is characterized by myocyte cell death through apoptosis and necrosis. Cardiomyocyte apoptosis peaks 6-8h following MI and secondary necrosis ensues as the surrounding cells are unable to phagocytose the majority of apoptosing cells [45]. Necrosis initiates an inflammatory response that signals the onset of the second stage of wound healing from 12h to 4 days post-MI [45]. The second stage of wound healing - acute inflammation - lasts for ~4 days and involves clearance of apoptotic cells and secondary necrosis. In this inflammatory stage, the extracellular matrix is degraded through an increase in matrix metalloproteinase (MMP) -1,-2, and -9 activity [46] facilitating migration of fibroblasts into the infarct area. Fibroblasts phenoconvert to myofibroblasts (fibroblasts with smooth-muscle like contractile properties) beginning ~4 days post MI [7] and populate the border zone and infarct area. These myofibroblasts synthesize and secrete collagens – mainly type I and type III. In the third stage of wound healing (~3 days - ~4weeks post-MI) new extracellular matrix (ECM) proteins are synthesized by the myofibroblasts and neovascularisation occurs resulting in the formation of granulation tissue. Collagen cross-linking occurs in this stage [47] contributing to an increase in tensile strength of the scar. In the fourth and final stage of wound healing, scar cellularity decreases due to apoptosis [48] however myofibroblasts continue to populate the scar for years afterward [7].

3. Fibroblasts and myofibroblasts

Cardiac fibroblasts are interstitial cells comprising the majority of cells in the adult heart [49]. These cells are of mesenchymal origin and are the main cell type involved in maintaining ECM homeostasis. While common to most tissues, fibroblasts display marked phenotypic and topographic diversity [50]. For example, myofibroblast dense tissues from various organs behave differently when exposed to different agonists [51, 52], suggesting a functional heterogeneity of myofibroblasts [53-55]. Wound healing/interstitial cardiac fibrosis is mediated by phenotypic variants of these cells termed myofibroblasts [42, 56-58]. Cardiac myofibroblasts are highly synthetic phenotypic variants [59], expressing α-smooth muscle actin (α-SMA), ED-A fibronectin, non-muscle myosin heavy chain b (SMemb), vimentin, AT_1 receptors, TGF-β receptors, LIFR/gp-130, ACE, and fibrillar collagens [11, 56, 60-64]. While a small population of myofibroblasts exists in the healthy heart at the valve leaflets, these cells arise mainly in the pathological state. The phenotype is induced by a variety of factors including TGF-β and *in vitro* culture at low seeding densities [25, 65, 66]. Myofibroblasts predominate [42] in post-MI infarct scar and in cultured adult cells; adult myofibroblasts are phenotypically stable [66].

Myofibroblasts that appear at the site of infarction are derived from a range of sources both proximal and distal to the infarct scar. Local sources include resident fibroblasts, smooth muscle cells and pericytes [67]. Degradation of the ECM occurs early after MI as matrix metalloproteinases 1, 2 and 9 (MMP1/2/9) are upregulated and begin to degrade the extensive collagen network in the infarct scar [46, 68]. Early degradation of the matrix aids in fibroblast migration and infiltration into the infarct scar [69, 70].

Epithelial-to-mesenchymal transition act as a source for myofibroblasts in lung [71] and has been shown to contribute to the fibroblast population in the heart [72, 73]. In addition, endothelial-mesenchymal transition serves as a source of fibroblasts in pressure overloaded hearts [74]. Bone marrow progenitor cells contribute to myofibroblast population of the heart following MI [75, 76] and can be enhanced by of hematopoietic stem cells with granulocyte colony stimulating factor to increase myofibroblast numbers in post-MI heart [77]. The contribution of each source is still uncertain however the many sources for myofibroblasts in scar tissue may signify the important role these cells play in reinforcing the scar following MI.

4. Extracellular matrix (ECM)

The myocardial extracellular matrix (ECM - composed mainly of fibrillar collagens but also proteoglycans, fibronectins, laminin, and others) is an organized network associated with cardiac function, serving to direct, transmit, and distribute myocyte-generated contractile force [78]. Together the cardiac ECM proteins participate in active restoration of sarcomeric length, via release of stored potential energy in matrix proteins thus making the heart a *de facto* suction pump [79, 80]. In addition, the ECM may regulate cell death, gene expression and parenchymal cell differentiation [81, 82]. The cardiac ECM is composed mainly of collagens type I and III [79, 80, 83, 84]. Collagen type I and type III provides tensile strength and resilience to distension of the heart. Together these proteins provide structural support, aid in transmission of force and help to maintain the shape of the heart.

Altered matrix synthesis and deposition participates in the development of heart failure through the development of cardiac fibrosis [41, 43, 44, 85-87]. Elevated fibrillar collagen expression, types I and III, may be responsible for changing heart function in heart disease based on its adverse influence on myocardial stiffness [88-91]. Pathological cardiac hypertrophy is associated with interstitial and perivascular fibrosis in remnant heart or as replacement fibrosis for necrosed muscle [43, 49, 92]. In the latter, ongoing collagen remodeling may contribute to decompensated cardiac function in severe heart failure [8, 85].

The majority of cells in the mature infarct scar and surviving myocardium are myofibroblasts [9, 42, 93]. Clinical and experimental studies [11, 31, 41, 49, 60, 85, 94-96] demonstrate fibrosis in left ventricle remote to the infarct site with increased myocardial stiffness and increased cross-linking of collagen fibrils [31, 88-90, 97]. However, regulation of collagen gene expression in post-MI heart tissues is not well understood.

At 3 weeks post-MI, scar formation is complete [98], yet the scar remains a metabolically active tissue due to the presence of myofibroblasts [42, 56, 99]. Myofibroblasts may persist in the infarct scar and remain active for months to years after MI [7-9, 42, 85], contributing to chronic remodelling of the myocardium through increased collagen content [98, 100, 101].

The scar is an anisotropic tissue with large collagen fibres oriented within 30 degrees of the local circumferential axis [10], thus limited fibrosis in the healing infarct scar may preserve ventricular function through selective resistance to circumferential deformation [10] and prevention of scar rupture. Myofibroblasts produce isometric tension

within granulation tissue *in vivo* and in cultures [102, 103]. This tension is exerted at the level of focal adhesions (FAs), which connect cells to matrix [65]. This mechanical force may be beneficial for cardiac pump function in post-MI heart by resisting circumferential stretch while allowing appropriate longitudinal and radial deformation with the noninfarcted myocardium [10]. In addition, myofibroblast contraction is an important means of matrix manipulation in wound healing [103].

5. Myofibroblast contraction

Myofibroblasts are contractile cells that produce isometric tension within granulation tissue and in culture [102, 103]. Contraction by these cells distorts the ECM during wound healing [103] as the tensile force opposes retractile forces and promotes scar contraction in the post-MI heart [104, 105]. Cellular tension is transmitted through the ECM via focal adhesion proteins [65] and enhancement of myofibroblast contraction is achieved through increased expression of α-SMA [106].

Myofibroblasts display spontaneous calcium oscillations of ~100 seconds (with quiescent fibroblast calcium oscillations ~220 seconds)[107]. These cells also express sodium calcium exchanger proteins and L-type calcium channels [108] and are electrically coupled to myocytes [109, 110]. Intercellular coupling is likely through gap junction proteins such as connexins 43 and 45 [111].

Myofibroblast contraction may be mediated through two main mechanisms. In the first model, elevated intracellular calcium results in the calcium/calmodulin-mediated activation of myosin light chain kinase. This kinase phosphorylates myosin light chain

and the phosphate is continuously removed causing rapid but transient contraction [112]. The second pathway is initiated with small GTPase RhoA activation leading to the activation of Rho-associated kinase (ROCK). The myosin light chain phosphatase is inactivated by ROCK through phosphorylation of the myosin-binding site [113]. In addition, ROCK phosphorylates myosin light chain [114] such that the net result is sustained phosphorylation of myosin light chain and persistent contraction [112].

As cardiac myofibroblasts are neither smooth muscle cells nor skeletal/cardiac myocytes, they likely use a unique mode of contraction that maybe be dependent on the cellular environment. While traditionally, Rho-ROCK regulated contraction was considered the main mechanism for myofibroblast contraction [103], Castella *et al* recently proposed a two-stage model of wound contraction with both Rho-ROCK and calcium mediated mechanisms [107]. In this model, the Rho-ROCK pathway maintains isometric tension on stress fibres. Calcium-induced contraction picks up the "slack" generated by the Rho-ROCK isometric cellular contraction and neo-matrix formation stabilizes the contracture. Once stabilized the stress fibres are able to support the new load and the cell may re-spread thereby allowing multiple cycles of incremental contracture. These pathways, in combination, may lead to contracture of the wound at a rate of ~1 cm per month [107]. In this fashion, ROCK may mediate stress fibres in the centre of the cell while MLCK may stimulate stress fibre assembly in the cell's periphery [112]. This hypothesis is relatively new and more study into the biomechanics of myofibroblast contraction is required.

Chronic cardiac wound healing leading to the development of fibrosis and congestive heart failure is a complex process and involves input from multiple factors [39, 88, 115-117]. In this regard, TGF-β_1 is a known modulator of fibrillar collagen expression [118-121] and elevated TGF-β_1 is associated with matrix remodelling in post-MI heart failure [11, 60, 61]. The sources of this TGF-β_1 include myocytes [122], platelets, fibroblasts, macrophages and latent TGF-β_1 held in the extracellular matrix which is released through ECM degradation and mechanical tension [123].

6. Transforming growth factor beta (TGF-β) signaling

TGF-β_1 mediates cell growth and differentiation, tissue wound repair and extracellular matrix production [124-126], including regulation of fibrillar collagens [57, 119-121, 127]. TGF-β is found as three separate isoforms (TGF-β_1, -β_2, and -β_3) in mammals, differing in combination of subunits allowing for distinct affinities for different receptors [128]. All three isoforms are highly conserved and present in mammals [129]. Two additional isoforms have been identified – TGF-β_4 in chicken and TGF-β_5 in frog [130, 131].

TGF-β_1, -β_2, and -β_3 are secreted as latent precursor molecules containing a latency associated peptide (LAP) region that is bound to a latent TGF-β-binding protein (LTBP)[132]. The LTBP may be removed by proteases (e.g. MMPs, plasmin, thrombin, transglutaminase, or endoglycosylases), by physical interactions of the LAP with other protein (e.g. thrombospondin-1)[133, 134] or through shear-induced mechanical release [135]. TGF-β_1 mRNA is the dominant form of TGF-β in the body and is expressed in numerous

cell types including endothelial, hematopoietic and connective tissue cells [136]. TGF-β_1 null mice exhibit a hyperinflammatory response affecting multiple organs, especially heart and lung [137]. TGF-β_2 mRNA expression is relegated mostly to epithelial and neuronal cells and TGF-β_2 null mice are perinatal lethal displaying multiple developmental defects in heart, lung, limbs, spine, and urogenital system [138, 139]. TGF-β_3 mRNA is expressed mainly by mesenchymal cells and mice lacking this isoform display cleft palate and delayed pulmonary development [140]. Cutaneous wound studies have shown that TGF-β_1 and -β_2 may act synergistically during wound repair and scar formation, while TGF-β_3 inhibits scar formation [141]. TGF-β_1 and TGF-β_3 are more powerful growth inhibitors than TGF-β_2 [129, 142] and induce differential responses in vascular cells [143]. Thus TGF-β isoforms have both distinct and overlapping functions that are likely dependent on cell type and environment.

TGF-β_1 is expressed in both the normal and hypertrophied myocardium [43, 44, 60, 125, 144, 145]. Abnormal TGF-β_1 ligand expression is linked to cardiac fibrosis [146], and TGF-β receptor mutations are associated with abnormal vasculature matrix [147]. Canonical TGF-β_1 signalling is mediated by Smads and their transcriptional partners including coactivators and corepressors [148-156]. The relative simplicity of the Smad signaling pathway contradicts the complex cellular responses mediated by TGF-β. Non-Smad pathways may be activated on TGF-β binding to TGF-β receptors. Through phosphorylation of tyrosine residues on TGF-β type I receptors, TGF-β can recruit and phosphorylate the ShcA protein promoting the formation of ShcA/Grb2/Sos complex [157]. This complex ultimately activates ERK signalling which is important in epithelial to mesenchymal transition [157-159]. TGF-β can trigger ubiquitination of TRAF6 to initiate

recruitment of TGF-β-activated kinase 1 (TAK1). This complex activates JNK and p38 pathways through the activation of MKK4 and MKK3/6 respectively [160-164] and is linked to TGF-β mediated apoptosis [165] and epithelial to mesenchymal transition [160]. RhoA may be induced by TGF-β in a Smad-independent manner to mediate epithelial to mesenchymal transition [166]. TGF-β induced activation of PI3K signal transduction occurs through non-Smad pathways as well [167] to effect changes in fibroblast proliferation and morphological transformation [167]. However, these, and other non-Smad TGF-β pathways, are beyond the scope of this thesis, thus we will focus on the Smad pathway.

TGF-β_1 signaling in fibroblasts of healthy hearts is the sum of different stimulatory (R-Smads) and inhibitory proteins e.g. Smad7 and Ski [19, 61, 156, 168]. TGF-β_1 ligand signalling from cell-surface receptors to the nucleus is transduced by Smads and their DNA-binding partners (Figure 1) [148-156, 168-170]. TGF-β_1 receptor type I and II (TβRI and TβRII respectively) are Ser/Thr kinase class proteins, and signal through receptor-regulated Smads (R-Smad2 or -3) by specific recognition and phosphorylation steps [171, 172]. TGF-β_1 binds to TβRII which induces autophosphorylation of serine and threonine residues. Bound TGF-β_1 is then recognized by TβRI and a heteromeric complex is formed resulting in the phosphorylation of TβRI [173]. Two FYVE-domain containing proteins, Smad anchor for receptor activation (SARA) protein and Hgs, function in cooperation to hold R-Smads in proximity to receptors for rapid activation, i.e. phosphorylation [174, 175]. R-Smads are phosphorylated at a conserved carboxy-terminal SSXS motif and then dissociate from the receptor/SARA/Hgs complex [176]. Phosphorylated R-Smads form a dimeric complex with common Smad4 (Co-Smad4) and

translocate to the nucleus [172, 177] where the Smad complex binds to nuclear DNA and is able to recruit either coactivators (e.g. p300) or corepressors (e.g. Ski) [19, 26, 149, 151, 156, 169, 178-183].

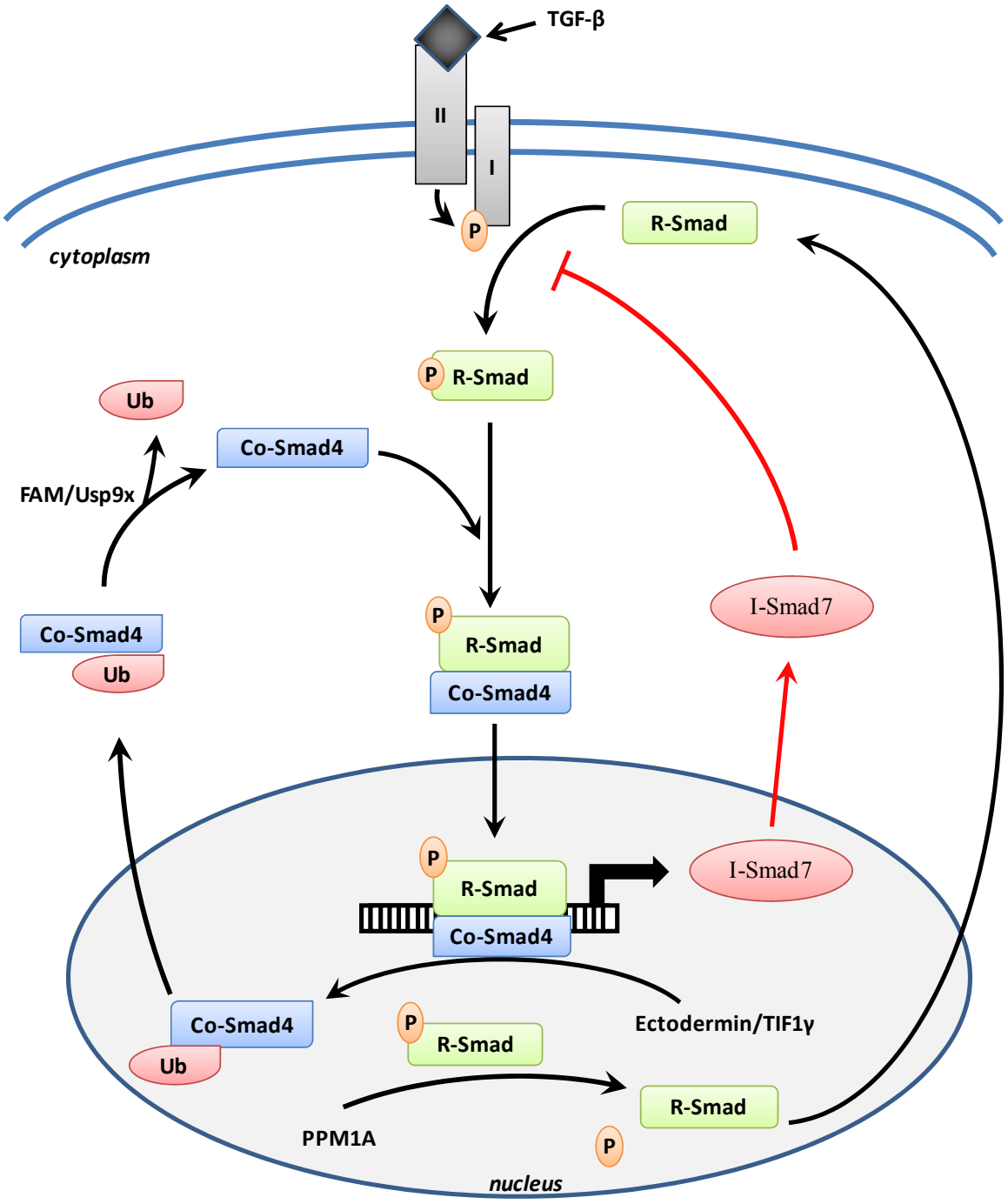
TGF-β
II
I
P
cytoplasm
R-Smad
P
R-Smad
Ub
Co-Smad4
FAM/Usp9x
Co-Smad4
Ub
P
R-Smad
Co-Smad4
I-Smad7
P
R-Smad
Co-Smad4
I-Smad7
Co-Smad4
Ub
P
R-Smad
Ectodermin/TIF1γ
PPM1A
R-Smad
P
nucleus

Figure 1. Canonical TGF-β signaling pathway. Binding of TGF-β to TGF-β receptor type II triggers a signalling cascade whereby R-Smads are "activated" by phosphorylation. Phosphorylated R-Smads (P-Smad) may bind with Co-Smad4 in the cytosol and translocate into the nucleus. P-Smad/Co-Smad4 complex binding to DNA activates I-Smad7 transcription. I-Smad7 is then shuttled into the cytosol where it may inhibit R-Smad phosphorylation at the TGF-β receptor type I. Dissociation of the P-Smad/Co-Smad4 complex is mediated by Ectodermin/TIF1γ which ubiquitinates Co-Smad4. Ubiquitinated Co-Smad4 is recycled by shuttling into the cytoplasm where it may be de-ubiquitinated by FAM/Usp9x. P-Smads may be dephosphorylated in the nucleus by PPM1A so that they too may also be recycled.

Smad4 is recycled through reversible ubiquitination in the nucleus that causes dissociation of Smads from phospho-Smads [184]. Smad4 is shuttled into the cytoplasm where it is de-uiquitinated for further binding to activated Smads [184]. R-Smad function relies on the quantity of R-Smad in the nucleus, and this activation is extensively regulated [156]. R-Smad activation has been linked to activation of collagen genes [185, 186]. Genes that are transcriptionally responsive to Smads contain Smad-binding elements (SBE) in their promoter regions [187]. Endogenous inhibitors of R-Smads include inhibitory Smad7 (I-Smad7) and nuclear Smad corepressors (e.g., Ski and SnoN) and they either competitively inhibit TβRI-mediated phosphorylation of R-Smads or stabilize inactive Smad complexes on DNA [26, 27, 179, 188-192]. I-Smad7 serves as a negative feedback mechanism in this system by binding and facilitating the degradation of TβRI, thereby turning off the receptor kinase and inhibiting R-Smad activation [188, 193]. I-Smad7 recruits Smad ubiquination regulatory factor 2 (Smurf2), an E3 ubiquitin ligase, to target TβRI for degradation [194].

7. c-Ski

7.1 Discovery/history

A study of chicken embryo cells infected with a Sloan Kettering avian retroviruses identified viral and cellular forms of Ski (v-Ski and c-Ski respectively [13], the viral form being truncated compared to the cellular homologue [195]. c-Ski is evolutionarily conserved among mouse, Xenopus and humans [13-16].

7.2 Alternative forms of c-Ski

Variants of c-Ski protein have been observed in early studies performed in chicken [195, 196], however more recent work rarely recognizes multiple forms. Original work identifying c-Ski described two c-Ski RNA transcripts of 8 and 5.7 kb [13]. Sutrave and Hughes described three types of c-Ski cDNA – one "full length" version comprised of 7 exons and two shorter versions lacking either exon2 or exon6. Sequence comparisons suggested that these variants were derived from alternatively spliced mRNAs [195]. Corroborating evidence of two alternatively spliced c-Ski – full length and lacking exon2 – were found by Grimes *et al.* in 1993 [196]. Further analysis failed to detect the c-Ski variant lacking exon6, however supporting evidence suggested that this version is a relatively rare c-Ski mRNA and not an artifact [195]. A subsequent study indicated that exon7 was actually two separate exons thus defining c-Ski as having a minimum of 8 exons in the chicken genome [197]. Human and *Xenopus* c-Ski have not been found to contain exon2 [15, 16]. Studies also describe 100 kDa and 66 kDa variants of c-Ski, with the larger protein being localized exclusively to the nucleus and the 66 kDa version detected in both cytosol and nuclei of a human leukemia cell line [198]. Early antibody preparations

recognized (full length) c-Ski at 90 kDa and (lacking exon2) 60 kDa and further described phosphorylation in the large version *vs* weak phosphorylation in the lower version. 90kDa c-Ski was found to be more stable, with a half life nearly 3X that of shorter c-Ski and both versions were noted to be localized to the nucleus [17].

7.3 *In vivo* studies

Studies have shown that c-Ski is ubiquitously expressed in all tissues of the developing mouse [199] including both cardiac and skeletal muscle tissues in adults and neonates [24]. c-Ski may play a role in early response to tissue injury as c-Ski mRNA was shown to be increased in regenerating tissues (early) in cells including myogenic cells [200]

Transgenic models of examining the roles of c-Ski in whole animals have shown that c-Ski overexpression leads to morphological transformation, anchorage independent growth and muscle differentiation in avian cells [13, 201]. Overexpression of c-Ski is associated with hypertrophy of type IIb muscle fibres [23] however evidence suggests that the increased muscle size is accompanied by muscle degeneration [22]. Supporting this observation, c-Ski overexpressing mice contain less contractile material in muscle fibres, poor alignment of Z-discs (with normal amounts and distribution of desmin) and abnormal mitochondria [202].

Ectopic expression in Xenopus embryos provides evidence that c-Ski is important in neural cell fate determination and body patterning [203, 204]. Supporting these observations, mouse models of c-Ski knockout are perinatal lethal, causing neural tube defects (associated with excessive apoptosis in cranial neuroepithelium) as well as cranial mesenchyme defects and reduction in skeletal muscle mass [21]. Thus these data suggest

that c-Ski is anti-apoptotic during development [21]. Interestingly, embryonic fibroblasts from c-Ski heterozygous knockout mice exhibit an increase proliferative potential and increased susceptibility to tumorigenesis [205]. Taken together these studies indicate that different concentrations of c-Ski protein may induce differential effects.

7.4 *In vitro* studies

While c-Ski was originally described as a nuclear protein [206], recent work describes a cytosolic role for c-Ski [27, 170, 183]. c-Ski will dimerize/-trimerize with itself or the related Ski-related novel protein (SnoN) via a C-terminal dimerization domain [207]. c-Ski is a phospho-protein [17, 18] and may be phosphorylated by cell division control protein 2 (cdc2) [208]. Evidence shows that phosphorylated c-Ski is more stable and is protected against proteasomal degradation [208, 209].

The nuclear function of c-Ski requires two distinct regions – the N-proximal amino acids 157-270 and C-terminal amino acids 595-728 for DNA binding activity [198]. c-Ski may bind specific DNA motifs to mediate transcriptional repression with its associated proteins [210-215]. Transcriptional repressor activity of c-Ski protein is accomplished through an N-terminal repressor domain [216]. In addition, c-Ski recruits other repressor proteins to form a transcriptional repression complex with N-CoR/SMRT (via an N-terminal cysteine-rich region) and mSin3A (through a C-terminal helical region) [212]. c-Ski also associates with histone deacetylase 1 (HDAC1) to repress gene activation [19]. Kokura *et al*. suggest that c-Ski is also necessary for MeCP2-mediated transcriptional repression [214]. In contrast, Ski is able to function as a co-activator for nuclear factor 1 (NF1) activated genes through binding with NF1 [217].

Regulation of c-Ski expression remains poorly understood. High concentrations of TGF-β ligand may trigger rapid degradation of c-Ski, while low TGF-β concentrations may increase c-Ski expression [218-220]. Conversely, c-Ski may regulate the biphasic effects of TGF-β on cell proliferation, i.e. c-Ski may enhance proliferation induced by low concentrations of TGF-β and augment the antiproliferative effects of high concentrations of TGF-β [218].

During the cell cycle c-Ski levels are reduced following mitosis (M-phase) and increase during the DNA synthesis phase (S-phase) [221]. This cell cycle regulation of c-Ski may occur through cdc34 – a ubiquitin-conjugating enzyme – causing c-Ski degradation [221]. Similarly, ubiquitination of c-Ski by the E3-ubiquitin ligase Arkadia may enhance TGF-β signaling through c-Ski degradation [222, 223]. This process of c-Ski regulation may be cell type dependent [220].

7.5 Effects of c-Ski on proliferation/cell viability

Involvement of c-Ski on cell viability, apoptosis and autophagy is likely cell-type and concentration dependent. Apoptosis of granulosa cells has been associated with elevated c-Ski expression [224] while c-Ski was able to reduce Smad3 induced apoptosis in response to radiation injury in skin [225]. In skin fibroblasts, c-Ski overexpression is linked to cell proliferation and reduced collagen type I expression [218, 226]. Further work needs to be done to ascertain the complex effects of c-Ski on cell viability.

7.6 c-Ski and TGF-β

c-Ski interacts with Smad2/3/4 and has been identified as an inhibitor of TGF-β signalling [19] [169], however, the exact mechanism is yet to be fully understood. Evidence suggests that the TGF-β repressor activity of c-Ski is dependent on the ability of c-Ski to bind Smad4 via an interaction loop preventing functional Smad complexes from forming [169, 227]. c-Ski mediated inhibition of TGF-β may be dependent on cell type and environment.

Suzuki *et al*. describe a disrupting bridge hypothesis involving "Smad complex trapping" by c-Ski on DNA, preventing transcriptional activation of target genes (Figure 2A) [26]. c-Ski also competes with the transcriptional co-activator p300 during TGF-β activation [19]. In this fashion c-Ski serves as a transcription repressor at the nuclear level.

A.

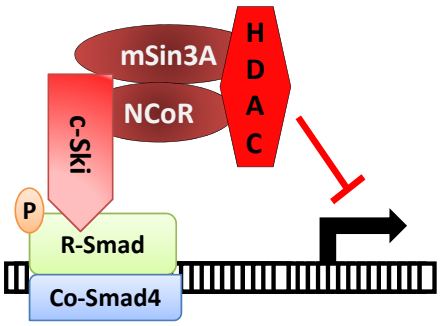
mSin3A
HDAC
NCoR
c-Ski
P
R-Smad
Co-Smad4

B.

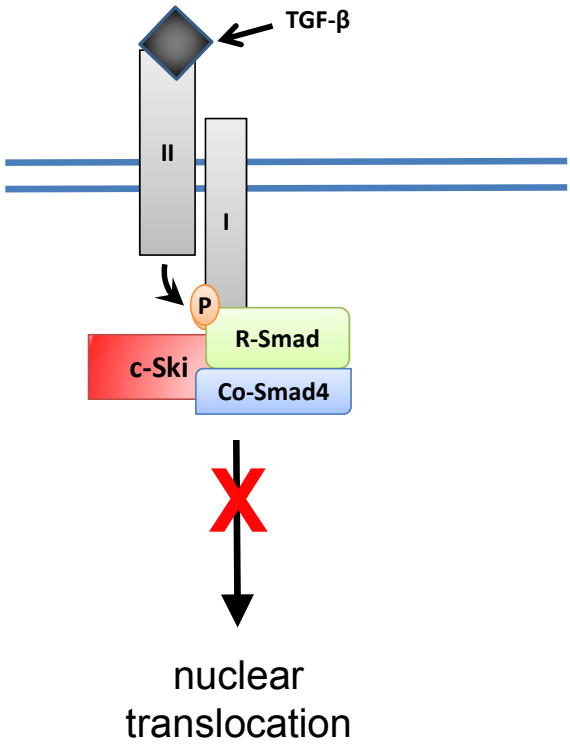
TGF-β
II
I
P
R-Smad
c-Ski
Co-Smad4
nuclear
translocation

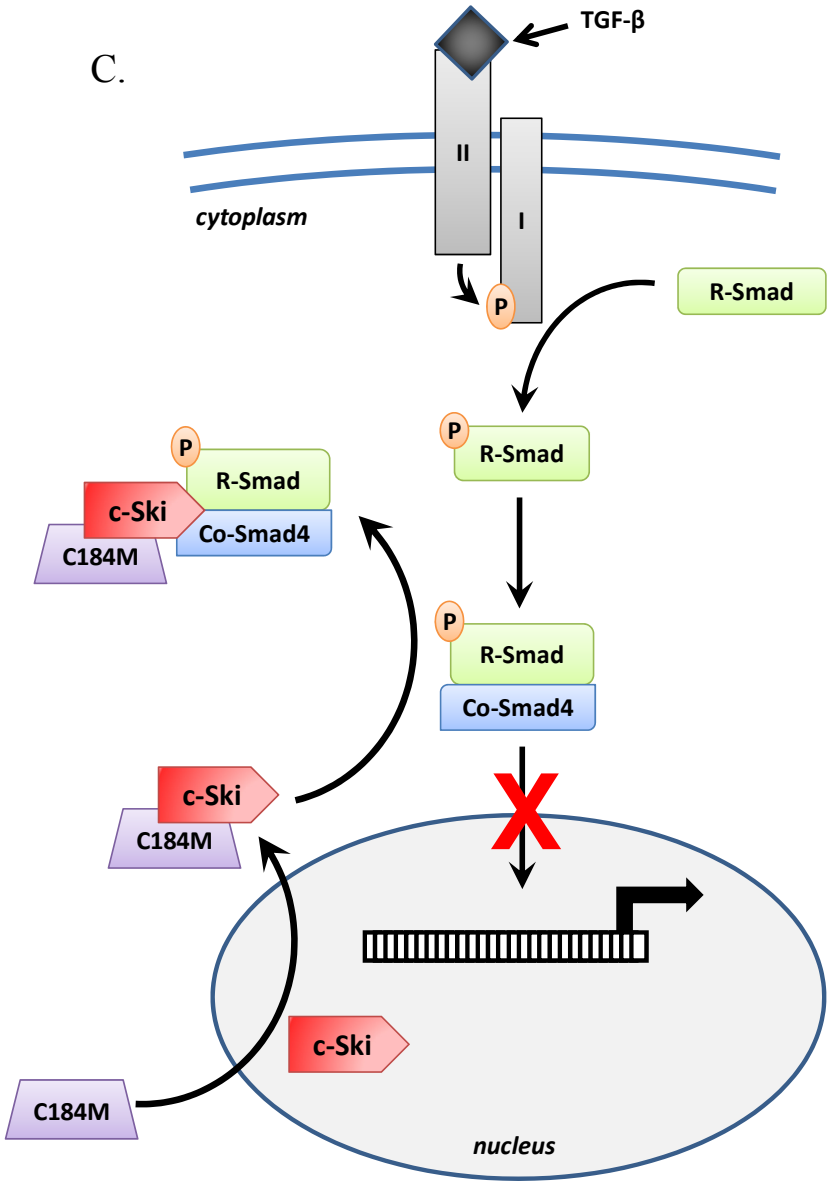

Figure 2. Possible mechanisms for c-Ski mediated inhibition of TGF-β. Panel A, Nuclear Smad "trapping" of c-Ski through binding to activated P-Smad/Co-Smad4 complex and recruitment of nuclear corepressors (mSin3A and N-CoR) and histone deacetylase to prevent target gene transcription. Panel B, c-Ski inhibits nuclear translocation of activated P-Smad/Co-Smad4 complex by preventing dissociation of complex from TGF-β receptor type I. Panel C, Cytosolic c-Ski/C184M complex binding to activated P-Smad/Co-Smad4 prevents nuclear translocation.

However, inhibition of TGF-β signaling persists in cells expressing c-Ski with a mutation of the nuclear localization signal [209]. c-Ski localization in the cytoplasm has been associated with TGF-β inhibition resulting from the inhibition of Smad2 phosphorylation and interaction at the TGF-β receptor type I to prevent nuclear translocation of R-Smad/Smad4 complexes (Figure 2B) [27, 209]. The novel C184M protein may aid this function as evidence shows that cytoplasmic co-localization of c-Ski and C184M inhibits nuclear translocation of Smad2 (Figure 2C) [170].

Although the precise mechanisms for the control of Ski expression/localization are unclear, its pluripotency implicates its participation in both physiologic and pathophysiologic processes especially with respect to TGF-β linked diseases

8. Meox proteins

8.1 Introduction to homeodomain proteins

Homeobox genes code for transcription factors that effect a range of cellular activities and are important for development, growth and differentiation [228]. These genes contain a homeodomain region consisting of a highly conserved 60 amino acid sequence that forms a DNA binding domain [229]. Homeobox genes have been shown to be involved in body patterning of the fruit fly, *Drosophila melanogaster* [230, 231] as well as a variety of disease states such as reduced expression in colorectal cancer (Cdx2) and Alzheimer's (Meox2) [232, 233].

There are many subfamilies of homeodomain proteins including the Hox gene family, the Paired-related homeobox (Prx) genes, the Hematopoietically expressed homeobox (Hhex) gene, Prospero-related homeobox (Prox) gene, and the Mesenchyme

homeobox (Meox) genes. Of these, adult Meox2 expression is restricted mainly to cardiovascular tissues, including heart, arterial smooth muscle cells, lung, and renal mesangial cells (check review).

The mesenchyme homeobox (Meox) proteins are a family of two homeodomain proteins that share 95% amino acid identity within their homeodomain region. Meox1 and Meox2 are expressed in the mesoderm and mesenchyme during embryonic development in mice [234] and their concerted action is believed to be important for somite development [235]. Yet, despite the similarity in homeodomain composition, Meox1 and Meox2 have both overlapping and distinct functions.

8.2 Meox1

Meox1 is evolutionarily conserved [236] and is expressed various tissues including colon, prostate, uterus and vascular smooth muscle cells (VSMC) [237]. It is important for the specification of the cardiac muscle lineage [236, 238] and is important in axial skeleton development [235]. Meox1 overexpression leads to anchorage independent growth and tumor formation [237]. Meox1 is a downstream target of another homeobox protein, Hoxa2, during development [239].

8.3 Meox2

Meox2 (also termed Mox2 or growth arrest specific homeobox gene - Gax) is expressed during the development of all muscle lineages as well as brain and other tissues [240]. Adult Meox2 expression is limited to cardiac tissue, vascular smooth muscle cells, lung and kidney tissues [241] and has been shown to be significantly downregulated in

cultured VSMCs exposed to serum [241]. This downregulation is also observed in vivo following balloon angioplasty injury, i.e. endothelial denudation, in rats [242]. Homozygous Meox2 knockout mice display a reduction in skeletal muscle mass [243] and a loss of Meox2 expression in brain endothelial cells has been shown to induce apoptosis [232].

Exogenous Meox2 expression in cardiomyocytes, VSMC and endothelial cells leads to inhibition of cell proliferation [244-246]. Evidence from other studies suggest that Meox2 may induce VSMC withdrawal from the cell cycle at the G0/G1 stage likely through upregulation of p21 to inhibit cyclin dependent kinase 2 (Cdk2) [245]. However, Meox2 may act to both inhibit cell growth and induce apoptosis through independent mechanisms [247]. While exogenous Meox2 inhibits cell proliferation through upregulation of p21 [245], apoptosis may be regulated by Meox2 via p21-independent mechanisms, i.e. Bax/Bcl-2 pathways in mitogen activated cells [247]. Interestingly, quiescent cells were not affected in this manner [247]. Meox2 expression may also inhibit mitogen-stimulated migration of VSMC through regulation of integrin expression [248]. The ability of Meox2 to regulate both migration and proliferation of VSMC has also been linked to inhibition of angiogenesis through inhibition of the NF-κB proangiogenic signalling pathway [249].

8.4 Meox2 and TGF-β

In the canonical pathway, TGF-β ligand signals through the Smad proteins to effect gene change and Meox2 has recently been linked to this pathway [250-252]. TGF-β was shown to increase the expression of Meox2 in HaCaT cell cultures and exogenous Meox2 overexpression in these studies enhanced TGF-β inhibition of cell proliferation [252]. However, although this study showed that Meox2 may enhance TGF-β-mediated effects,

it may also act as a TGF-β antagonist, i.e. Meox2 blocked TGF-β_1 induced epithelial to mesenchymal transition (EMT) [252]. Myofibroblasts may arise from both EMT and endothelial to mesenchymal transition (EndMT) [74, 253]. Increased expression of Meox2 *in vivo* was associated with reduced inflammation and vascular remodeling by adventitial cells and these data were also linked to reduced Smad/TGF-β1 levels describing a direct influence of Meox2 overexpression on the expression of these proteins [250, 251]. A recent study provides evidence that Meox2 expression may be negatively regulated via Zeb2 (also known as Smad interacting protein or SIP1)[254]. Zeb2 is a nuclear factor that is induced by TGF-β stimulation [255] and may act as a transcriptional repressor to enhance EMT through a reduced expression of intercellular junctional proteins [255, 256]. In addition, Zeb2 has been shown to repress Meox2 expression and this repression may be relieved through microRNA-221 targeting of Zeb2 [254]. Further regulatory mechanisms of Meox2 expression have yet to be elucidated. In summary, while Meox2 has been studied largely in VSMC and endothelial cells and is able to exert effects on a range of cellular process, the role/regulation of this protein in cardiac myofibroblasts is unknown.

III. Rationale and hypothesis

A critical feature of cardiac wound healing following myocardial infarction is the appearance of myofibroblasts at the site of injury. These phenoconverted cells are responsible for the deposition of extracellular matrix, e.g. fibrillar collagens, which serve to reinforce the infarct in the acute phase of MI but ultimately tip the balance towards decomponsated heart failure through excessive matrix deposition with additional time. Abnormal matrix and excessive collagen may impair coordinated electrical conduction, lead to myocardial stiffening, and therefore to diastolic dysfunction. In addition, myofibroblasts exert tractional force on the injured areas leading to scar contracture. TGF-β_1 is an important inducer of collagen deposition and phenotypic conversion of fibroblasts into myofibroblasts post-MI. TGF-β signalling is regulated through a cascade of activators, e.g. R-Smads, and inhibitors, e.g. I-Smad7 and c-Ski, however the exact role of each of these proteins are not yet completely understood. The general premise of this investigation is that an imbalance between TGF-β activators and inhibitors in the infarct scar results in abnormal wound healing leading to heart failure. The aim of this thesis is to gain further the knowledge of the role of endogenous TGF-β inhibitors in cardiac myofibroblasts during myocardial remodelling following MI, including collagen deposition and phenotypic conversion.

Background: Enzymatic activation and mechanical release of latent TGF-β1 in the extracellular matrix following MI ends in receptor binding and activation of canonical R-Smad signalling. TGF-β1 stimulation of these cells induces de novo expression of α-SMA, ED-A fibronectin, SMemb (among other markers) and fibrillar collagens thus

marking phenoconversion of fibroblasts into myofibroblasts. In these cells, the normal balance between TGF-β_1 activation and inhibition is ultimately disrupted in favour of collagen production however the mechanisms causing phenoconversion and imbalance toward Smad activation are unclear. A potential strategy for treatment of post-MI wound healing may be found in the modulation of the phenotype of these cells through use of endogenous inhibitors, e.g. c-Ski, to reduce chronic collagen deposition that leads to decompensated heart failure.

Research question: What is the role of c-Ski in the infarct scar – i.e. how does this protein affect myofibroblast function and phenotype and by what mechanisms does it exert these effects?

Hypothesis: c-Ski inhibits myofibroblast function(s) and causes a reversion to the non-secretory fibroblastic phenotype.

Objectives: 1) Investigate the effect of c-Ski on myofibroblast functions, e.g. collagen synthesis, secretion and contraction

2) Elucidate the mechanism of TGF-β inhibition by c-Ski in cardiac myofibroblasts

3) Characterize the effects of c-Ski overexpression on cardiac myofibroblast phenotype.

4) Identify a mechanism for c-Ski mediated modulation of myofibroblast phenotype.

Approach: 1) Develop viral gene delivery system to overexpress c-Ski in cultured cardiac myofibroblasts and characterize both endogenous and exogenous c-Ski expression and localization using immunoblotting and immunofluorescence. In c-Ski overexpressing cells, collagen type I expression will be monitored using immunofluorescence. Quantitative assessment of mature type I collagen will be performed by measuring the cleaved amino terminal globular heads of collagen type I with a procollagen type I amino terminal peptide enzyme immunoassay. A two-dimensional collagen gel deformation assay will measure the effect of c-Ski overexpression on myofibroblast contractility in the presence and absence of TGF-β1. 2) Immunofluorescence and immunoblotting of nuclear and cytosolic protein fractions will be used to investigate the effect of c-Ski on P-Smad2 localization following TGF-β stimulation. Immunoprecipitation of c-Ski from myofibroblasts will be performed to ascertain the ability of this protein to bind to activated P-Smad2. 3) The effects of c-Ski overexpression on myofibroblast phenotype will be assessed using Western blotting of well known myofibroblast phenotype markers α-SMA, ED-A fibronectin, and SMemb. 4) A recently discovered link between fibroblast to myofibroblast differentiation and reduced Meox1 and Meox2 mRNA expression provides a potential mechanism for c-Ski mode of action. Investigation of the association of these proteins will be performed by assessing the influence of c-Ski overexpression on Meox1 and Meox2 mRNA expression in both the presence and absence of TGF-β1 using quantitative real-time PCR. The relevant links will be tested against myofibroblast phenotype using adenoviral overexpression. Immunoblotting for the phenotypic markers outlined in approach 3 will serve as endpoints in these experiments. Known modifiers of

Meox expression will be examined as a potential mechanism for c-Ski influence on Meox mRNA expression.

Significance: This study addresses the modulation of TGF-β_1 signalling pathway to influence myofibroblast mediated contraction and collagen synthesis as well as myofibroblast phenotype. A more complete understanding of the mechanisms underlying the phenoconversion of fibroblasts into myofibroblasts will allow for the therapeutic manipulation of these cells to treat heart failure in patients who have suffered MI. As these cells are also implicated in the pathogenesis of other cardiovascular diseases, e.g. hypertension and diabetic cardiomyopathy, this investigation will have broader implication in describing the underlying mechanisms contributing to these diseases. This study will ultimately identify the c-Ski protein as a potential target for development of novel therapeutic treatments of heart failure.

IV. Materials and Methods

1. Isolation of primary fibroblasts/myofibroblasts

Fibroblasts: Rats (150-200g) were injected with Ketamine/Xylazine cocktail to anesthetise them. On loss of reflex activity, heparin was injected into either the tail vein or the femoral vein. Next the chest cavity was cut open and the heart excised. The heart was then placed into a 100mm dish with 20ml DMEM-F12. Excess material was trimmed away and the heart was hung from the aorta on a cannula and secured using silk suture thread. DMEM-F12 was perfused through the heart for 5 minutes followed by a 5 minute perfusion with SMEM, a calcium-free medium, to stop the heart from beating.

Next a 0.1% collagenase type II(298 U/mg)/SMEM solution was run through the heart for 20 minutes. Afterwards, the heart was removed from the cannula into a 100 mm dish containing a 0.05% collagenase type II (298 U/mg)/SMEM solution and the dish was taken to the biological safety hood where tweezers were used to tear the heart into small segments. The dissociated heart was then placed in a 37^{o}C tissue culture incubator for 15 min to complete the digestion and liberate as many fibroblasts as possible. Digestion was halted by adding 10 ml of 10% DMEM-F12 to the plate, then transferring the entire solution to a 50ml tube where the remaining large segments of myocardium were allowed to settle out for 1 – 2 min. Leaving the relatively large pieces of tissue undisturbed, the supernanant was transferred to a new 50 ml tube which was then spun down at 2000rpm for 7 min. For retroviral infection of P0 cells, the supernatant was aspirated off, the pellet resuspended in 9 ml of 10% DMEM-F12, and 1 ml added to each of 9 wells of a 24 well dish. For all other experiments, the cell pellet was resuspended in 40ml of 10%DMEMF12 + 100 U/ml penicillin + 100 µg/ml streptomycin + 1.2g/L sodium bicarbonate + 1 µM acorbic acid and plated in 4 X T-75 flasks (Corning). After 2 h, cells were washed twice with 1X PBS and then 1ml of fresh media was added per well. These cells were considered P0 fibroblasts. Media was changed again the next morning without washing this time. Following 72 hours of incubation, cells were passaged into P1 myofibroblasts.

2. Retroviral construction and infection

Subcloning of c-ski into pMxie retroviral vector - Ski into pCDNA3.1NHA

Ski/pCMVtag2B was obtained from Dr. Shunsuke Ishii (Japan). c-Ski gene was cut from 10 µg of vector DNA using *NcoI* in NEB4 buffer, and BSA for a total volume of 99.05 µl – this was incubated 3 h at 37°C. Next, 33 uM dNTP and Klenow fragment enzyme were added and reaction was incubated at 25°C for 15 min followed by an incubation at 75°C for 20 min to inactivate all of the enzymes. DNA reaction products were purified using Qiaquick PCR purification columns and DNA was eluted with nuclease-free water (Ambion, # 9937) and absorbance checked on a Milton Roy spectrophotometer 1001 plus. Samples were then stored at 4°C until next step. 10 µg of pcDNA3.1-N-HA (Dr. Michael Czubryt, ICS, Winnipeg) was cut using *BamHI* in Buffer B (Roche) and BSA in a total volume of 98.99 µl and incubated at 37°C for 3 h. Next, 1µl of Mung Bean nuclease was added and the reaction was incubated at 30°C for 30 min. SDS was then added (0.01% of reaction volume) to inactivate the enzyme. DNA was purified using Qiaquick PCR purification columns and the absorbance checked as described above. Next, Antarctic Phosphatase (NEB) and Antarctic phosphatase buffer was added as per NEB protocol and the reaction was incubated at 37°C for 15 min. The enzyme was heat inactivated at 65°C for 15 min, and then the reaction mixture was stored at 4°C until the next step.

Linearized Ski/pCMV (9.52 µg) from above was cut with *XbaI* in NEB2 buffer with BSA in a total volume of 95 µL. The reaction was incubated at 37°C for 3 h, and then the enzymes were heat inactivated at 65°C for 20 min.

Linearized pcNDA3.1-N-HA (5.22 µg) from above was cut with *XbaI* in NEB2 buffer with BSA at 37^{o}C for 3 h. Next, Antarctic phosphatase buffer and enzyme were added as per NEB instructions. The reaction was incubated at 37^{o}C for 15 min, followed by heat inactivation at 65^{o}C for 20 min.

DNA loading buffer was added to the samples, which were run on a 0.8% medium agarose gel with ethidium bromide at 120V for 1 h 20 min. Appropriate bands were exised from the gel using scalpel blades over a BLAK RAY Lamp (Model UVL-21, Upland – borrowed from the laboratory of Dr. Larry V. Hryshko, ICS, Winnipeg). DNA extraction from gel was performed using GenElute gel extraction kit (Sigma) and absorbance was checked to determine DNA concentration.

The ligation was performed using NEB Quick Ligation Kit (#M2200S) with a 3:1 molar ratio of insert to vector and a total of 121.43 ng DNA per reaction. Each reaction was incubated (Vector alone and vector plus insert) at 25^{o}C for 15 min then transformed using Max efficiency cells (Invitrogen #18258-012) following Max efficiency protocol in 1.5 ml Eppendorff tubes. After 1 h incubation period, cells were spun down at 14000 rpm (~16000 X g) in the microcentrifuge for 10 sec. All but ~ 100 µl of SOC media was aspirated and the cells were resuspended in the SOC media remaining in the tube. Then the ~100 µl of the cell suspension was plated on ampicillin (50 µg/ml) agar plates and spread using a glass "hockey stick". Next, without flaming, the "hockey stick" was spread on a second ampicillin agar plate. Plates were incubated at 37^{o}C overnight in a Precision Gravity Convection Oven (Dr. Elissavet Kardami's Lab, ICS). The next day,

colonies were counted and it was determined whether double the number of colonies were present on the Vector plus insert plate versus the Vector alone.

Eight colonies from the ligation plate were selected and grown overnight in Ampicillin LB broth for minipreps application. DNA was then cut using *NheI* and *XbaI* in NEB2 buffer with BSA in a total volume of 10 µl (a vector only sample was cut for the purpose of comparison) and incubated at 37^{o}C for 1 h. Samples were run on a small 0.8 % agarose gel at 90V for 1 h and a picture of the DNA was taken using a Polaroid camera with 667 film. Six of the eight samples taken initially showed the insert. The cleanest looking samples and some linearized vector were used to confirm the result using the PCR technique.

PCR was performed using LA-Taq (TAKARA) using 25 ng template with GCI and GCII buffers. Primers used were:

L-SKIJ (Forward) Primer1: 5'-TAATGGATCCTGGAGGCGGCGGCAGGC-3'

R-SKI (Reverse) Primer2: 5'-TAAAGATATCCTACGGCTCCAGCTCCGC-3'

We then set the PCR machine to run 25 cycles on (Robocycler 40 - Stratagene):

1 X 2 min @ 98^{o}C

14 X 30 sec @ 98^{o}C, 2 min 30 sec @ 72^{o}C

15 X 20sec @ 98^{o}C, 2 min 15 sec @ 70^{o}C

We then programmed the cycler to store samples at 6^{o}C when the reactions were complete.

After this round of PCR was complete, a 5 µl sample was run on a small 0.8% agarose gel at 90V for 1 h. Next, a linearized fragment was cut with *XbaI* and then purified as above. A band size of ~2200 bp showed up on ligation samples but not vector only thus confirming insertion of Ski into pcDNA3.1-N-HA.

Insertion of HA-Ski into pMxie vector

pcDNA3.1-HA-Ski was amplified for DNA stocks using a Qiagen Maxiprep kit. In order to add appropriate restriction sites on either side of the HA tagged ski gene for further cloning of DNA, PCR was performed on pcDNA3.1-N-HA-Ski. Primers used were:

HASkiupstream1: 5'-GCATTACTCGAGCCATGTACCCATACGATGTTCCAG-3'

HASKIdownstream1:5'-
GACTTAGGATCCGAATGTTCCAGCAAGCAGAGGACC-3'

PCR was accomplished using Platinum *Pfx* using 25 ng of template, 5 µl of 10X amplification buffer, 6 µl 2.5mM dNTP mix, 1 µl 50mM MgSO4, 1.5 µl of 10µM primer mix, 1µl DNA polymerase, 15 µl of 10X Enhancer solution (final Enhancer concentration of 3X), and nuclease free water to 50 µl. 1-2 drops of mineral oil was placed over each sample to prevent evaporation. The hot start method was used as follows:

- 94^{o}C for 1 minute
- add DNA polymerase
- 25 X 94^{o}C for 30 seconds then 2 min 45 sec at 65^{o}C
- 1X 94^{o}C for 30 sec then 65^{o}C for 4 min

- store at 6°C

Next, samples were transferred to new 500 µl eppendorf tubes by taking 47 of the 50µl from each tube. Contamination by mineral oil was prevented by using gel loading tips and injecting air and dispensing the air once through the oil layer. Then sample was removed without disturbing oil layer and transferred to a new tube.

A 5 µl sample was run on a small 0.8% agarose gel to confirm successful PCR amplification of the HA-Ski gene. Samples were then purified with Qiaquick PCR purification columns, eluted in nuclease free water and then stored at -20°C until ready to use.

For the ligation, 10 µg of pMxie vector was cut using *BamHI* and *XhoI*, using Roche buffer B and BSA in a total volume of 100 µl. Reactions were incubated at 37°C for 6 h then heat inactivated at 70°C for 15 minutes. Next, 1/10 of reaction volume of Antarctic phosphatase buffer was added to the reaction along with a volume of Antarctic phosphatase enzyme equal to the amount of DNA present in micrograms eg, 10 µg DNA add 10 µl enzyme. The reaction was incubated at 37°C for 15 min, followed by heat inactivation at 65°C for 20 min. Next, samples were purified using the Qiaquick PCR purification columns.

HA-Ski PCR product (1.5 µg) was cut using *BamHI* and *XhoI* as was done with the pMxie vector again cutting for 6 h at 37°C and inactivating at 70°C for 15 min. DNA was purified using Qiaquick PCR purification columns.

Ligation of vector (pMxie) and insert (HA-Ski) was performed using Rapid DNA ligation kit from Roche with a molar ratio of 3:1 insert to vector. Reaction was incubated at room temperature for 30 min then used 1 – 2 µl of the reaction to transform into subcloning efficiency DH5α cells as described above. Cut vector was used as a negative control for the ligase reaction and a sample of vector without ligase was tested as well. Cells were plated on ampicillin agar plates and incubated at 37^{o}C overnight. The next morning colonies on each plate were counted and compared. Four colonies were picked and inoculated into ampicillin containing LB broth for plasmid minipreps.

Once DNA was isolated, test cuts were performed using *BamHI* and *XhoI* in Roche buffer B with BSA and a final volume of 10 µl to excise and identify the inserted HA-Ski gene. Two of the successful clones were then used for further minipreps and required amounts of DNA for sequencing were purified using Qiaquick PCR purification columns. DNA was sent out for DNA sequencing to (Cortec Kingston, ON) using the following primers as the starting point:

pMxieupstream#1: 5'-GCAGCTTGGATACACGCC-3'

pMxiedownstream#1: 5'-CATATAGACAAACGCACACCG-3'

Cortec then designed subsequent primers until the HA-Ski insert was fully sequenced. Sequence data was analysed using the Bioedit software. DNA from clones in which there were no errors was selected for Maxiprep using HiSpeed plasmid Maxi Kit (Qiagen) cell culture. Eco-phoenix (J. Wigle) cells were used for retrovirus production. Cells were

cultured at 37^{o}C in 10% FBS/DMEM + 100 U/ml penicillin + 100 µg/ml streptomycin + 2 mM L-glutamine + 3.7 g/L sodium bicarbonate.

NIH-3T3 cells were used for retrovirus titration and were cultured at 37^{o}C in 10 % FBS/DMEM + 100 U/ml penicillin + 100 µg/ml streptomycin + 1.5g/L sodium bicarbonate.

3. Adenovirus construction and infection

pcDNA3.1-N-HA-Ski and pShuttle2 were cut with *NheI* and *XbaI* in buffer NEB2 for 3 h. The pShuttle2 restriction digest was heat inactivated at 65^{o}C for 20 min before the removal of the 5' phosphate using Antarctic phosphatase (37^{o}C for 20 min then heat inactivation for 20 min at 65^{o}C). The pShuttle2/Antarctic phosphatase mixture was purified using Qiaquick PCR purification columns to remove the <100 bp nucleotide sequences. The digested pcDNA3.1-N-HA-Ski plasmid was run on a 0.8% agarose gel with SYBR Safe detection reagent and the appropriate ~ 2530 bp band was excised over a UV box and purified using Millipore gel purification columns. Ligations were performed using a Roche Rapid DNA ligation kit with a 5:1 molar ratio of insert to vector. The ligation product was transformed into Bioline alpha-select chemically competent cells (bronze efficiency) and positive colonies were selected for miniprep DNA isolations. Restriction digests using NheI/XbaI were performed to test for the presence of the appropriate sized insert. A successful clone was amplified in large scale and purified using a Qiagen Hispeed maxiprep. pAdeno-X Expression System 1

(Clontech) was used for generation of pAdenox-HA-Ski adenovirus according to manufacturer's directions. Titers were determined using a rapid titer kit from Clontech.

4. Protein isolation

Adult primary cardiac fibroblast P0 cells were passaged and plated on either 60mm or 100mm plates as P1 cells and left to grow until 60-70% confluency was reached. When using retrovirus (Rv-pMixie or Rv-pMixie-HA-Ski), cells were infected as P0 fibroblasts 24 h - 48 h after isolation and then passaged into P1 cells for experiments. Infection with adenovirus (Ad-LacZ or Ad-HA-Ski) occurred as P1 cells were plated for experiments. Once the desired confluency was reached, cells were starved using DMEM-F12 for 24 h. Stimulation with TGF-β_1 (10ng/ml) was then performed and TGF-β_1 containing medium was refreshed every 24 h as required. Once the stipulated stimulation time was completed, cells were removed from the incubator and washed twice with 1 X PBS. Cells were left in the second wash and placed on ice until ready to scrape. RIPA lysis buffer pH = 7.6 containing 150 mM NaCl, 1.0% nonidet P-40 (NP-40), 0.5% deoxcholate, 0.1% sodium dodecyl sufate (SDS), 50 mM Tris, phosphatase inhibitors (10 mM NaF, 1 mM Na_3VO_4, and 1 mM EGTA), and protease inhibitors (4 μM leupeptin, 1 μM pepstatin A, and 0.3 μM aprotinin) was used to lyse the cells by adding 120 μl of lysis buffer per 100 mm plate and scraping using a rubber cell scraper. Cells were collected and placed into 1.5 ml eppendorf tubes and left on ice for 1 h. Next cells were sonicated for 5-10 sec three times and then centrifuged at 14000 rpm in a microcentrifuge for 15 min at 4^{o}C. After centrifugation, supernatant was transferred to

new 1.5 ml eppendorf tubes being careful not to disturb the pellet. Samples were then stored at -20^{o}C until protein assay was carried out.

5. Protein assay

Protein was thawed and put on ice after removing from -20^{o}C freezer. Dilutions of 1/5 were prepared using RIPA buffer, allowing for 10 µl of protein per well of a 96 well dish. Standards of 0, 0.2, 0.4, 0.8, 1.0, 2.0 µg/µl were prepared diluting Albumin standard (Pierce) in RIPA buffer. Standards and protein dilution were loaded into wells in triplicate using 10 µl of standard/sample per well. Next a solution of 50:1 Bicinchoninic acid to Copper (II) sulfate was prepared and 200 µl added per well. 96-well plate was incubated for 30 minutes at 37^{o}C before reading on a plate reader..

6. Western blot analysis

Protein lysates used for running SDS-polyacrylamide gel electrophoresis were prepared by combining aliquots of lysates with Laemmli buffer (125 mM Tris-HCl (pH6.8), 5 % glycerol, 2.5 %SDS, 5 % 2-mercaptoethanol, and 0.125 % bromophenol blue) and boiling for 5 minutes. Equal amounts of protein (10-20 µg) were loaded on a 6% SDS-polyacrylamide gel along with Benchmark prestained ladder for identification of protein size. Proteins were separated at 175V for ~1 h and then transferred onto a 0.45 µM polyvinylidene difluoride (PVDF) membrane at 100V (40 mA) for 1.5 h. Membranes were blocked overnight in tris-buffered saline with 0.2% Tween 20 (TBS-T)

containing 5% skim milk at 4^{o}C with shaking. Membranes were then washed 4 X 10 minutes with TBS-T. Primary antibodies were diluted in TBS-T with 5% skim milk and incubated for 1.5 h at room temperature or overnight at 4^{o}C followed by 4 X 10 minute washes in TBS-T. Secondary antibodies (horseradish peroxidase (HRP)-labeled anti-mouse IgG or HRP-labeled anti-rabbit IgG) were diluted in TBS-T with 1 % skim milk and incubated at room temperature for 1.5 h. ECL+ Plus was used to visualize proteins and was developed on Kodak film. Protein loading was confirmed by using immunoblotting against β-tubulin or through Ponceau S staining solution (0.1 % Ponceau S in 5 % acetic acid).

7. Immunofluorescence

Adult primary cardiac fibroblasts entering their exponential growth phase (~20% confluent) were either mock infected, pMxie infected or pMxie-HA-Ski infected (MOI 150). Following 12-24 hours of infection, media was replaced with fresh 10% FBS/DMEM-F12 and left to grow to ~ 90 % confluency. Cells were then passaged from P0 into P1's and plated in a 6 well dish with coverslips. Counting was usually not required as cells were infected in a 24 well dish and passaged thereby limiting cellular proliferation. Cells were left to grow at 37^{o}C in 10 % FBS/DMEM-F12 until 60-70% confluent. Cells were then starved by washing 2X with 1X PBS and 0 % FBS/DMEM-F12 media was then added. After 24 h of starvation, cells were either left unstimulated or stimulated with TGF-β_1 (10 ng/ml) (R&D, Minneapolis, MN, USA). Upon stimulation of cultures for more than 24 h, fresh media + TGF-β_1 was added every 24 h. Once the

stimulation period was completed, culture media was aspirated and cells were washed once quickly, then 3X 7 min with cold 1X PBS. Cells were then fixed with 4 % paraformaldehyde for 10 minutes at room temperature. Cells were washed again as described above. 0.1% Triton-X100 was then added to permeabilize the cells and was incubated for 15 min at room temperature. Cells were again washed once quickly, then 3 X 7 min with cold 1X PBS. After aspiration of the last wash, primary antibody was added. Antibody for Sp1.D8 (type I procollagen – Hybridoma Bank) was used at 1/1000, Smad2 (Cell Signaling) used at 1/20, PSmad2 (Upstate) was used at 1/20, Ski (Upstate) was used at 1/200 and Alexa Fluor 488 conjugated anti-EGFP (Molecular Probes) was used at 1:700. Cells were incubated with primary antibody overnight at 4^{o}C. The next day, cells were washed as above and secondary antibody applied – Alexa Fluor 568 or 594 (Molecular Probes) at a dilution of 1:700. Secondary antibody was left on cells for 90 min and the cells were then washed as above. After the last wash, cells were left in PBS until ready to be mounted on slides. The coverslip was removed from the well and was gently aspirated until dry. A drop of Slowfade Gold with DAPI was put on the slide and the coverslip mounted cell side down. Coverslips were then sealed with clear nail polish and stored at 4^{o}C until ready to view. Pictures were taken with a 12.3 megapixel Nikon D90 digital camera on a Nikon Eclipse E600 fluorescent microscope.

8. MTT assay

First passage (P1) rat cardiac myofibroblasts were infected with Ad-LacZ, Ad-HA-Ski or left uninfected and then plated at 5000 cells/well in 96-well plates. Each

treatment was performed in triplicate. Cells were allowed to grow/adhere for 24 hours in the presence of 10% FBS before changing the media to 0.2 µl of serum free media. After 24 hours of starvation, the media was again replaced with fresh serum free media or serum free media with 10 ng/ml of TGF-β_1 (R & D Systems, Minneapolis, MN, USA). After various time points, 20 µl of MTT solution (5 mg/ml of MTT in PBS, sterile filtered with 0.45 µm filter) was added to each well and incubated at 37^{o}C for a further 3 hours. The media/MTT mixture was then removed by pipetting and replaced with 200 µl of dimethyl sulfoxide (DMSO) and then the plates were allowed to sit for 5 min. Each well was then mixed by pipetting and absorbances were measured at 570 nm to calculate cell viability.

9. Measurement of apoptosis by flow cytometry

Apoptosis was measured using the Nicoletti method [257, 258]. Briefly, infected cells grown in 12-well plates (pre-starved in FBS free medium for 24 h) were treated with TGF-β_1 (10 ng/ml) for 48 h. After scraping, the cells were harvested by centrifugation at 1500 x g for 5 min, washed once with PBS, and then resuspended in a hypotonic propidium iodide (PI) lysis buffer (1% sodium citrate, 0.1% Triton X-100, 0.5 mg/ml RNase A, 40 µg/ml propidium iodide). Cell nuclei were then incubated for 30 minutes at 30°C and subsequently analyzed by flow cytometry. Nuclei to the left of the G_1 peak (sub G_1) containing hypodiploid DNA were considered to be apoptotic.

10. Procollagen type I Amino terminal peptide enzyme immunoassay (P1NP EIA)

P1 cardiac myofibroblasts were seeded on 100mm^2 cell culture dishes and either remained uninfected or were infected with LacZ adenovirus (Ad-LacZ) (100 multiplicity of infection (MOI)) or Ad-HA-Ski (100 MOI) adenoviruses and then allowed to grow overnight to ~75% confluency. Cells were then serum starved for 24 h by washing twice with PBS and adding starvation media (serum free DMEM-F12 with 100 U/ml penicillin, 100 μg/ml streptomycin, and 1 μM ascorbic acid). Next, cells were either treated with TGF-β_1 (10 ng/ml) for 24 h or left untreated. Once the treatment period was complete, media was removed to a 15 ml tube and cells from that plate were scraped and added to the tube with the media. Next, tubes were subjected to 5 rapid freeze thaws in liquid nitrogen/37^{o}C water bath. 5μl of this media/cell solution was used for the procollagen type I amino terminal peptide enzyme immunoassay (P1NP EIA) following kit instructions.

11. RNA isolation

First passage cardiac myofibroblasts in 100 mm^2 dishes were harvested for RNA using GenElute Mammalian Total RNA miniprep kit (Sigma) according to manufacturer's instructions. RNA was diluted in 10 mM Tris (pH 7.5) and the absorbance at 260 nm (A_{260}) used to determine RNA concentrations. RNA purity was assessed using the ratio of absorbance at 260 nm to absorbance at 280 nm (A_{260}/A_{280}).

12. qPCR

Isolated RNA was DNase I treated for 30 minutes at 37°C. Stop solution was added and then tubes were incubated at 65°C for a further 10 minutes. Primer sets for Meox1 and Meox2 are found in Table 1.

Table 1. Primer sequences for quantitative real-time PCR

rat Meox2 primers:	
ratMEOX2forward	5'-ttagcgggctctgctcaaac-3'
ratMEOX2reverse	5'-ttcacgaaggtcccaaagtc-3'
(Amplicon size = 114 bp)	
rat Meox1 primers:	
ratMEOX1forward	5'-tcgcccaccataactacctg-3'
ratMEOX1reverse	5'-ccttcacacgcttccacttc-3'
(Amplicon size = 123 bp)	
GAPDH primers:	
GAPDH forward	5'-tgcaccaccaactgcttagc-3'
GAPDH reverse	5'-ggcatggactgtggtcatgag-3'
(Amplicon size = 86 bp)	

PCR master mix was prepared containing 2.5 µl RNA (used 250ng/reaction for Meox2), 12.5 µl Sybr Green, 1 µl primer mix (10 µM –each forward and reverse) and 8.5 µl DEPC treated water yielding a 25 µl total volume per reaction. Samples were run in triplicate including a no template control and a no reaction with template control eg, no reverse transcriptase enzyme was added in this case. After sealing the plate with optical tape, samples were run on a BioRad iQ5 light cycler using the following PCR thermocycler program:

cycle 1: (Reverse Transcriptase) step - 1 X @ 50.0°C for 10 min

cycle 2: (Amplification steps) - 1 X @ 95.0°C for 5 min

cycle 3 40 X @ 95.0°C for 10 sec, 65.0°C for 30 sec

cycle 4: (Melt curve) - 1 X @ 95.0°C for 1 min

cycle 5: 1 X @ 55.0°C for 1 min

cycle 6: 81 X @ 55.0°C - 95°C for 10 sec - increasing by 0.5°C every cycle

Data was analyzed using the BioRad iQ5 software.

13. 2D collagen gel contraction

Collagen gels were made by combining 7 ml of cold collagen solution (Stem Cell Technologies) with 2 ml 5X concentrated DMEM-F12 and adusting the pH to ~7.4. Total volume was brought to 10 ml with sterile double distilled water. 600 µl of the mixture was added to each well of a 24-well dish and allowed to solidify a minimum of 3 h to overnight at 37^{o} C in a 5 % CO_2 incubator. P1 cardiac myofibroblasts were seeded onto solidified collagen gels at 1 X 10^5 cells per well and either left uninfected or infected with Ad-LacZ (100 MOI) or Ad-HA-Ski (100 MOI) at the time of plating. Cells were allowed to grow and adhere for ~24 h and then were serum-starved for 24 h. Prior to addition of TGF-β_1 (10ng/ml) to the appropriate wells, gels were released from the walls of the dish using a scalpel blade or circular cutting tool. Once gels were released around the edges, cytokine was added, and pictures taken (t = 0). Pictures were then taken 24 h following the initial treatment and analyzed using IDL Measure gel software to determine gel surface area at each time point.

14. Immunoprecipitation

P1 cardiac myofibroblasts were plated and infected with Ad-HA-c-Ski (100 MOI) or Ad-LacZ (100 MOI) control virus. Following 24 h of incubation, cells were washed twice with PBS and then lysed with 500 µl of mild RIPA lysis buffer (150mM NaCl, 1% NP-40, 50mM Tris, pH8) containing protease inhibitor cocktail (Sigma) and phosphatase inhibitors (10 mM NaF, 1 mM sodium orthovanadate, and 20 mM β-glycorophosphate). Cell lysates were used for immunoprecipiation using Dynabeads Protein G (Invitrogen) following the manufacturer's protocol using gentle elution to remove protein complexes bound to beads.

15. Reagents/antibodies

c-Ski antibody (Upstate/Millipore), HA antibody (Rockland Immunochemicals), phospho-Smad2 ser456/467 antibody (Upstate/Millipore), α-smooth muscle actin (α-SMA) (Sigma), non-muscle myosin heavy chain b (SMemb) (Abcam), eukaryotic elongation factor 2 (eEF2) (Cell Signaling), β-tubulin (Abcam), ED-A fibronectin (Chemicon) procollagen type I antibody (sp1.D8) (Hybridoma Bank), antibodies for Lamin A and Hsc70 (Abcam), TGF-β_1 cytokine (cell signaling), Zeb2 (Sigma), Collagen gel solution (Stem cell technologies/Advance Biomatrix Purcol), procollagen type I amino terminal peptide enzyme immunoassay (PINP EIA) from Immuno-Diagnostic Systems.

16. Statistics

Data are expressed as mean ± SEM. Data were entered and processed using the SigmaStat statistics program. Groups were compared using one-way ANOVA with Student-Newman-Keuls *post hoc* test for multiple group comparisons. $P < 0.05$ was considered to be significant unless otherwise indicated in the legend.

V. Results

1. Characterization of viruses: c-Ski has mainly been studied in the context of transformed cell lines. Studies performed in primary cells have been lacking or absent, and the latter is true with respect to studying c-Ski expression in the heart. As myofibroblasts are central to post-MI wound healing and cardiac fibrosis and as these processes are closely associated with TGF-β/Smad signaling [43, 259], we investigated the expression of c-Ski in first passage (P1) cardiac myofibroblasts. HeLa nuclear extract was used as a standard for c-Ski expression. We consistently observed an abundant 105 kDa c-Ski band regardless of treatment (serum starved, 10% FBS or 10 ng/ml TGF-β1 treatment) (Figure 3A) along with two less abundant bands at 95 and 115 kDa, which were revealed with longer exposure times (data not shown). To assess the effectiveness of our adenoviral overexpression system, we infected P1 cardiac myofibroblasts with various MOI's of adenoviral hemagglutinin-tagged c-Ski (Ad-HA-Ski). Adenoviral overexpression of c-Ski resulted in an increase in the intensity of the 95 kDa band in a dose dependent manner compared to uninfected and adenoviral LacZ (Ad-LacZ) infected cells (Figure 3B). Localization of overexpressed c-Ski was determined through immunofluorescent analysis. Using a HA-antibody we were able to detect exogenous c-Ski localization in a distinct nuclear localization compared to uninfected and Ad-LacZ infected controls. Nuclei were DAPI stained and the actin cytoskeleton was stained with phalloidin to delineate the outline of the cell (Figure 4).

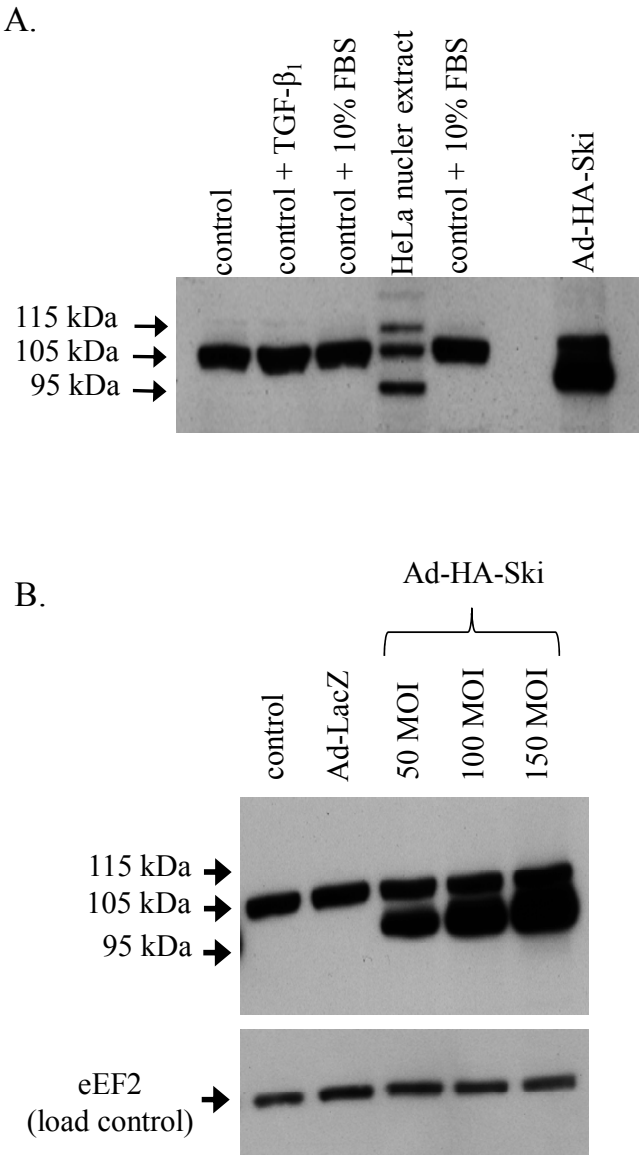

Figure 3. Characterization of c-Ski in uninfected and Ad-HA-Ski infected P1 myofibroblasts. Panel A, Cardiac myofibroblasts express 115, 105 and 95 kDa forms of c-Ski. Expression of endogenous c-Ski was performed using Western blot analysis of normal P1 cardiac myofibroblasts under serum-starved, 10% FBS or TGF-β1 stimulated conditions. Ad-HA-Ski overexpression lane was done with MOI of 100 vp/cell. HeLa nuclear extract (Upstate) was used as a control for c-Ski expression. Panel B, Ad-HA-Ski overexpresses 95 kDa c-Ski. P1 cardiac myofibroblasts were left uninfected or infected with Ad-LacZ (100 MOI) or at various MOI's with Ad-HA-Ski for 24 hours. Total c-Ski expression was examined using Western blot using eEF2 as a loading control. Images are representative of n = 3 different experiments.

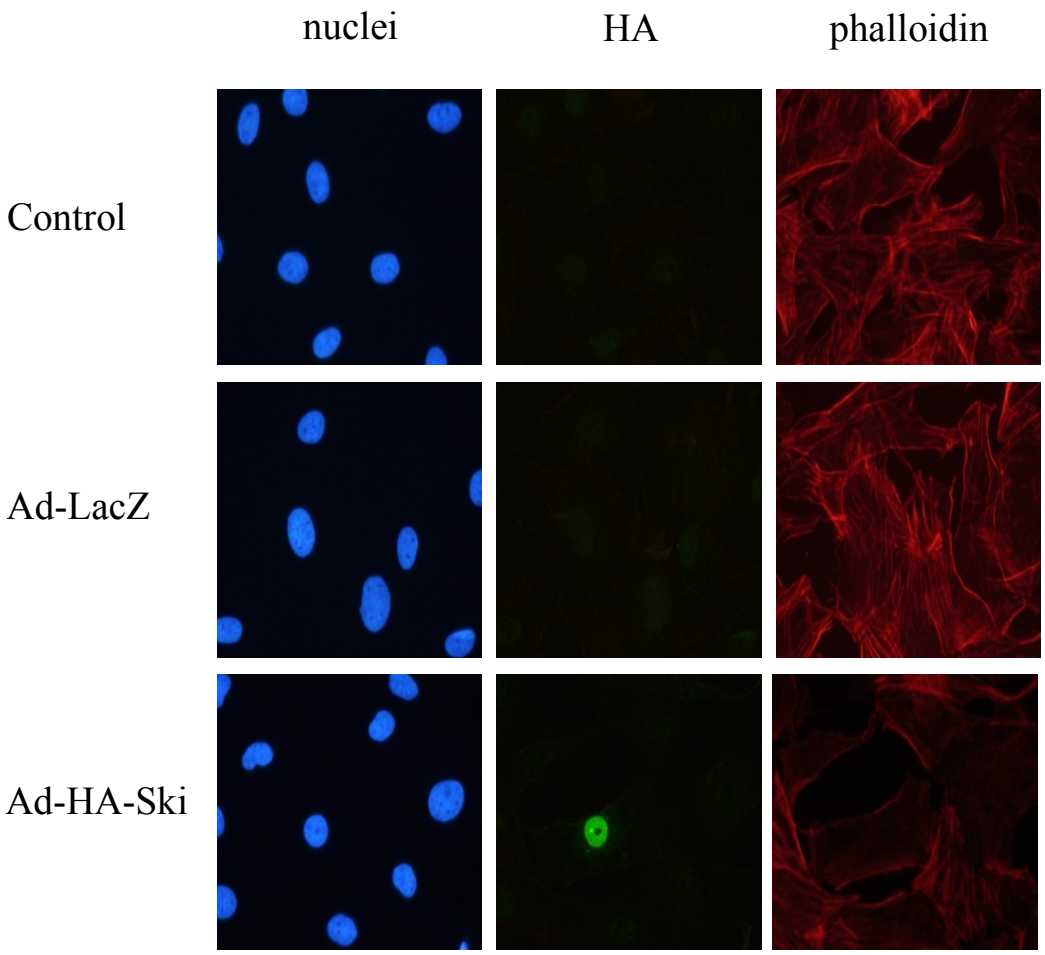

Figure 4. Exogenously expressed c-Ski is nuclear. P1 cardiac myofibroblasts were left uninfected or infected with Ad-LacZ (100 MOI) or Ad-HA-Ski (MOI 100) for 24 hours. Cells were fixed and immunostained using hemagglutinin (HA) antibody and DAPI nuclear stain. Phalloidin stain was used to delineate cell outline. Images are representative of 3 different experiments.

2. Effect of c-Ski overexpression on collagen synthesis/secretion: Previous studies have shown that c-Ski is able to inhibit TGF-β signalling [26, 27]. As this cytokine is profibrotic and implicated in cardiac fibrosis following MI [25, 146] and induces myofibroblast contraction of collagen gel matrices when cells are plated in two dimensions [260], we assessed the ability of c-Ski overexpressing cells to modulate these TGF-β induced effects. As the retroviral plasmid contains an eGFP reporter gene, we were able to detect retroviral infection in RV-pMxie and RV-HA-Ski infected cells. Monomeric procollagen expression within cells was monitored by immunostaining with procollagen type I antibody (sp1.D8). We observed a reduction of procollagen type I staining in retroviral-HA-Ski infected cells compared to uninfected and eGFP-only (Rv-pMxie) infected cells (Figure 5). To quantify the changes in myofibroblast collagen type I secretion, we used a procollagen type I amino terminal peptide enzyme immune assay to measure the cleaved globular end produced on mature extracellular collagen formation. Collagen type I secretion by Ad-HA-Ski infected cells was significantly reduced in TGF-β_1 stimulated (10 ng/ml for 24 hours) and unstimulated cells compared to Ad-LacZ and uninfected controls (Figure 6).

3. Effect of c-Ski overexpression on myofibroblast contraction: Myofibroblast contractility was measured using a two-dimensional collagen gel deformation assay. We observed an inhibition of myofibroblast gel contraction under both basal conditions and TGF-β_1 (10 ng/ml for 24 hours) stimulated conditions compared to uninfected and Ad-LacZ infected controls (Figure 7). In combination with the c-Ski overexpression characterization data, these data suggest an important role for the 95 kDa form of c-Ski in

the modulation of cardiac myofibroblast function, i.e. in the physical remodelling of the extracellular matrix.

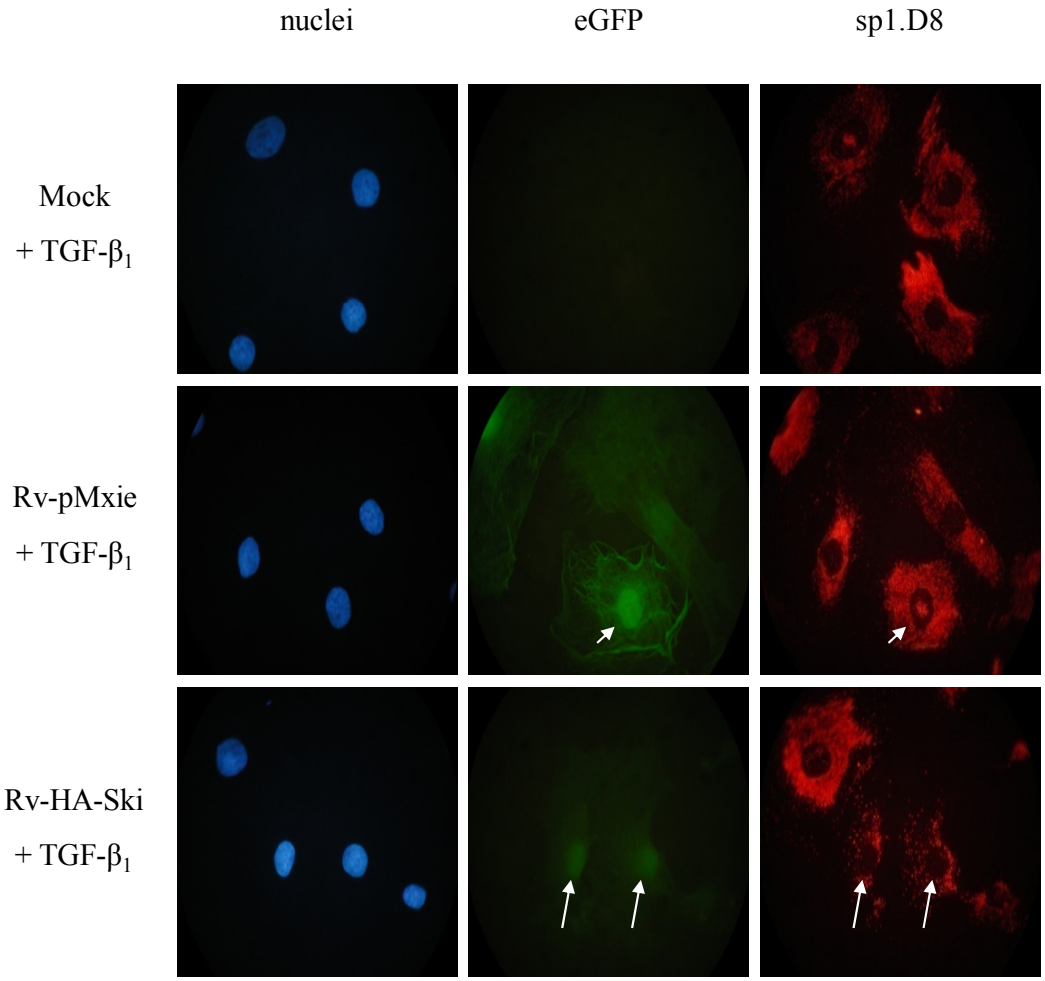

Figure 5. Overexpression of c-Ski inhibits collagen type I synthesis. Retrovirus-infected cells and uninfected (mock) control cells were stimulated with TGF-β_1 (10 ng/ml, 30 minutes) to induce expression of procollagen type I, fixed and immunostained with procollagen type I antibody (sp1.D8) with eGFP as a reporter for infection. Nuclei were stained with DAPI. Images are representative of n = 3 different experiments.

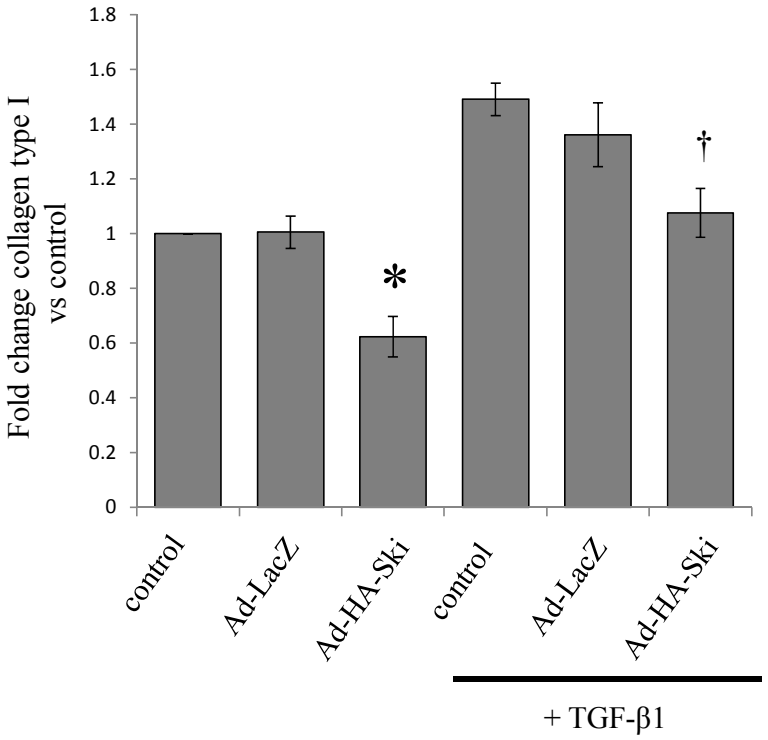

Figure 6. Overexpression of c-Ski inhibits collagen type I secretion. Uninfected (control) or Ad-LacZ/Ad-HA-Ski infected cells were serum starved for 24 hours and then treated with TGF-β_1 (10ng/ml) for 24 hours or left unstimulated. Cleaved amino globular heads of procollagen type I molecules were assayed using PINP EIA on the media/cell solution. Data was normalized to control within each group. Data are n=6, * $P < 0.001$ *vs* control; † $P< 0.01$ *vs* control +TGF-β_1.

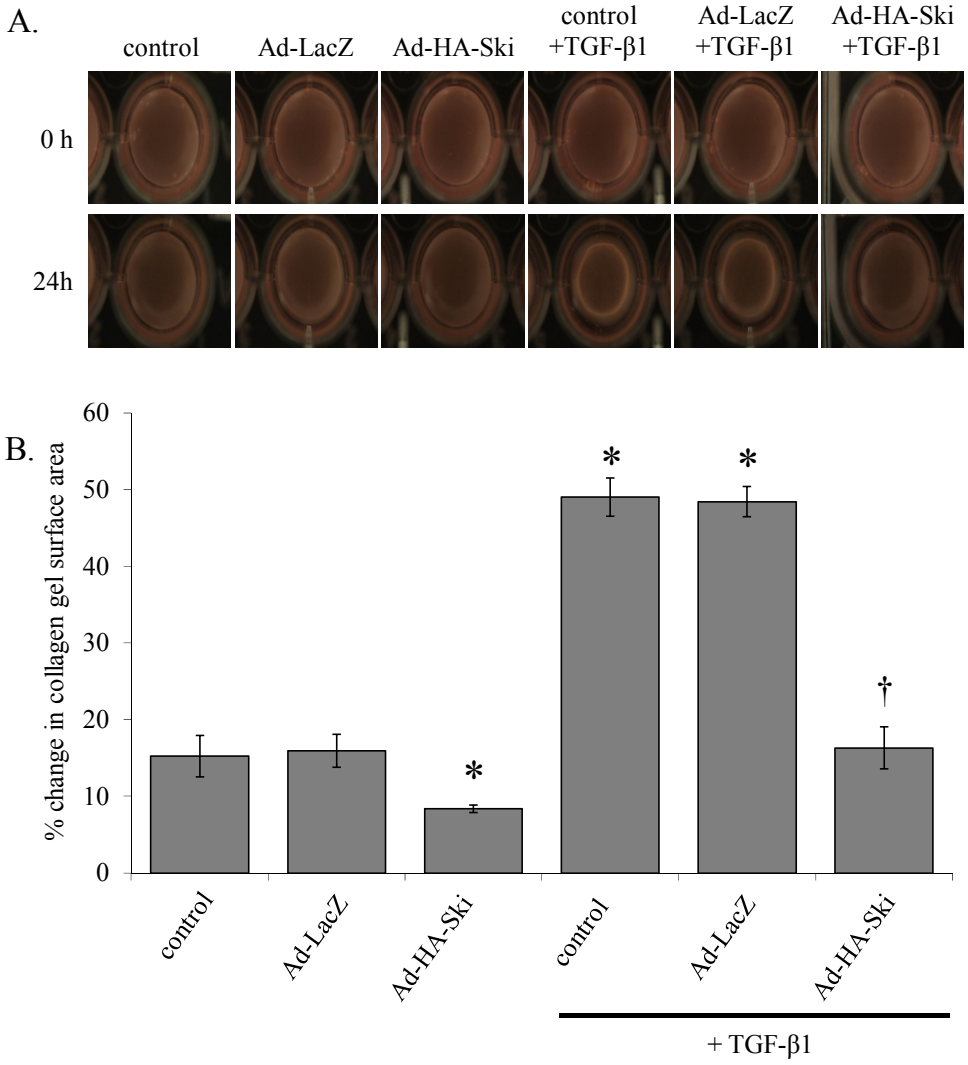

Figure 7. Ad-HA-Ski overexpression inhibits basal contractility and TGF-β_1 induced contractility of P1 cardiac myofibroblasts. Two-dimensional semi-floating gel contraction was carried out on uninfected (control) and Ad-LacZ (100 MOI) or Ad-HA-Ski (100 MOI) infected cells. Cells were serum starved for 24 hours then gels were released from the walls of the well and left unstimulated or treated with TGF-β_1 (10 ng/ml, 24 hours). Panel A: Pictures of gels were taken at time 0 and 24 hours following stimulation and changes in surface area measured using IDL based computer software. Panel B: Histographical representation of n=4 is shown. * $P < 0.001$ *vs* control; † $P< 0.001$ *vs* control +TGF-β_1.

4. Effect of TGF-β_1 stimulation on c-Ski localization: Stimulation of cells with TGF-β has been shown to induce degradation of c-Ski [223]. To ascertain the impact of TGF-β_1 (10 ng/ml) stimulation on c-Ski localization in primary cardiac myofibroblasts, we used immunofluorescent staining to monitor c-Ski expression and localization. We found that c-Ski staining at early time points (≤12 hours) was mainly diffuse throughout the cell, however at 24 and 48 hours of TGF-β_1 (10 ng/ml) stimulation, c-Ski was mainly localized to the nucleus (Figure 8).

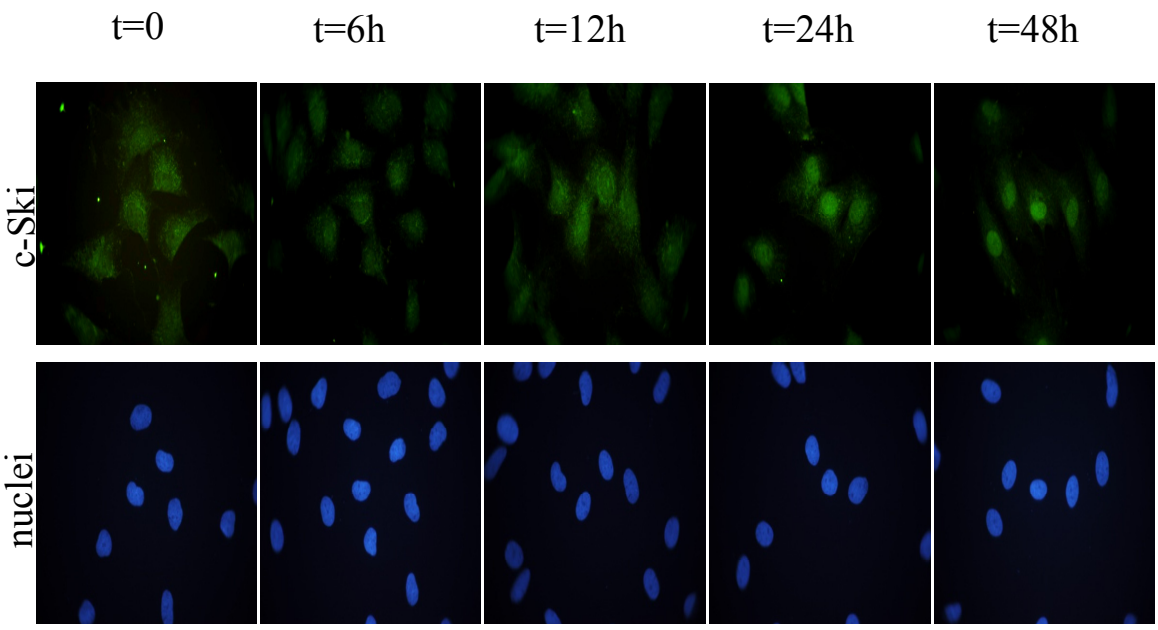

Figure 8. TGF-β_1 stimulates nuclear translocation of c-Ski in P1 cardiac myofibroblasts. P1 cardiac myofibroblasts at ~75% confluency were serum-starved for 24 h before treatment with TGF-β_1 (10 ng/ml) for various times. Immunofluorescent staining of c-Ski in serum-starved cells (DAPI nuclear stain) at selected time points under oil immersion (400 X). Pictures are representative of n = 4 individual experiments.

5. Mechanism for c-Ski mediated inhibition of collagen type I synthesis/secretion:

TGF-β signals through the canonical Smad signal transduction pathway [148, 149, 154]. Several potential mechanisms for c-Ski-mediated inhibition of TGF-β have been described using numerous cell lines including both nuclear and cytosolic mechanisms [26, 27]. To elucidate the actions of c-Ski in cardiac myofibroblasts, we examined the effects of c-Ski overexpression on the nuclear translocation of phospho-Smad2 (P-Smad2) using immunostaining and nuclear/cytosolic fractionation. Following TGF-β_1 (10 ng/ml) stimulation for 30 minutes, P-Smad2 translocated to the nucleus in all groups including uninfected, Ad-LacZ and Ad-HA-Ski infected cells. This result was demonstrated with immunofluorescence showing strong nuclear P-Smad2 staining in all cells (Figure 9A). We confirmed this result using nuclear/cytoplasmic fractionation showing robust P-Smad2 expression in the nuclear fractions of TGF-β_1 (10 ng/ml for 30 minutes) stimulated cells (Figure 9 B and C). A trend towards reduced P-Smad2 expression in nuclei of Ad-HA-Ski infected cells compared to uninfected and LacZ expressing cells was noted but found to be not significant and there was no increase in P-Smad2 levels in the cytoplasm of Ad-HA-Ski infected cells. To further identify the mechanism of c-Ski mediated inhibition of TGF-β_1, we examined the potential interaction of c-Ski and P-Smad2 in primary cardiac myofibroblasts. The association of these two proteins was assayed using co-immunoprecipitation. Following co-immunoprecipitation with c-Ski antibody, we observed significant levels of P-Smad2 in the uninfected and Ad-HA-Ski infected cell extracts (Figure 10). These data, taken together with the above experimental observations, provide evidence that nuclear 95 kDa c-Ski may function to inhibit TGF-β_1 through binding with P-Smad2. These data suggest a nuclear mechanism for c-Ski

mediated inhibition of TGF-β_1 through P-Smad2 binding. Inhibition may occur through P-Smad2 sequestering in the nucleus - either bound to DNA or through prevention of DNA binding. While our study does not definitively distinguish between these mechanisms, when taken with published data from other labs, our results support Suzuki *et al*.'s "disrupting bridge" hypothesis of c-Ski binding with phospho-Smads on DNA and preventing target gene activation.

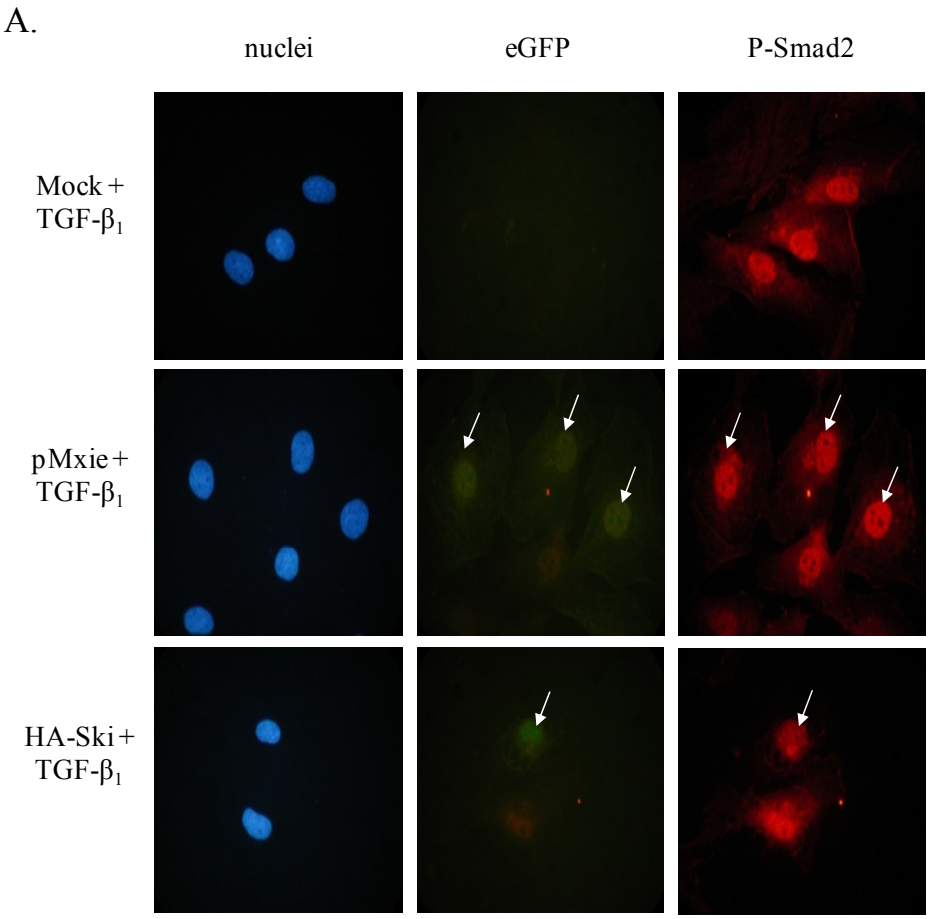

B.

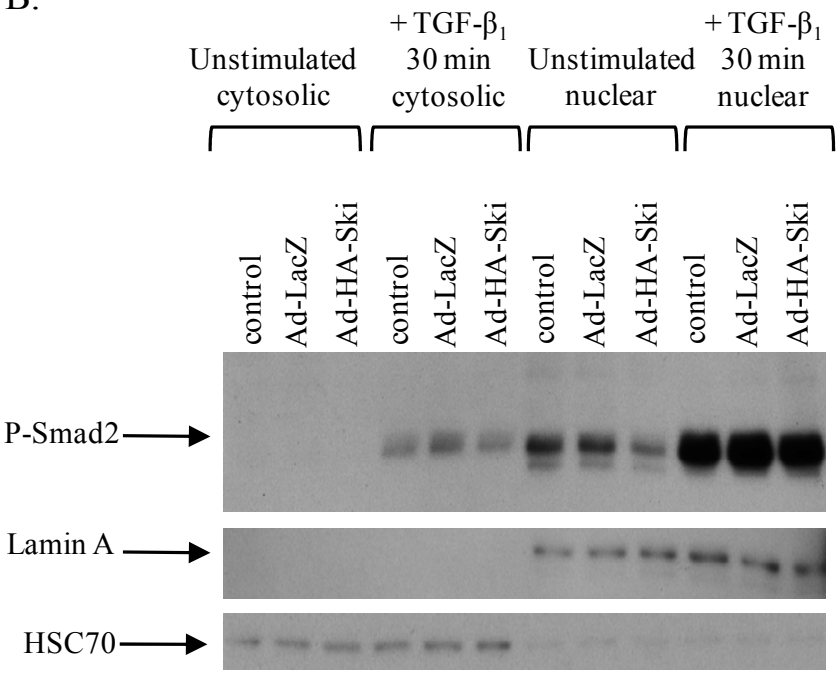
Unstimulated cytosolic
+ TGF-β1 30 min cytosolic
Unstimulated nuclear
+ TGF-β1 30 min nuclear
control
Ad-LacZ
Ad-HA-Ski
P-Smad2
Lamin A
HSC70

C.

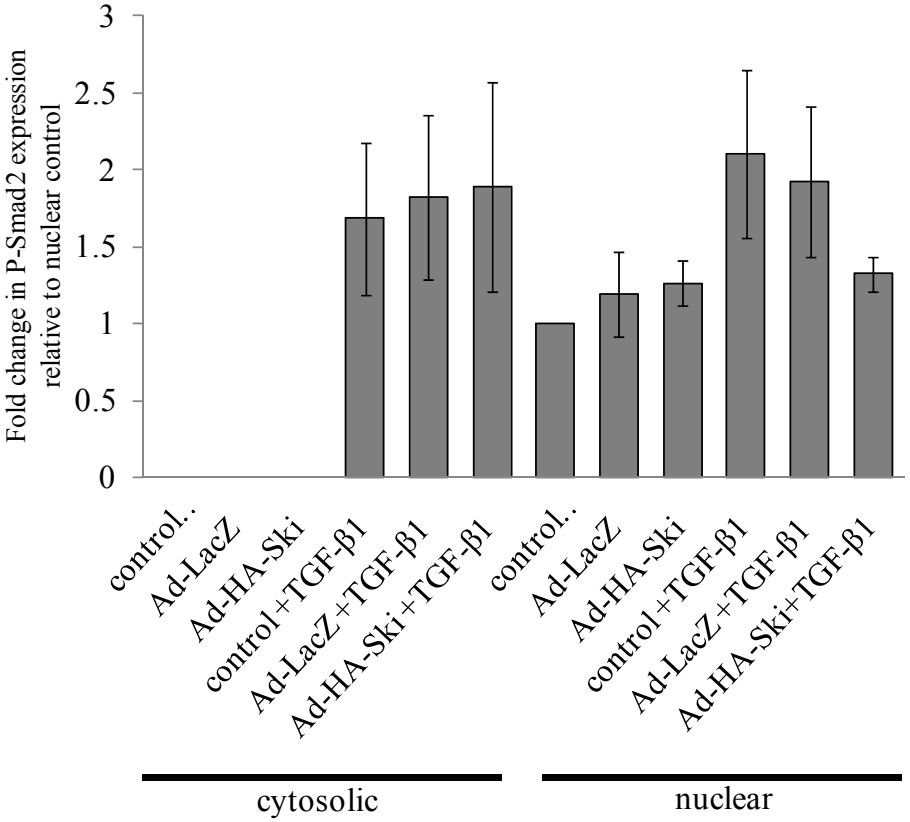
Fold change in P-Smad2 expression relative to nuclear control
3
2.5
2
1.5
1
0.5
0
control..
Ad-LacZ
Ad-HA-Ski
control+TGF-β1
Ad-LacZ+TGF-β1
Ad-HA-Ski+TGF-β1
cytosolic
nuclear

Figure 9. Overexpression of c-Ski does not inhibit nuclear translocation of P-Smad2. Panel A, Rv-HA-Ski infected P1 cardiac myofibroblasts (MOI 150) were treated with TGF-β_1 (10 ng/ml, 30 minutes) to stimulate phosphorylation and nuclear translocation of Smad2. Cells were immunostained for P-Smad2. The reporter gene eGFP was used to identify infected c-Ski overexpressing cells. P-Smad2 antibody was used to assess localization of "activated" Smad2 and nuclei were stained with DAPI. Images are representative of 3 independent experiments.
Panel B, Representative Western blots of nuclear and cytoplasmic fractions of uninfected, Ad-LacZ and Ad-HA-Ski infected cells that were unstimulated and stimulated for 30 min with TGF-β_1 (10 ng/ml) to induce Smad2 phosphorylation and nuclear translocation. LaminA and Hsc70 were used as nuclear and cytoplasmic loading controls, respectively.
Panel C, Histographical representation of data in (B). Data are n = 4 separate experiments.

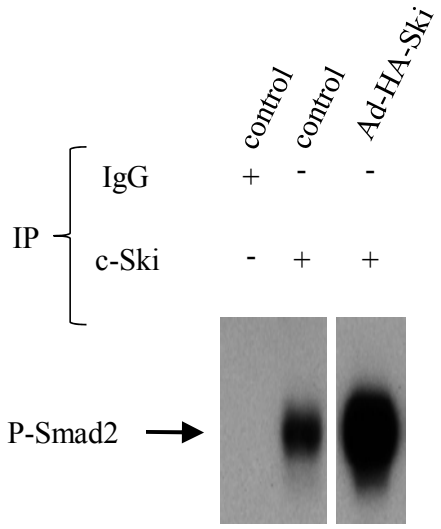

Figure 10. c-Ski forms a complex with P-Smad2 *in vitro*. Immunoprecipitation was performed on P1 cardiac myofibroblasts that were either uninfected or Ad-HA-Ski infected (50 MOI). Immunoprecipitation was performed using c-Ski antibody or IgG antibody as a control. Western blot was probed for P-Smad2 protein. Image is representative of n=6.

6. Effects of c-Ski on myofibroblastic phenotype: Cardiac fibroblasts phenoconversion into myofibroblasts results from a range of factors including TGF-β_1 stimulation [261, 262] and low density plating on rigid substrate [263]. Smad transduction of TGF-β signal is associated with this fibroblast to myofibroblast differentiation [25, 261, 264]. As we have shown above c-Ski is a potent inhibitor of TGF-β mediated effects including collagen type I synthesis/secretion and collagen gel contraction – two important characteristics of the myofibroblast phenotype. Thus we examined the effect of c-Ski overexpression on the phenotype of primary cardiac myofibroblasts through expression of recognized myofibroblast markers: α-SMA (Figure 11), ED-A fibronectin (Figure 12) and SMemb (Figure 13). Overexpression of 95 kDa c-Ski at various MOI's resulted in a marked reduction in α-SMA and ED-A fibronectin expression in Ad-HA-Ski infected cells relative to uninfected and Ad-LacZ infected cells. Changes in SMemb expression were not significant suggesting that 95 kDa c-Ski may diminish the myofibroblastic phenotype without fully reversing it.

7. Effects of c-Ski on myofibroblast cell viability: c-Ski has been shown to play a role in apoptosis [224] and is also associated with the regulation of cell proliferation [218, 226]. The roles of c-Ski are cell type dependant and the effects of c-Ski expression on viability of cardiac myofibroblasts are unknown. To examine the effects of c-Ski overexpression on the viability of P1 cardiac myofibroblasts we used MTT assays (Figure 14). Cells were exposed to serum-free medium or TGF-β_1 (10 ng/ml) for 48 hours. We observed a significant reduction in cell numbers in Ad-HA-Ski infected cells compared to uninfected and Ad-LacZ infected cells at seeding desities of 5000 cells per well. However, this

effect was partially lost at lower seeding densities (Figure 14). Flow cytometric analysis using propidium iodide staining revealed that reduction in cell viability was likely due to significant levels of apoptosis in c-Ski overexpressing cells relative to Ad-LacZ infected and uninfected control groups (Figure 15 A and B).

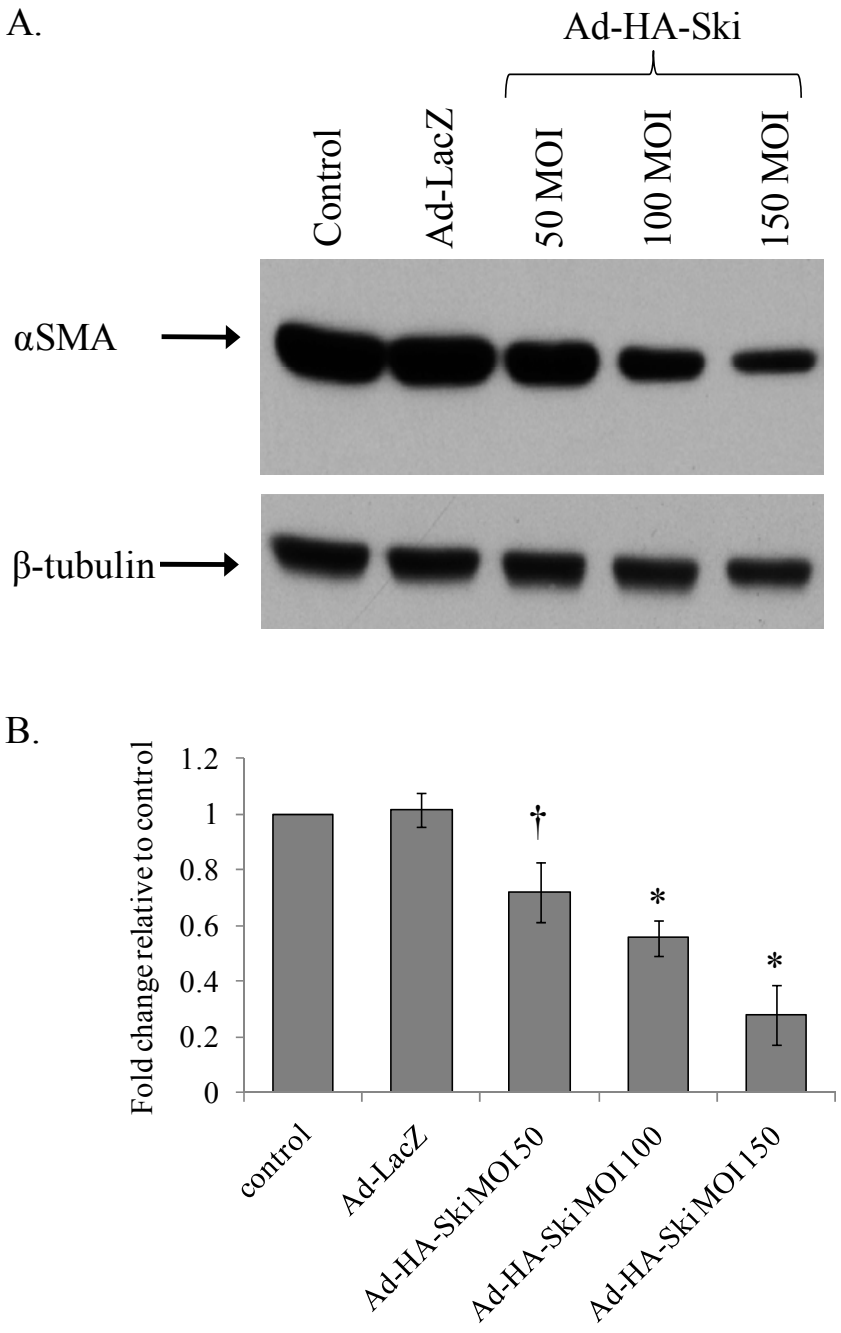

Figure 11. α-SMA expression decreases in 95 kDa c-Ski overexpressing cells. P1 cardiac myofibroblasts were infected with either Ad-LacZ (100 MOI) or Ad-HA-Ski (50, 100, 150 MOI) for 24 h. Uninfected cells served as a control. Panel A: Total αSMA expression was examined using Westerns using β-tubulin antibody as a loading control. Panel B: Histographical representation of data obtained in (A). Image shown is representative of n=3. † $P < 0.05$ *vs* controls; *$P < 0.01$ *vs* control values.

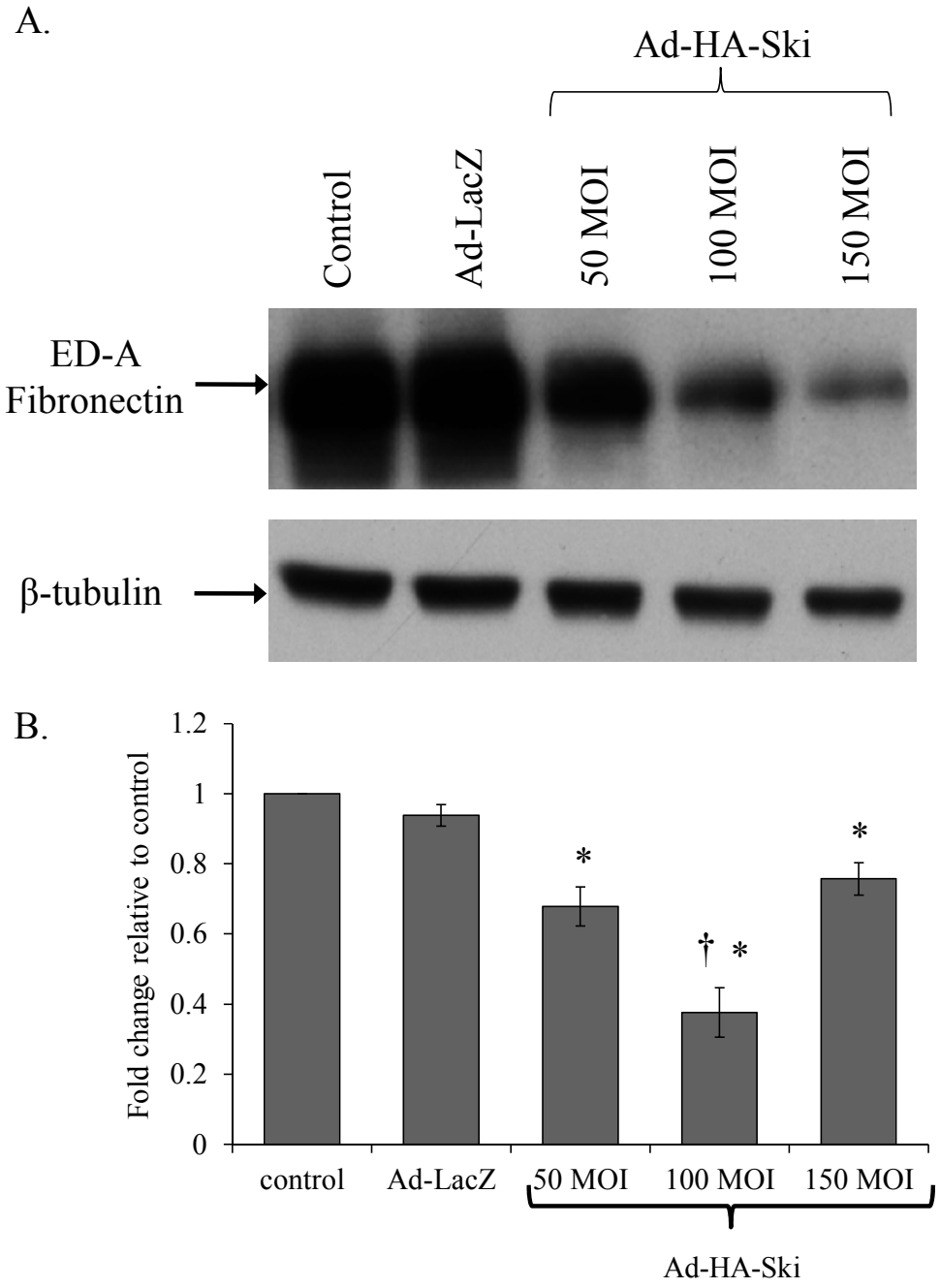

Figure 12. ED-A fibronectin is decreased in 95 kDa c-Ski overexpressing cells. P1 cardiac myofibroblasts were infected with either Ad-LacZ (100 MOI) or Ad-HA-Ski (50, 100, 150 MOI) for 24 h. Uninfected cells served as a control. Panel A, Total ED-A fibronectin expression was examined using Westerns using β-tubulin antibody as a loading control. Panel B, Histographical representation of data obtained in (A). Image

shown is representative of n = 4 independent experiments. *P < 0.01 *vs* control values; † P < 0.01 *vs* 50 MOI and 150 MOI.

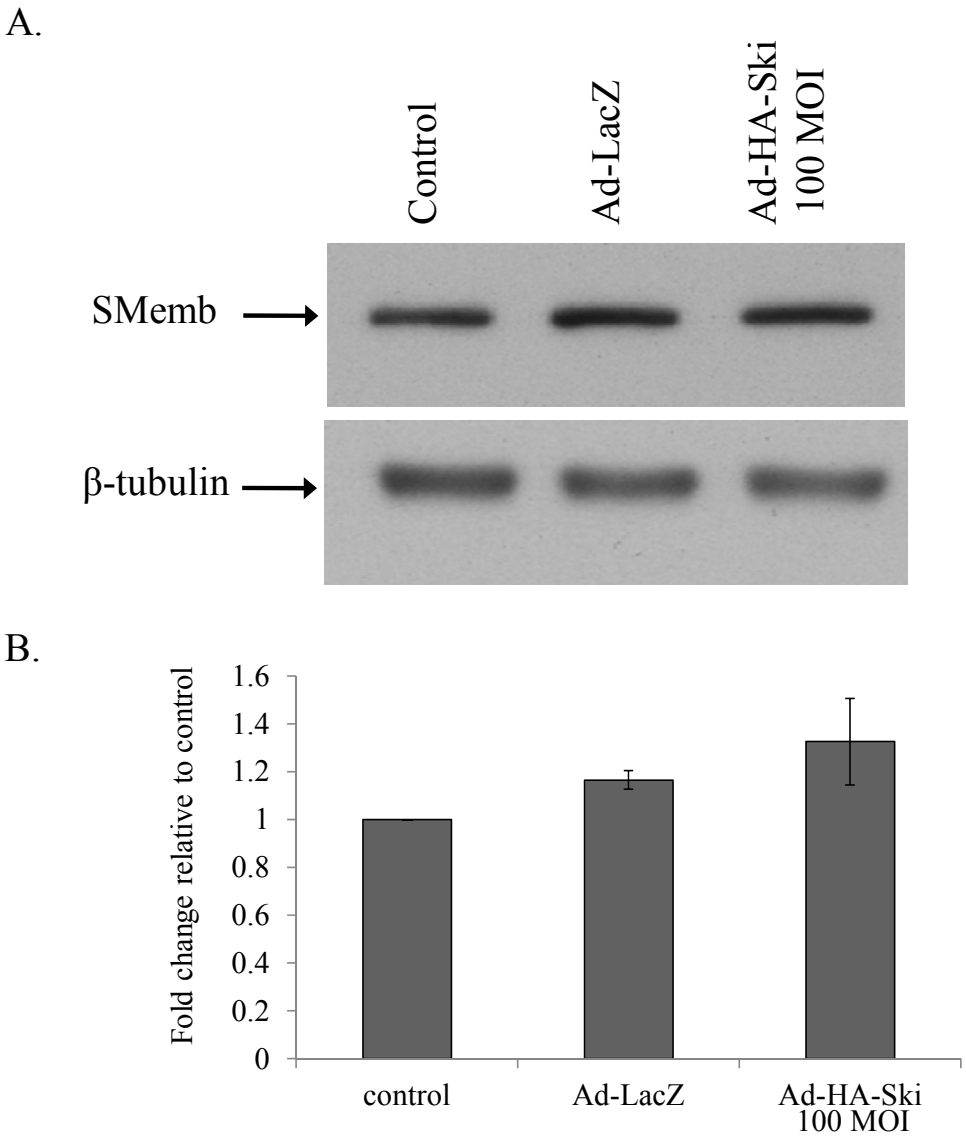

Figure 13. SMemb is not significantly altered with Ad-HA-Ski infection. P1 cardiac myofibroblasts were infected with either Ad-LacZ (100 MOI) or Ad-HA-Ski (100 MOI) for 48 h. Uninfected cells served as a control. Panel A, Total SMemb expression was examined using Western blot analysis using β-tubulin expression as a loading control. Panel B, Histographical representation of data obtained in (A). Image shown is representative of n = 3 independent experiments.

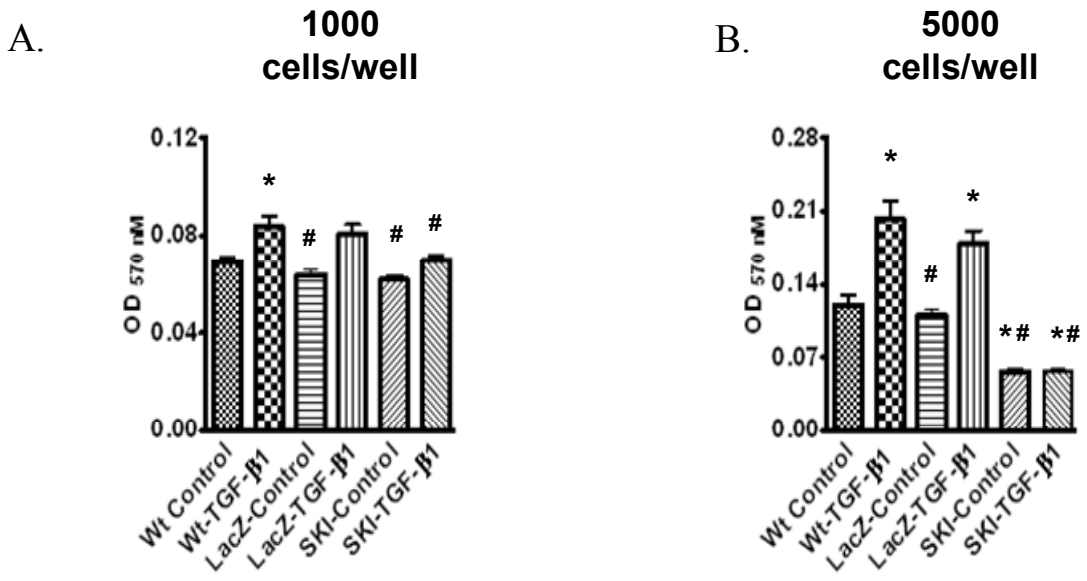

Figure 14. c-Ski overexpression reduces rat ventricular myofibroblast viability. Panels A and B, Cells were seeded at (A) 1000 cells/well or (B) 5000 cells/well in 96-well plates and left uninfected (wild type – Wt) or infected with Ad-LacZ (100 MOI) (LacZ) or Ad-HA-Ski (100 MOI) (SKI) and allowed to grow and adhere overnight. Cell were then serum starved for 24 hours before treatment with TGF-β_1 (10 ng/ml) for a further 48 hours. Serum free conditions for 48 hours served as a control. Cell viability was assessed by MTT-assays. Results are expressed as percentage of corresponding control and represent the means ± SE of 9 independent experiments in three different sets of rat ventricular cells. [Panel A, * = $P < 0.01$ *vs* Wt control; # = $P < 0.05$ *vs* Wt + TGF-β_1; Panel B, * = $P < 0.01$ *vs* Wt control; # = $P < 0.001$ *vs* Wt + TGF-β_1].

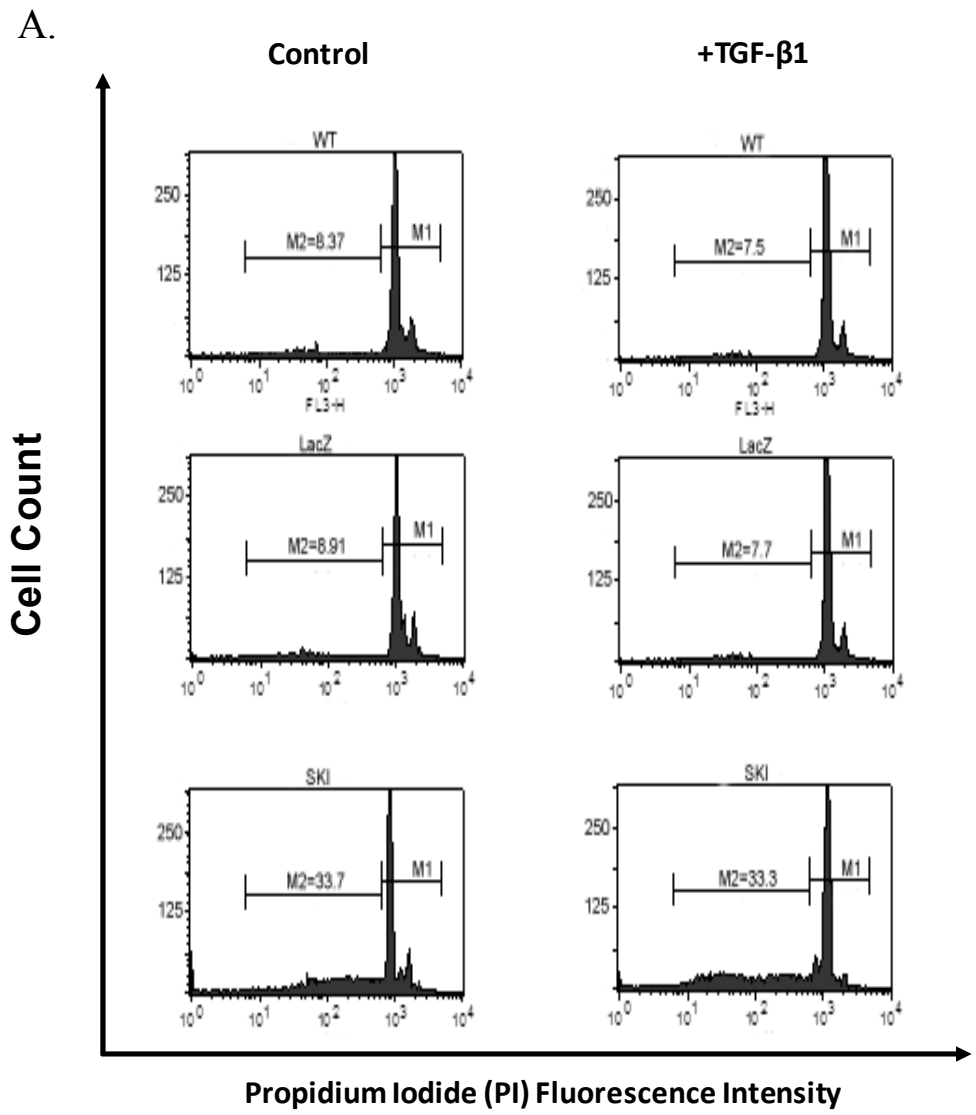

Figure 15: c-Ski overexpression induces apoptosis in first passage cardiac myofibroblasts. Panel A, DNA histograms of rat ventricular cells (Nicoletti method) from FACS analysis of uninfected (wild type – WT), Ad-LacZ (100MOI) (LacZ), and Ad-HA-Ski (100MOI) (SKI) infected P1 cardiac myofibroblasts. M2 (statistical marker) has been placed to mark sub-diploid DNA that is low on control histograms. The diploid (G1), and tetraploid (G2) DNA is visible in a form of two peaks in the far-right part of the histograms. G1 and G2 peaks are still preserved and sub-diploid peak corresponding to apoptotic cells was also clearly visible to the left from both peaks that represent normal cells. Panel B, Histographical representation of FACS data. n = 3 separate experiments. [* = $P < 0.01$ *vs* WT; # = $P < 0.01$ *vs* WT + TGF-β_1].

B.

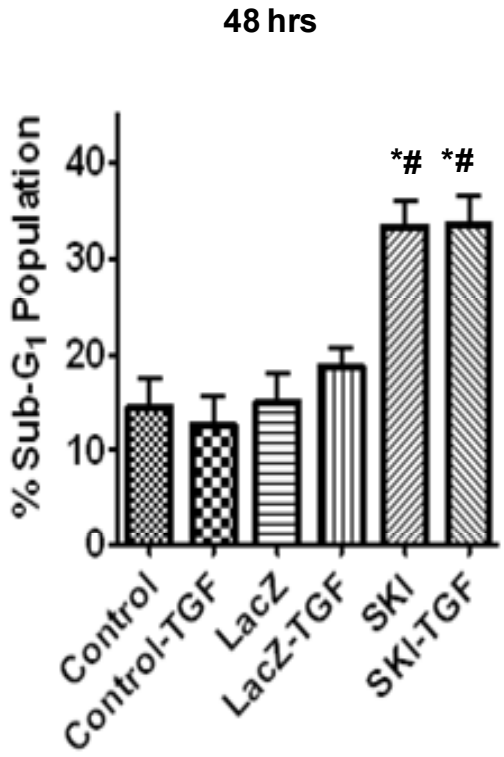

8. c-Ski effects on Meox1 and Meox2 mRNA expression: Primary (P0) fibroblast to myofibroblast (P1 and P2) phenoconversion is associated with increased levels of α-SMA [265], ED-A fibronectin [266] and SMemb [101] as well as a dramatic reduction in Meox1 and Meox2 mRNA expression (unpublished data). As shown above, c-Ski overexpression was able to diminish the myofibroblastic phenotype. As higher Meox1 and Meox2 levels are associated with the relatively quiescent fibroblast phenotype, we examined the effect of c-Ski overexpression on Meox1 and Meox2 mRNA expression. Using qPCR we observed an induction of Meox2 mRNA expression in Ad-Ski infected P1 cardiac myofibroblasts compared to uninfected and Ad-LacZ infected controls (Figure 16). A

trend of reduced Meox1 mRNA expression in c-Ski overexpressing cells was observed but not found to be significant. These data indicate that c-Ski may be involved in regulating the expression of the Meox2 homeobox protein but not a closely related protein, Meox1.

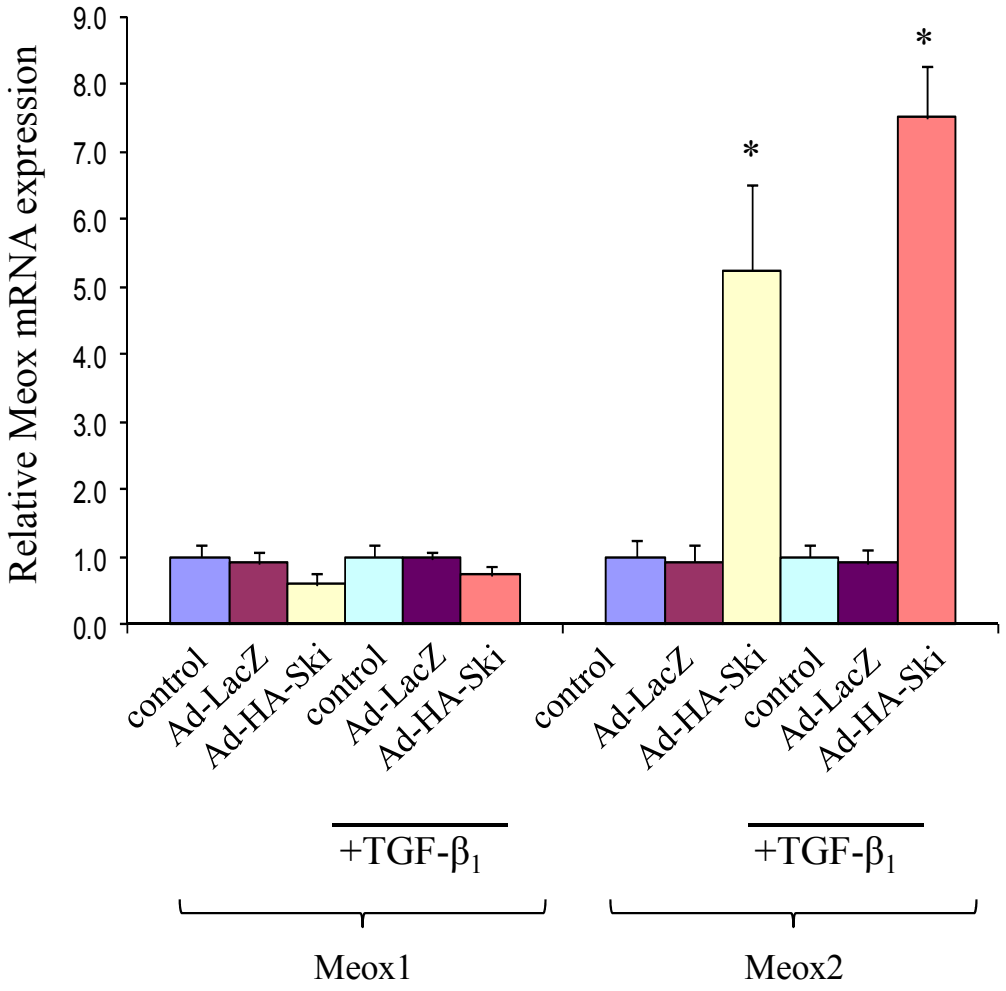

Figure 16. Overexpression of c-Ski upregulates Meox2 mRNA expression. P1 cardiac myofibroblasts were either infected with Ad-LacZ (100 MOI), Ad-HA-Ski (100 MOI) or left uninfected. Cells were starved for 24 hours before treatment with TGF-β_1 (10 ng/ml for 24 h). Total RNA was isolated and two-step qPCR performed with Meox1 and Meox2 primers. GAPDH primers were used to control for loading. * = $P < 0.005$ vs control. Data are n = 4 independent experiments. qPCR and analysis performed by J. Douville.

9. Effects of Meox2 protein overexpression on myofibroblast phenotype

The data shown above in this section led us to suggest a possible mechanism for c-Ski modulation of myofibroblastic phenotype through Meox2 induction. To test the hypothesis that Meox2 may influence the phenotype of our cells, we overexpressed FLAG-tagged Meox2 (Ad-FLAG-Meox2) in cardiac myofibroblasts and examined phenotypic markers through Western blot. Similar to c-Ski, Meox2 overexpression was able to significantly reduce both α-SMA and ED-A fibronectin protein expression but not alter SMemb levels (Figure 17). These effects on phenotype are similar to those or c-Ski overexpression. Thus, we feel that a putative link exists between these two proteins and represents a putative novel pathway for the modulation of the myofibroblastic phenotype.

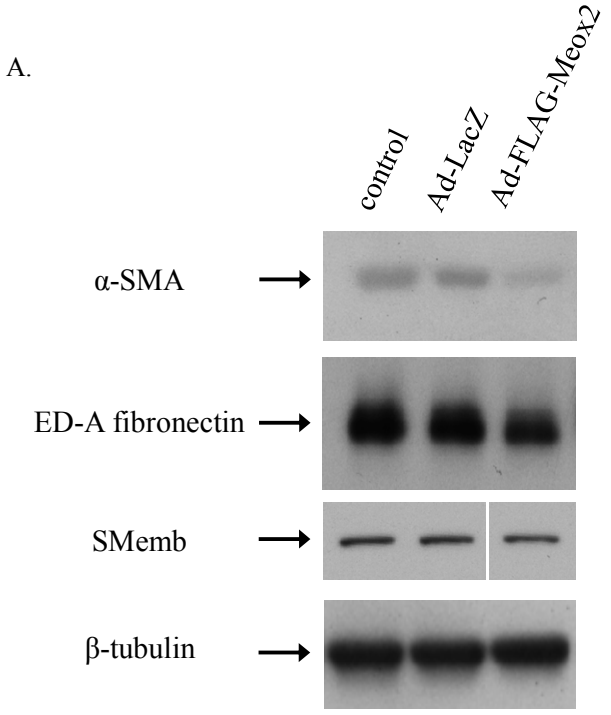

Figure 17. Meox2 overexpression causes diminution of myofibroblast phenotype. Panel A, P1 cardiac myofibroblasts were infected with Ad-LacZ (100 MOI) or Ad-

FLAG-Meox2 (200 MOI). Uninfected cells were cultured as an additional control. Cells were allowed to grow in the presence of virus for 48 h before harvesting for Western blot analysis. Myofibroblast phenotype was assessed using α-SMA, ED-A fibronectin and SMemb antibodies with β-tubulin expression used as a loading control. Images are representative of n = 4 independent experiments.
Panel B, Histographical representation of Western blots in (A). α-SMA, * = $P < 0.01$ vs control; ED-A fibronectin, † = $P < 0.05$ vs control; SMemb data was not significant. Data obtained from n = 4 independent experiments.

B.

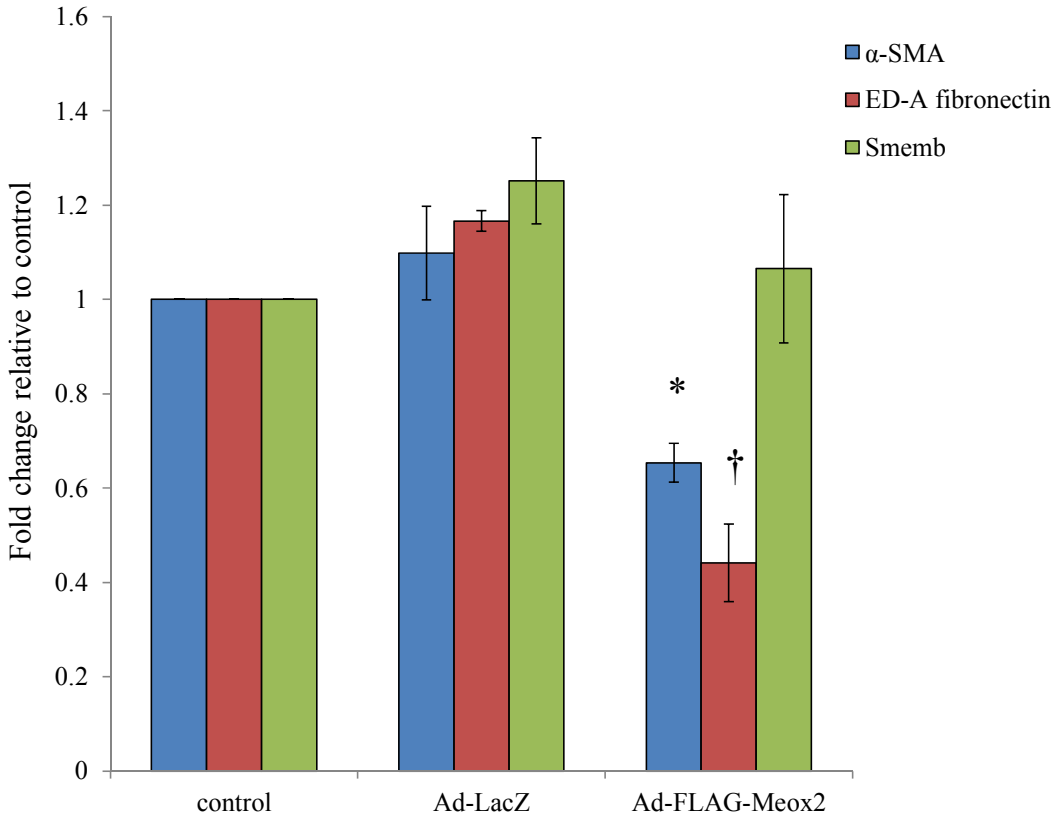

10. Mechanism for c-Ski mediated increase in Meox2 expression

A variety of mechanisms may be responsible for c-Ski induction of Meox2 mRNA expression, including direct binding of c-Ski to the Meox2 promoter and indirectly modulating Meox2 repressor proteins. To examine the possibility of indirect activation, we investigated the expression of Zeb2, a recently identified inhibitor of Meox2 [254]. Using Western blot analysis,we observed robust Zeb2 protein expression in uninfected and Ad-LacZ infected myofibroblasts. However, individual overexpression of c-Ski and Meox2 induced a significant reduction in Zeb2 levels in P1 cells (Figure 18). These results indicate an indirect mechanism for c-Ski mediated increases in Meox2 mRNA expression. To date this is the first time c-Ski has been linked to Zeb2 protein expression and provides a novel mechanism for c-Ski mediated diminution of myofibroblast phenotype.

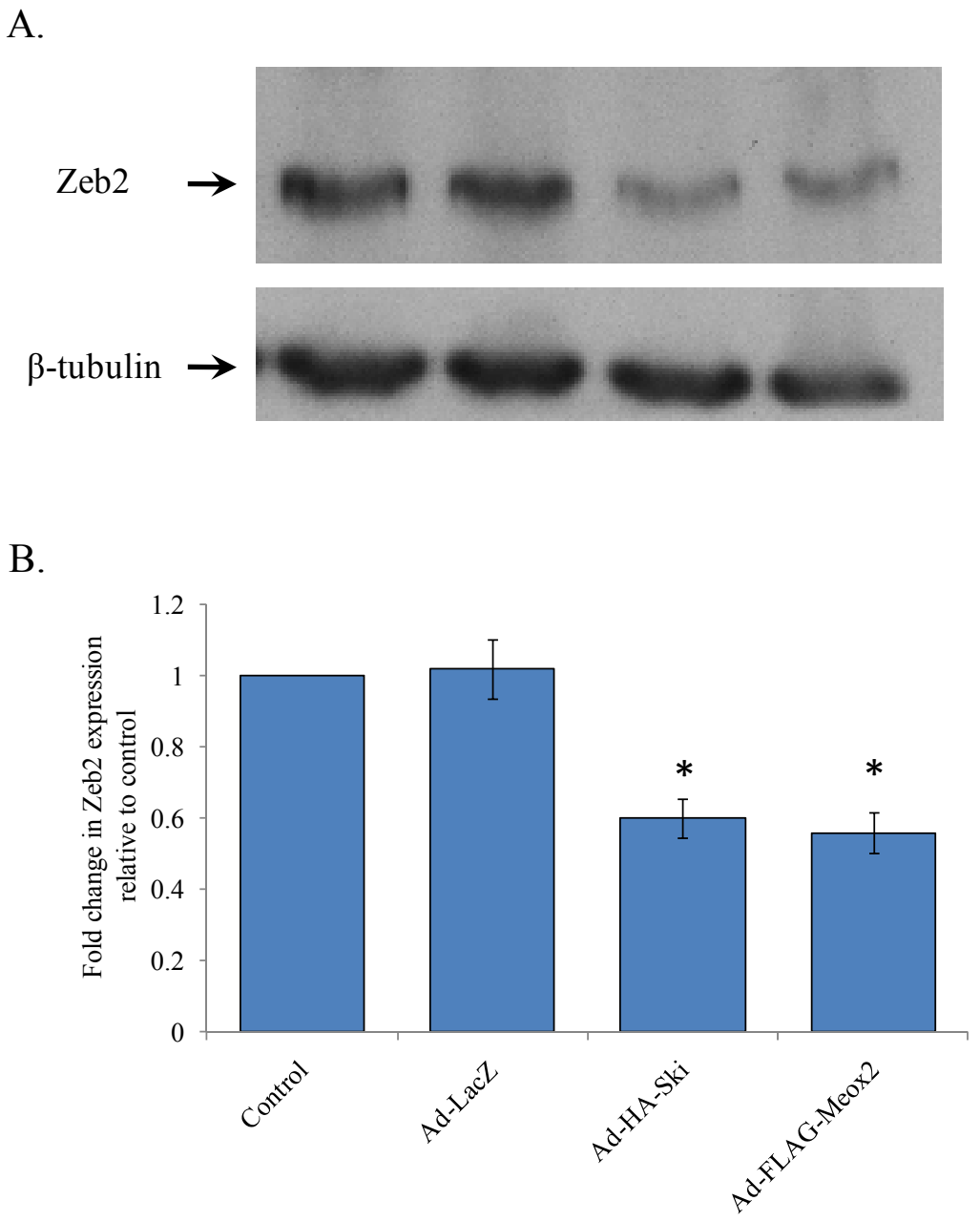

Figure 18. Overexpression of c-Ski or Meox2 reduces Zeb2 protein expression. P1 cardiac myofibroblasts were infected with Ad-LacZ (100 MOI), Ad-HA-Ski (50 MOI), Ad-FLAG-Meox2 (200 MOI). Uninfected cells were cultured as an additional control. Cells were allowed to grow in the presence of virus for 48 h before harvesting for Western blot analysis. Panel A, Total Zeb2 expression was examined using Western blot using β-tubulin antibody as a loading control. Panel B, Histographical representation of data obtained in (A). Image shown is representative of n=3 independent experiments. *P < 0.01 vs control values.

VI. Discussion

In this thesis, we have summarized our work that for the first time identifies a role for c-Ski protein in controlling the phenotype of primary cardiac myofibroblasts. Previous work in our lab has demonstrated a dramatic increase in cytosolic levels of c-Ski in post-MI infarct scar cardiac myofibroblasts beginning at 48 hours through 4 weeks post-MI (Figure 19) [267]. These data identified c-Ski as a potential target for study of cardiac remodeling following myocardial infarction. We have observed the three distinct forms of c-Ski expressed in cardiac myofibroblasts corresponding to 95, 105, and 115 kDa Western bands and we were able to overexpress the 95 kDa version with our adenoviral overexpression system. It has been suggested by others that alternate forms of c-Ski arise from differential phosphorylation of the 95 kDa form [17, 18]. We found that the main isoform in myofibroblast infected with adenoviral-c-Ski was the 95 kDa form. On the other hand, degradation of c-Ski occurs through a ubiquitin-mediated pathway via interaction with Arkadia [222]. Thus it is possible that the attachment of ubiquitin groups to the c-Ski protein may also account for one or more of the detected c-Ski forms. In addition the Ski-related novel protein (SnoN) has been shown to have many parallel functions with c-Ski [182, 268] and possesses small ubiquitin-like modifier-1 (SUMO-1) binding sites [269]. As SnoN and c-Ski are both structurally and functionally related it is possible that c-Ski sumoylation is partly responsible for one or more of the additional c-Ski bands detected by Western blotting. Whether sumoylation of Ski has any effect on Ski function is unclear. However Wrighton and coworkers found that sumoylation of SnoN does not affect its TGF-β inhibitory potential [269]. Although we are not increasing

the levels of the most common form of cellular c-Ski, the fundamental functional differences between 95 and 105 kDa c-Ski may be minimal. Nonetheless this suggestion is purely speculative and requires further study. The 105 kDa form appears as the most prominent form of c-Ski in normal preparations in our hands and we assume that the Ski protein at this band may be modified with one or more of these post-translational changes. Adenoviral overexpression of c-Ski induced overexpression of (apparently) unmodified c-Ski and this protein significantly altered the function and phenotype of primary cardiac myofibroblasts. That there was no detectable increase in 105 kDa c-Ski may signify that the enzyme(s) responsible for post-translational modification of c-Ski are rate limiting factors and the addition of exogenous c-Ski therefore created a cellular excess of c-Ski available for modification without the mechanisms to do so. An alternate hypothesis to post-translational modification of c-Ski is that we may be observing alternative splicing [195, 196]. Early studies with c-Ski identified three alternative splice variants [195]. Differences in sub-nuclear localizations were evident between the different forms [195], however the implications of this finding have not been explored. Experiments with truncated versions of the full length c-Ski cDNA showed equal effectiveness at inducing morphological transformation of chicken embryo fibroblasts and induction of muscle in cells from quail embryo [270]. While the functions of each different form of c-Ski remain unclear, we have identified numerous effects of 95 kDa c-Ski on cardiac myofibroblast phenotype and function.

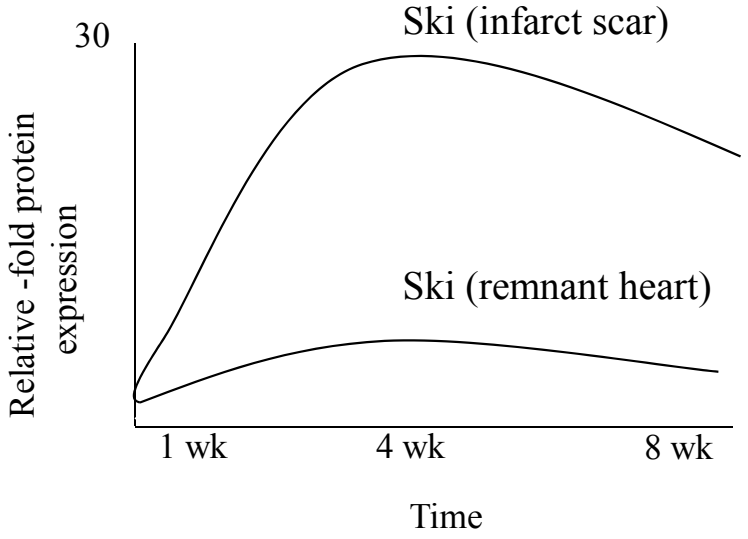

Figure 19. c-Ski expression in post-MI rat heart. Schematic representation of 105 kDa c-Ski expression in cytosolic fraction of cells in post-MI rat heart: infarct scar (myofibroblasts) and remnant heart.

It is well known that cardiac myofibroblasts deposit extracellular matrix proteins (namely fibrillar collagens) following MI and that the overexpression and net accumulation of these proteins in both the damaged myocardium and in the extracellular space of the noninfarcted myocardium results in overt cardiac fibrosis and heart failure [41, 43, 44, 85-87]. Furthermore, induction of collagen secretion is in large part due to chronically elevated TGF-β [146]. One of the main findings of the current work was that adenoviral overexpression of 95 kDa c-Ski was linked to the inhibition of collagen synthesis and secretion in primary cardiac myofibroblasts. This effect was observed in both unstimulated and TGF-β_1 stimulated cells. Thus we have identified c-Ski as a potential therapeutic target for treatment of a variety of etiologies of heart disease associated with cardiac fibrosis. As specific antifibrotic therapies for cardiac fibrosis are currently lacking within the armament of clinical therapy, the ability of c-Ski to directly modulate collagen

synthesis and secretion by myofibroblasts is clincally relevant. We suggest that c-Ski targeted treatment post-MI, as well as inclusion in the arsenal of therapies for hypertension and diabetes (and other etiologies) may represent a potential method to delay/prevent cardiac fibrosis and heart failure in these disease states.

Scar contracture is mediated by cardiac myofibroblasts [271]. Myofibroblast contraction may be regulated through a range of mechanisms including Ca^{2+} signalling [112], Rho/ROCK signalling and α-SMA expression [106, 272]. Our results show that c-Ski is able to inhibit myofibroblast contraction in both unstimulated and TGF-β_1 stimulated cells. This result may be due in part to a reduced expression of α-SMA observed in Ad-HA-Ski infected cells (Figure 11). Alternatively, basal inhibition of contraction in c-Ski overexpressing cells may signal an effect of c-Ski on isometric tension generated by myofibroblasts. Castella *et al*. have proposed that Rho/ROCK signalling influences isometric tension in myofibroblasts [107], thus c-Ski induced inhibition of myofibroblast contraction in unstimulated cells may signify an effect of c-Ski on the kinases regulating isometric tension within these cells. TGF-β_1 induces collagen gel contraction *in vitro* [273], an effect we observed in our uninfected and Ad-LacZ infected control samples. However, c-Ski overexpressing cells exhibited minimal changes in contraction under the same conditions. The differences between uninfected, Ad-LacZ and Ad-HA-Ski infected cells cannot be attributed to inhibition of isometric tension alone. As TGF-β induces the expression of α-SMA [261, 274] and α-SMA is directly related to myofibroblast contraction [106, 272], reduction of α-SMA levels in c-Ski overexpressing cells may be the mechanism for reduced myofibroblast contraction under TGF-β_1 stimulation. These data demonstrate that c-Ski is a powerful inhibitor of TGF-β mediated effects.

c-Ski has been characterized as an inhibitor of TGF-β signaling [19, 169] yet there is some debate as to the precise mechanisms involved in c-Ski mediated inhibition. Suzuki *et al.* have proposed a "Smad trapping" mechanism whereby nuclear c-Ski binds to phosphorylated R-Smad and Co-Smad4 on DNA creating a stable inactive complex thereby preventing transcription of TGF-β target genes [26]. Ferrand *et al.* have shown that c-Ski may bind the TGF-β type I receptor with R-Smad and Smad4 forming an inactivated complex that prevents nuclear translocation of the R-Smad/Smad4 complex [27]. In addition, the novel protein C184M may bind c-Ski and co-localize to the cytoplasm to inhibit R-Smad/Smad4 nuclear translocation [170]. We have shown that overexpressed 95 kDa c-Ski is nuclear (Figure 4) and that this exogenous c-Ski does not inhibit P-Smad2 nuclear translocation (Figure 9). Therefore the mechanism of 95 kDa c-Ski function in P1 cardiac myofibroblasts is likely through sequestration of P-Smad2 in the nucleus (Figure 20). The data presented herein identifies a nuclear mechanism for 95 kDa c-Ski but does not distinguish between P-Smad2 trapping in association with DNA or simply within the nuclear membrane (Figure 20). However, taken with other studies, our results support Suzuki's Smad trapping model. A confirmation of this hypothesis in our cells could be achieved by studying the DNA binding ability of the c-Ski/P-Smad2 complex in cardiac myofibroblasts. We have not examined the binding ability of c-Ski and non-phosphorylated Smad2 in our study, however this experiment may help further define the role of c-Ski in the TGF-β_1 pathway. Each form of c-Ski may act differentially to inhibit TGF-β and specific mechanisms involved likely depend on the cell type being studied. In addition, the majority of literature to date does not distinguish the form of c-Ski involved.

We have observed a nuclear function for 95 kDa c-Ski, however, 105 and 115 kDa c-Ski may function in either or both the nucleus and cytoplasm.

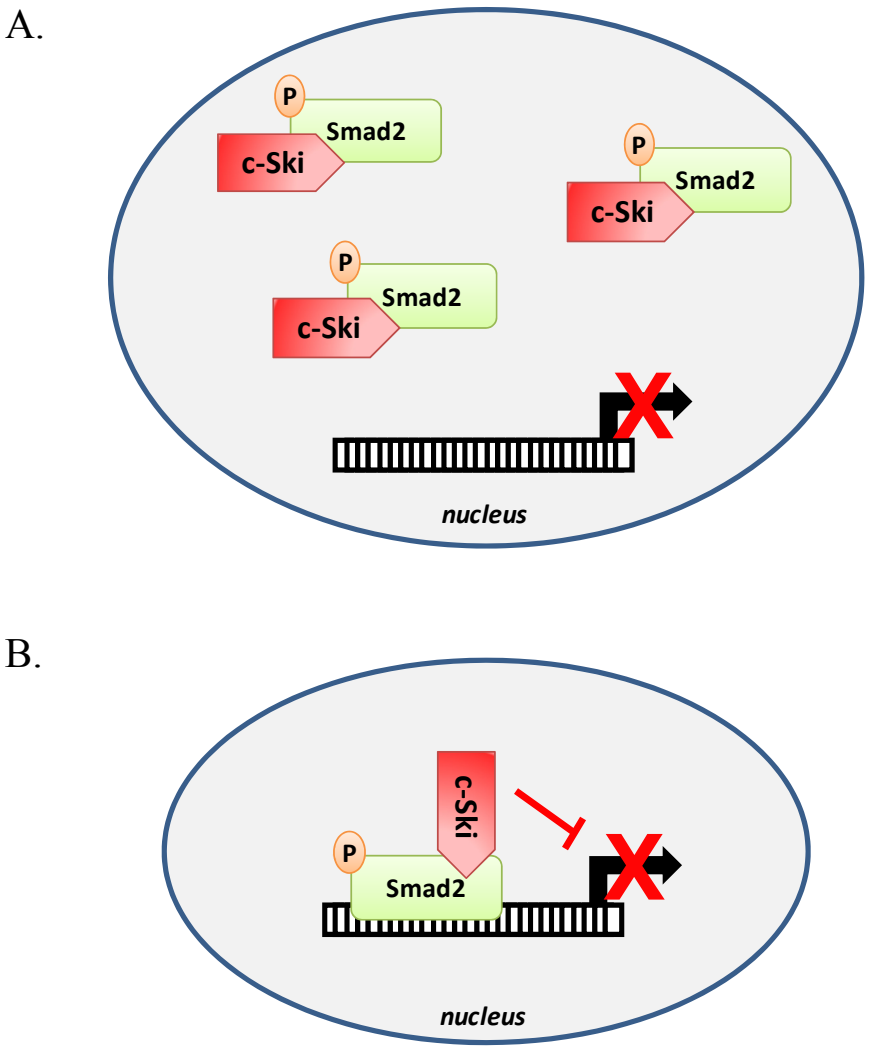

Figure 20. **Putative mechanism for 95 kDac-Ski mediated inhibition of TGF-β_1 in cardiac myofibroblasts**. Our results indicate a nuclear mechanism for 95 kDa c-Ski mediated repression of TGF-β_1. Panel A, c-Ski may inhibit TGF-β_1 signaling by sequestering P-Smad2 in the nucleus .Panel B, c-Ski may also inhibit TGF-β_1 through inactivation of P-Smad2/Co-Smad4 complexes on DNA thereby preventing transcriptional activation.

Classical definitions of c-Ski describe a nuclear localization [19, 212], while more recent work demonstrates cytosolic localization [27, 209]. We observed diffuse total cellular staining of c-Ski in unstimulated and TGF-β_1 stimulated cells at early time points (0-12 hours) and nuclear c-Ski accumulation occurred following 24 hours of stimulation (Figure 8). Unstimulated cells were not assayed under the same conditions to serve as a control for this experiment however this research is ongoing and will be completed by our lab in the near future. Nevertheless, this finding may signify a delayed negative feedback mechanism similar to the more rapid I-Smad7 activation. Whereas I-Smad7 shifts from a nuclear to cytosolic localization, c-Ski works in reverse, suggesting c-Ski may reside in the cytoplasm in the form of a latent cellular pool – ready for activation under strong stimulus. As we observe 105 kDa c-Ski most prominently in cardiac myofibroblasts, this nuclear c-Ski accumulation may be attributed to the 105 kDa form. This result, taken together with the *in vivo* finding of cytosolic c-Ski accumulation in post-MI infarct scar [267], may signify a malfunction in the TGF-β inhibitory functions of c-Ski post-MI through as yet undefined mechanisms. I-Smad7 expression is reduced in post-MI scar tissue [61] while R-Smad expression is increased in these tissues [43] demonstrating an imbalance in antifibrotic/profibrotic signals. That c-Ski is a potent antifibrotic and is increased in cytosolic fraction of infarct scar [267] without a reduction in collagen production [43] indicates that this cytosolic c-Ski may not be inhibitory under such conditions. As Hao *et al*. have demonstrated a reduction in TβRI expression in infarct scar [43] and c-Ski may function through binding to this receptor [27] it is possible that c-Ski is concentrated into the cytoplasm due to undescribed stimuli where it is no longer able to

efficiently function. A clearer understanding of the mechanisms regulating c-Ski localization is necessary to ascertain the function of c-Ski in the post-MI heart.

Cardiac fibroblast to myofibroblast phenoconversion is characterized by the *de novo* expression of α-SMA [265], ED-A fibronectin [266] and SMemb [275] as well as increased expression of fibrillar collagens [9] and contractile ability [276]. We observed a reduction in myofibroblast function as well as phenotypic markers α-SMA and ED-A fibronectin. As these are all known "hallmarks" of myofibroblasts, we suggest that c-Ski is able to induce a diminution of myofibroblastic phenotype into a more fibroblastic one. While we have also observed an induction of apoptosis with c-Ski overexpression, phenotyping data was adjusted for equal loading of protein to rule out changes due to cell viability. As myofibroblasts remain in the healed infarct scar months and years after the initial insult [7] and as these cells maintain excessive extracellular matrix proteins over this time period, the ability to modulate cardiac myofibroblast function and phenotype is of great therapeutic value in treating cardiac fibrosis and heart failure [9].

We have also begun to elucidate a potential mechanism, through induction of Meox2 expression, for c-Ski induced myofibroblast dedifferentiation. Others have shown that cardiac fibroblast to myofibroblast phenoconversion is associated with a dramatic decrease of Meox1 and Meox2 mRNA expression (J. Douville and J. Wigle unpublished data) suggesting that these proteins function to maintain the fibroblastic phenotype. The loss of these homeodomain proteins may "release the brakes" and allow the progression of fibroblasts into myofibroblasts. We have shown that c-Ski overexpression induces a diminution in myofibroblastic phenotype and is associated with an increase in Meox2

mRNA expression (Figure 16). Thus c-Ski may serve to "re-apply the brake" to the cell cycle and cell differentiation pushing cells into a proto-myofibroblast, or more fibroblastic, phenotype. Through overexpression of Meox2 we observed a similar diminution in myofibroblastic phenotype (as with c-Ski overexpression). Thus we have identified a putative mechanism for c-Ski induced reductions of myofibroblast markers (Figure 20). Meox2 expression levels may be regulated by the Zeb2 protein such that high levels of Zeb2 results in repression of Meox2 and expression of the Zeb2 protein may be regulated by microRNA-221 [254]. We demonstrated a reduction in Zeb2 with overexpression of either c-Ski or Meox2 (Figure 18), thereby identifying a putative mechanism for c-Ski induction of Meox2 (Figure 21). Given that Zeb2 may be regulated by microRNA-221 [254], a future study of this mechanism should include the effects of c-Ski on microRNA-221 expression. Simultaneous c-Ski overexpression and silencing of Zeb2 would confirm this link. Similarly, simultaneous c-Ski overexpression and ablation of Meox2 would determine a direct or indirect effect on myofibroblast phenotype. Thus in the context of our observations, c-Ski may either be acting directly on Meox2 gene expression or through decreasing Zeb2 to increase levels of Meox2. It also cannot be discounted that c-Ski utilizes multiple mechanisms, including Meox2 upregulation, to diminish myofibroblast phenotype as c-Ski induces a relatively small increase of 6-fold of Meox2 mRNAexpression compared to the near 20-fold reduction in expression observed in P0-P1 fibroblast to myofibroblast differentiation. This observation may also account for the lesser degree of myofibroblast diminution in Meox2 overexpressing cells compared with c-Ski overexpressing cells. Regardless, further work needs to be done to

determine the extent of myofibroblast reversion due to c-Ski overexpression, i.e. migratory potential and other markers of phenotype.

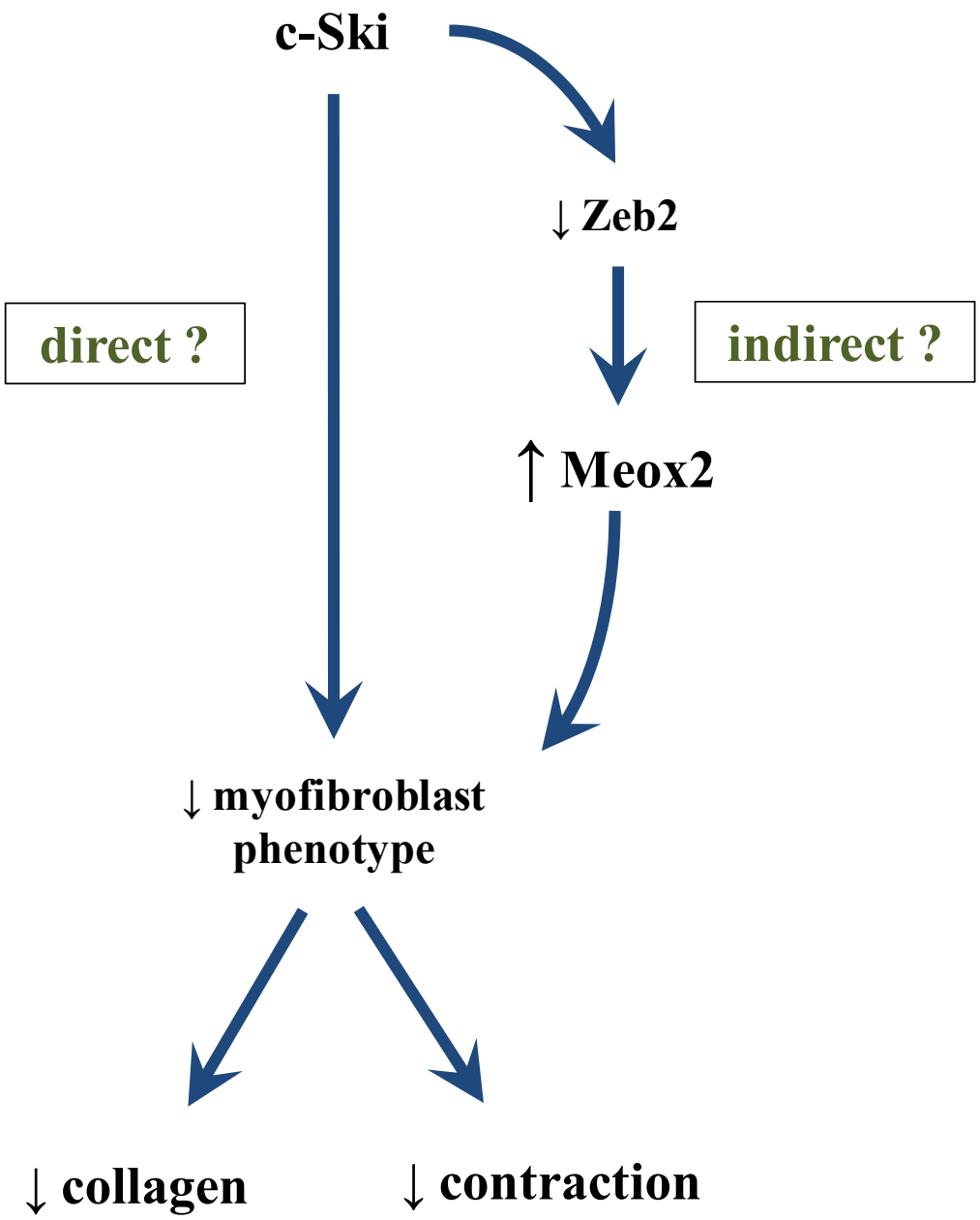

Figure 21. **Putative mechanism for c-Ski modulation of myofibroblast phenotype and function**. c-Ski may signal directly, or through upregulation of Meox2, to modulate myofibroblast phenotype.

There is debate as to the effects of c-Ski overexpression on cell viability. Some have observed significant increases in apoptosis with c-Ski knockout in the cranial neuroepithelium thereby linking loss of c-Ski with a reduction in cell viability [21], whereas others have linked increased levels of c-Ski to apoptosis of granulosa cells [224]. In addition, c-Ski overexpression has displayed an anti-apoptotic effect in skin cells [225] and a hypertrophic response in skeletal muscle [270]. These studies suggest that the apoptotic effects of c-Ski are likely concentration dependent and cell type specific. Although we have shown an increase in apoptosis with high levels of c-Ski overexpression under starvation conditions (Figure 15), the effect of lower concentrations, e.g. lower MOI, may yield different effects. Our data indicate that c-Ski may play a role in cell death when myofibroblasts are under stressed conditions, however the propidium iodide staining and MTT assays used in our studies to detect apoptosis may mask a possible autophagic response. Autophagy is a process whereby intracellular proteins are sequestered for degradation in autophagosomes and can promote cell survival or induce apoptosis depending on the stimuli [277-279]. Under starvation conditions, high levels of c-Ski may function though autophagic pathways to "tip the balance" in favour of apoptosis or survival which could not be detected in our assays. Further investigation of autophagy, using protein markers, e.g. LC3, is recommended to explore this possibility. The conflicting cell viability effects between this study and other findings likely result from cell type specific effects, culture conditions, as well as c-Ski concentration specific effects.

VII. Conclusions and future directions

In summary, our results show that 95 kDa nuclear c-Ski is a powerful regulating factor in a variety of cardiac myofibroblast cell processes, including collagen synthesis/secretion, contraction, differentiation and apoptosis. Through our mechanistic study, our data supports a nuclear function for 95 kDa c-Ski through "Smad-trapping" to inhibit TGF-β_1, however, experiments showing the c-Ski/P-Smad2 complex bound to DNA would provide definitive evidence supporting Suzuki *et al.*'s hypothesis. While further research into the mechanism of c-Ski function is required, we believe that c-Ski may be an important therapeutic target for the treatment of cardiac fibrosis and potentially other fibrotic diseases. As we have shown c-Ski's ability to inhibit collagen synthesis and secretion, a natural extension of this study is to test for MMP activation. To confirm and enhance our findings, knockout studies of c-Ski would be useful in clarifying its role in myofibroblast phenotype and function. Further elucidation of the mechanism of c-Ski effects through Meox2 upregulation could be described with combined c-Ski overexpression and Meox2 ablation. Investigation of the mechanism for c-Ski mediated inhibition of myofibroblast contraction through Rho/ROCK or calcium signaling would be of great value in demonstrating the role of these pathways in myofibroblast contraction. In addition, in light of the potential role for c-Ski in cell death, in depth studies using c-Ski overexpression on the induction of cell death through apoptosis/autophagy would yield novel findings and help to describe the role of c-Ski *in vivo*. Once the mechanisms of c-Ski function have been further characterized *in vitro*, this knowledge could be used for *in vivo* studies with infarct scar targeted overexpression/knockdown of c-Ski post-MI via intracardiac injection.. These studies

would reveal the therapeutic potential of c-Ski in preventing cardiac fibrosis and delaying the onset of heart failure.

VIII. References

1. Mathers CD, Boerma T, Ma Fat D. Global and regional causes of death. *Br Med Bull*. 2009;92:7-32
2. Roger VL, Go AS, Lloyd-Jones DM, Adams RJ, Berry JD, Brown TM, Carnethon MR, Dai S, de Simone G, Ford ES, Fox CS, Fullerton HJ, Gillespie C, Greenlund KJ, Hailpern SM, Heit JA, Ho PM, Howard VJ, Kissela BM, Kittner SJ, Lackland DT, Lichtman JH, Lisabeth LD, Makuc DM, Marcus GM, Marelli A, Matchar DB, McDermott MM, Meigs JB, Moy CS, Mozaffarian D, Mussolino ME, Nichol G, Paynter NP, Rosamond WD, Sorlie PD, Stafford RS, Turan TN, Turner MB, Wong ND, Wylie-Rosett J. Heart disease and stroke statistics--2011 update: A report from the american heart association. *Circulation*. 2011;123:e18-e209
3. Statistics_Canada. Mortality, summary, list of causes - 2006. 2010;Catalogue #84F0209X
4. Leal J, Luengo-Fernandez R, Gray A, Petersen S, Rayner M. Economic burden of cardiovascular diseases in the enlarged european union. *Eur Heart J*. 2006;27:1610-1619
5. Wielgosz A, Arango, M., Bancej, C., Bienek, A., Johansen, H., Lindsay, P., Luo, W., Luteyn, A., Nair, C., Quan, P., Stewart, P., Walsh, P., Webster, G. Tracking heart and stroke in canada. 2009
6. WHO. Cardiovascular diseases - fact sheet #317. 2011
7. Willems IE, Havenith MG, De Mey JG, Daemen MJ. The alpha-smooth muscle actin-positive cells in healing human myocardial scars. *Am J Pathol*. 1994;145:868-875

8. Cleutjens JP, Blankesteijn WM, Daemen MJ, Smits JF. The infarcted myocardium: Simply dead tissue, or a lively target for therapeutic interventions. *Cardiovasc Res*. 1999;44:232-241

9. Cleutjens JP, Verluyten MJ, Smits JF, Daemen MJ. Collagen remodeling after myocardial infarction in the rat heart. *Am J Pathol*. 1995;147:325-338

10. Holmes JW, Nunez JA, Covell JW. Functional implications of myocardial scar structure. *Am J Physiol*. 1997;272:H2123-H2130

11. Weber KT. Fibrosis, a common pathway to organ failure: Angiotensin ii and tissue repair. *Semin Nephrol*. 1997;17:467-491

12. Thum T, Gross C, Fiedler J, Fischer T, Kissler S, Bussen M, Galuppo P, Just S, Rottbauer W, Frantz S, Castoldi M, Soutschek J, Koteliansky V, Rosenwald A, Basson MA, Licht JD, Pena JT, Rouhanifard SH, Muckenthaler MU, Tuschl T, Martin GR, Bauersachs J, Engelhardt S. Microrna-21 contributes to myocardial disease by stimulating map kinase signalling in fibroblasts. *Nature*. 2008;456:980-984

13. Li Y, Turck CM, Teumer JK, Stavnezer E. Unique sequence, ski, in sloan-kettering avian retroviruses with properties of a new cell-derived oncogene. *J Virol*. 1986;57:1065-1072

14. Ludolph DC, Neff AW, Parker MA, Mescher AL, Smith RC, Malacinski GM. Cloning and expression of the axolotl proto-oncogene ski. *Biochim Biophys Acta*. 1995;1260:102-104

15. Nomura N, Sasamoto S, Ishii S, Date T, Matsui M, Ishizaki R. Isolation of human cdna clones of ski and the ski-related gene, sno. *Nucleic Acids Res.* 1989;17:5489-5500

16. Sleeman JP, Laskey RA. Xenopus c-ski contains a novel coiled-coil protein domain, and is maternally expressed during development. *Oncogene*. 1993;8:67-77

17. Sutrave P, Copeland TD, Showalter SD, Hughes SH. Characterization of chicken c-ski oncogene products expressed by retrovirus vectors. *Mol Cell Biol*. 1990;10:3137-3144

18. Nagata M, Nagata S, Yuki K, Isogaya K, Saitoh M, Miyazono K, Miyazawa K. Identification of a phosphorylation site in c-ski as serine 515. *J Biochem*. 2010

19. Akiyoshi S, Inoue H, Hanai J, Kusanagi K, Nemoto N, Miyazono K, Kawabata M. C-ski acts as a transcriptional co-repressor in transforming growth factor-beta signaling through interaction with smads. *J Biol Chem*. 1999;274:35269-35277

20. Atanasoski S, Notterpek L, Lee HY, Castagner F, Young P, Ehrengruber MU, Meijer D, Sommer L, Stavnezer E, Colmenares C, Suter U. The protooncogene ski controls schwann cell proliferation and myelination. *Neuron*. 2004;43:499-511

21. Berk M, Desai SY, Heyman HC, Colmenares C. Mice lacking the ski proto-oncogene have defects in neurulation, craniofacial, patterning, and skeletal muscle development. *Genes Dev.* 1997;11:2029-2039

22. Bowen RA, Reed ML, Schnieke A, Seidel GE, Jr., Stacey A, Thomas WK, Kajikawa O. Transgenic cattle resulting from biopsied embryos: Expression of c-ski in a transgenic calf. *Biol Reprod*. 1994;50:664-668

23. Leferovich JM, Lana DP, Sutrave P, Hughes SH, Kelly AM. Regulation of c-ski transgene expression in developing and mature mice. *J Neurosci*. 1995;15:596-603

24. Claycomb WC, Lanson NA, Jr. Proto-oncogene expression in proliferating and differentiating cardiac and skeletal muscle. *Biochem J*. 1987;247:701-706

25. Evans RA, Tian YC, Steadman R, Phillips AO. Tgf-beta1-mediated fibroblast-myofibroblast terminal differentiation-the role of smad proteins. *Exp Cell Res*. 2003;282:90-100

26. Suzuki H, Yagi K, Kondo M, Kato M, Miyazono K, Miyazawa K. C-ski inhibits the tgf-beta signaling pathway through stabilization of inactive smad complexes on smad-binding elements. *Oncogene.* 2004;23:5068-5076

27. Ferrand N, Atfi A, Prunier C. The oncoprotein c-ski functions as a direct antagonist of the transforming growth factor-{beta} type i receptor. *Cancer Res*. 2010;70:8457-8466

28. Gonzalez-Vilchez F, Ayuela J, Ares M, Pi J, Castillo L, Martin-Duran R. Oxidative stress and fibrosis in incipient myocardial dysfunction in type 2 diabetic patients. *Int J Cardiol*. 2005;101:53-58

29. Ihm SH, Youn HJ, Shin DI, Jang SW, Park CS, Kim PJ, Kim HY, Chang K, Seung KB, Kim JH, Choi KB. Serum carboxy-terminal propeptide of type i procollagen (pip) is a marker of diastolic dysfunction in patients with early type 2 diabetes mellitus. *Int J Cardiol*. 2007;122:e36-38

30. Gonzalez A, Lopez B, Querejeta R, Diez J. Regulation of myocardial fibrillar collagen by angiotensin ii. A role in hypertensive heart disease? *J Mol Cell Cardiol*. 2002;34:1585-1593

31. Pelouch V, Dixon IM, Sethi R, Dhalla NS. Alteration of collagenous protein profile in congestive heart failure secondary to myocardial infarction. *Mol Cell Biochem*. 1993;129:121-131

32. Devereux RB, Roman MJ, Paranicas M, O'Grady MJ, Lee ET, Welty TK, Fabsitz RR, Robbins D, Rhoades ER, Howard BV. Impact of diabetes on cardiac structure and function: The strong heart study. *Circulation*. 2000;101:2271-2276

33. Pick R, Janicki JS, Weber KT. Myocardial fibrosis in nonhuman primate with pressure overload hypertrophy. *Am J Pathol*. 1989;135:771-781

34. Colucci WS, Braunwald E. Pathophysiology of heart failure. In: Braunwald E, ed. *Heart disease*. Philadelphia: W.B.Saunders Company; 1997:394-420.

35. Kannel WB. Epidemiology of heat failure in the united states. In: Poole-Wilson PA, Colucci WS, Massie BM, Chatterjee K, Coats AJS, eds. *Heart failure*. New York: Churchill Livingstone; 1997:279-288.

36. Mettauer B, Zoll J, Garnier A, Ventura-Clapier R. Heart failure: A model of cardiac and skeletal muscle energetic failure. *Pflugers Arch.* 2006;.

37. Saha M, Ferro A. Cardiac stem cell therapy: Present and future. *Br J Clin Pharmacol*. 2006;61:727-729

38. Wollert KC, Drexler H. Clinical applications of stem cells for the heart. *Circ Res*. 2005;96:151-163

39. Nian M, Lee P, Khaper N, Liu P. Inflammatory cytokines and postmyocardial infarction remodeling. *Circ Res*. 2004;94:1543-1553

40. Pfeffer JM, Pfeffer MA. Angiotensin converting enzyme inhibition and ventricular remodeling in heart failure. *Am J Med*. 1988;84:37-44

41. Ju H, Zhao S, Jassal DS, Dixon IM. Effect of at1 receptor blockade on cardiac collagen remodeling after myocardial infarction. *Cardiovasc Res*. 1997;35:223-232

42. Peterson DJ, Ju H, Jianming Hao PM, Chapman D, Dixon IMC. Expression of gia2 and gsa in myofibroblasts localized to the infarct scar in heart failure due to myocardial infarction. *Cardiovasc Res*. 1998;41:575-585

43. Hao J, Ju H, Zhao S, Junaid A, Scammell-LaFleur T, Dixon IM. Elevation of expression of smads 2, 3, and 4, decorin and tgf-beta in the chronic phase of myocardial infarct scar healing. *J Mol Cell Cardiol*. 1999;31:667-678

44. Dixon IMC, Hao J, Reid NL, Roth M. Effect of chronic at1 receptor blockade on cardiac smad overexpression in hereditary cardiomyopathic hamsters. *Cardiovasc Res*. 2000;46:286-297

45. Haunstetter A, Izumo S. Apoptosis: Basic mechanisms and implications for cardiovascular disease. *Circ Res*. 1998;82:1111-1129

46. Cleutjens JP, Kandala JC, Guarda E, Guntaka RV, Weber KT. Regulation of collagen degradation in the rat myocardium after infarction. *J Mol Cell Cardiol*. 1995;27:1281-1292

47. Holmes JW, Borg TK, Covell JW. Structure and mechanics of healing myocardial infarcts. *Annu Rev Biomed Eng*. 2005;7:223-253

48. Desmouliere A, Redard M, Darby I, Gabbiani G. Apoptosis mediates the decrease in cellularity during the transition between granulation tissue and scar. *Am J Pathol*. 1995;146:56-66

49. Weber KT, Brilla CG. Pathological hypertrophy and cardiac interstitium. Fibrosis and renin- angiotensin-aldosterone system. *Circulation*. 1991;83:1849-1865

50. Chang HY, Chi JT, Dudoit S, Bondre C, van de RM, Botstein D, Brown PO. Diversity, topographic differentiation, and positional memory in human fibroblasts. *Proc Natl Acad Sci USA*. 2002;99:12877-12882

51. Gabbiani G, Hirschel BJ, Ryan GB, Statkov PR, Majno G. Granulation tissue as a contractile organ. A study of structure and function. *J Exp Med*. 1972;135:719-734

52. Ryan GB, Cliff WJ, Gabbiani G, Irle C, Montandon D, Statkov PR, Majno G. Myofibroblasts in human granulation tissue. *Hum Pathol*. 1974;5:55-67

53. McCulloch CA, Bordin S. Role of fibroblast subpopulations in periodontal physiology and pathology. *J Periodontal Res*. 1991;26:144-154

54. Fries KM, Blieden T, Looney RJ, Sempowski GD, Silvera MR, Willis RA, Phipps RP. Evidence of fibroblast heterogeneity and the role of fibroblast subpopulations in fibrosis. *Clin Immunol Immunopathol*. 1994;72:283-292

55. Torry DJ, Richards CD, Podor TJ, Gauldie J. Anchorage-independent colony growth of pulmonary fibroblasts derived from fibrotic human lung tissue. *J Clin Invest*. 1994;93:1525-1532

56. Sun Y. Local angiotensin ii and myocardial fibrosis. In: Zanchetti, et al., eds. *Hypertension and the heart*. New York, NY: Plenum Press; 1997:55-61.

57. Powell DW, Mifflin RC, Valentich JD, Crowe SE, Saada JI, West AB. Myofibroblasts. I. Paracrine cells important in health and disease. *Am J Physiol*. 1999;277:C1-C9

58. Eghbali M, Czaja MJ, Zeydel M, Weiner FR, Zern MA, Seifter S, Blumenfeld OO. Collagen chain mrnas in isolated heart cells from young and adult rats. *J Mol Cell Cardiol*. 1988;20:267-276

59. Frangogiannis NG, Smith CW, Entman ML. The inflammatory response in myocardial infarction. *Cardiovasc Res*. 2002;53:31-47

60. Hao J, Wang B, Jones SC, Jassal DS, Dixon IMC. Interaction between angiotensin ii and smad proteins in fibroblasts in failing heart and in vitro. *Am.J Physiol*. 2000;279:H3020-H3030

61. Wang B, Hao J, Jones SC, Yee MS, Roth JC, Dixon IM. Decreased smad 7 expression contributes to cardiac fibrosis in the infarcted rat heart. *Am J Physiol Heart Circ Physiol*. 2002;282:H1685-H1696

62. Sun Y, Cleutjens JP, Diaz-Arias AA, Weber KT. Cardiac angiotensin converting enzyme and myocardial fibrosis in the heart. *Cardiovasc Res*. 1994;28:1423-1432

63. Sun Y, Weber KT. Angiotensin ii receptor binding following myocardial infarction in the rat. *Cardiovasc Res*. 1994;28:1623-1628

64. Hildebrand A, Romaris M, Rasmussen LM, Heinegard D, Twardzik DR, Border WA, Ruoslahti E. Interaction of the small interstitial proteoglycans biglycan, decorin and fibromodulin with transforming growth factor beta. *Biochem J*. 1994;302:527-534

65. Dugina V, Fontao L, Chaponnier C, Vasiliev J, Gabbiani G. Focal adhesion features during myofibroblastic differentiation are controlled by intracellular and extracellular factors. *J Cell Sci*. 2001;114:3285-3296

66. Masur SK, Dewal HS, Dinh TT, Erenburg I, Petridou S. Myofibroblasts differentiate from fibroblasts when plated at low density. *Proc Natl Acad Sci USA*. 1996;93:4219-4223

67. Gabbiani G. The cellular derivation and the life span of the myofibroblast. *Pathol Res Pract*. 1996;192:708-711

68. Etoh T, Joffs C, Deschamps AM, Davis J, Dowdy K, Hendrick J, Baicu S, Mukherjee R, Manhaini M, Spinale FG. Myocardial and interstitial matrix metalloproteinase activity after acute myocardial infarction in pigs. *Am.J Physiol Heart Circ.Physiol*. 2001;281:H987-H994

69. Guo C, Piacentini L. Type i collagen-induced mmp-2 activation coincides with up-regulation of membrane type 1-matrix metalloproteinase and timp-2 in cardiac fibroblasts. *J Biol Chem*. 2003;278:46699-46708

70. Stawowy P, Margeta C, Kallisch H, Seidah NG, Chretien M, Fleck E, Graf K. Regulation of matrix metalloproteinase mt1-mmp/mmp-2 in cardiac fibroblasts by tgf-beta1 involves furin-convertase. *Cardiovasc Res*. 2004;63:87-97

71. Willis BC, Liebler JM, Luby-Phelps K, Nicholson AG, Crandall ED, du Bois RM, Borok Z. Induction of epithelial-mesenchymal transition in alveolar epithelial cells by transforming growth factor-beta1: Potential role in idiopathic pulmonary fibrosis. *American J Pathol*. 2005;166:1321-1332

72. van Tuyn J, Atsma DE, Winter EM, van der Velde-van Dijke I, Pijnappels DA, Bax NA, Knaan-Shanzer S, Gittenberger-de Groot AC, Poelmann RE, van der Laarse A, van der Wall EE, Schalij MJ, de Vries AA. Epicardial cells of human adults can undergo an epithelial-to-mesenchymal transition and obtain characteristics of smooth muscle cells in vitro. *Stem Cells*. 2007;25:271-278

73. Zhou B, von Gise A, Ma Q, Hu YW, Pu WT. Genetic fate mapping demonstrates contribution of epicardium-derived cells to the annulus fibrosis of the mammalian heart. *Dev biol*. 2010;338:251-261

74. Zeisberg EM, Tarnavski O, Zeisberg M, Dorfman AL, McMullen JR, Gustafsson E, Chandraker A, Yuan X, Pu WT, Roberts AB, Neilson EG, Sayegh MH, Izumo S, Kalluri R. Endothelial-to-mesenchymal transition contributes to cardiac fibrosis. *Nat Med*. 2007;13:952-961

75. Mollmann H, Nef HM, Kostin S, von Kalle C, Pilz I, Weber M, Schaper J, Hamm CW, Elsasser A. Bone marrow-derived cells contribute to infarct remodelling. *Cardiovasc Res*. 2006;71:661-671

76. van Amerongen MJ, Bou-Gharios G, Popa E, van Ark J, Petersen AH, van Dam GM, van Luyn MJ, Harmsen MC. Bone marrow-derived myofibroblasts contribute functionally to scar formation after myocardial infarction. *J Pathol*. 2008;214:377-386

77. Fujita J, Mori M, Kawada H, Ieda Y, Tsuma M, Matsuzaki Y, Kawaguchi H, Yagi T, Yuasa S, Endo J, Hotta T, Ogawa S, Okano H, Yozu R, Ando K, Fukuda K. Administration of granulocyte colony-stimulating factor after myocardial

infarction enhances the recruitment of hematopoietic stem cell-derived myofibroblasts and contributes to cardiac repair. *Stem Cells*. 2007;25:2750-2759

78. Caulfield JB, Borg TK. The collagen network of the heart. *Lab Invest*. 1979;40:364-372

79. Robinson TF, Factor SM, Sonnenblick EH. The heart as a suction pump. *Sci Am*. 1986;254:84-91

80. Robinson TF, Cohen-Gould L, Factor SM. Skeletal framework of mammalian heart muscle. Arrangement of inter- and pericellular connective tissue structures. *Lab Invest*. 1983;49:482-498

81. Birchmeier C, Birchmeier W. Molecular aspects of mesenchymal-epithelial interactions. *Annu Rev Cell Biol*. 1993;9:511-40:511-540

82. Simon-Assmann P, Kedinger M, De Arcangelis A, Rousseau V, Simo P. Extracellular matrix components in intestinal development. *Experientia*. 1995;51:883-900

83. Bashey RI, Martinez Hernandez A, Jimenez SA. Isolation, characterization, and localization of cardiac collagen type vi. Associations with other extracellular matrix components. *Circ Res*. 1992;70:1006-1017

84. Weber KT, Jalil JE, Janicki JS, Pick R. Myocardial collagen remodeling in pressure overload hypertrophy. A case for interstitial heart disease. *Am J Hypertens*. 1989;2:931-940

85. Ju H, Zhao S, Tappia PS, Panagia V, Dixon IMC. Expression of gqalpha and plc-beta in scar and border tissue in heart failure due to myocardial infarction. *Circulation*. 1998;97:892-899

86. Pelouch V, Dixon IM, Golfman L, Beamish RE, Dhalla NS. Role of extracellular matrix proteins in heart function. *Mol Cell Biochem*. 1993;129:101-120

87. Dixon IMC, Reid NL, Ju H. Angiotensin ii and tgf-b in the development of cardiac fibrosis, myocyte hypertrophy, and heart failure. *Heart Failure Reviews*. 1997;2:107-116

88. Makino N, Hata T, Sugano M, Dixon IMC, Yanaga T. Regression of hypertrophy after myocardial infarction is produced by the chronic blockade of angiotensin type 1 receptor in rats. *J Mol Cell Cardiol*. 1996;28:507-517

89. Jalil JE, Doering CW, Janicki JS, Pick R, Shroff SG, Weber KT. Fibrillar collagen and myocardial stiffness in the intact hypertrophied rat left ventricle. *Circ Res*. 1989;64:1041-1050

90. Thiedemann KU, Holubarsch C, Medugorac I, Jacob R. Connective tissue content and myocardial stiffness in pressure overload hypertrophy. A combined study of morphologic, morphometric, biochemical, and mechanical parameters. *Basic Res Cardiol*. 1983;78:140-155

91. Brown L. Cardiac extracellular matrix: A dynamic entity. *Am J Physiol Heart Circ Physiol*. 2005;289:H973-H974

92. Bartosova D, Chvapil M, Korecky B, Poupa O, Rakusan K, Turek Z, Vizek M. The growth of the muscular and collagenous parts of the rat heart in various forms of cardiomegaly. *J Physiol (Lond.)*. 1969;200:285-295

93. van Krimpen C, Schoemaker RG, Cleutjens JP, Smits JF, Struyker-Boudier HA, Bosman FT, Daemen MJ. Angiotensin i converting enzyme inhibitors and cardiac remodeling. *Basic Res Cardiol*. 1991;86 Suppl 1:149-55:149-155

94. Liu KZ, Jackson M, Sowa MG, Ju H, Dixon IMC, Mantsch HH. Modification of the extracellular matrix following myocardial infarction monitored by ftir spectroscopy. *Biochim Biophys Acta*. 1996;1315:73-77

95. Dixon IMC, Ju H, Jassal DS, Peterson DJ. Effect of ramipril and losartan on collagen expression in right and left heart after myocardial infarction. *Mol Cell Biochem*. 1996;165:31-45

96. Weber KT. Extracellular matrix remodeling in heart failure: A role for de novo angiotensin ii generation. *Circulation*. 1997;96:4065-4082

97. Dixon IMC, Ju H, Reid NL. The role of angiotensin ii in post-translational regulation of fibrillar collagens in fibrosed and failing rat heart. In: Dhalla NS, Zahradka P, Dixon IMC, Beamish RE, eds. *Angiotensin ii receptor blockade: Physiological and clinical implications*. Boston: Kluwer Academic Publishers; 1998:471-498.

98. Fishbein MC, Maclean D, Maroko PR. Experimental myocardial infarction in the rat: Qualitative and quantitative changes during pathologic evolution. *Am J Pathol*. 1978;90:57-70

99. Sun Y, Weber KT. Angiotensin converting enzyme and myofibroblasts during tissue repair in the rat heart. *J Mol Cell Cardiol*. 1996;28:851-858

100. Jugdutt BI, Amy RW. Healing after myocardial infarction in the dog: Changes in infarct hydroxyproline and topography. *J Am Coll Cardiol*. 1986;7:91-102

101. Santiago JJ, Dangerfield AL, Rattan SG, Bathe KL, Cunnington RH, Raizman JE, Bedosky KM, Freed DH, Kardami E, Dixon IM. Cardiac fibroblast to myofibroblast differentiation in vivo and in vitro: Expression of focal adhesion

components in neonatal and adult rat ventricular myofibroblasts. *Dev Dyn*. 2010;239:1573-1584

102. Serini G, Gabbiani G. Mechanisms of myofibroblast activity and phenotypic modulation. *Exp Cell Res*. 1999;250:273-283

103. Tomasek JJ, Gabbiani G, Hinz B, Chaponnier C, Brown RA. Myofibroblasts and mechano-regulation of connective tissue remodelling. *Nat Rev Mol Cell Biol*. 2002;3:349-363

104. Lijnen P, Petrov V, Fagard R. Transforming growth factor-beta 1-mediated collagen gel contraction by cardiac fibroblasts. *J Renin Angiotensin Aldosterone Syst*. 2003;4:113-118

105. Grinnell F. Fibroblasts, myofibroblasts, and wound contraction. *J Cell Biol*. 1994;124:401-404

106. Hinz B, Celetta G, Tomasek JJ, Gabbiani G, Chaponnier C. Alpha-smooth muscle actin expression upregulates fibroblast contractile activity. *Mol Biol Cell*. 2001;12:2730-2741

107. Castella LF, Buscemi L, Godbout C, Meister JJ, Hinz B. A new lock-step mechanism of matrix remodelling based on subcellular contractile events. *J Cell Sci*. 2010;123:1751-1760

108. Raizman JE, Komljenovic J, Chang R, Deng C, Bedosky KM, Rattan SG, Cunnington RH, Freed DH, Dixon IM. The participation of the na+-ca2+ exchanger in primary cardiac myofibroblast migration, contraction, and proliferation. *J Cell Physiol*. 2007;213:540-551

109. Kohl P, Camelliti P, Burton FL, Smith GL. Electrical coupling of fibroblasts and myocytes: Relevance for cardiac propagation. *J Electrocardiol*. 2005;38:45-50

110. Chilton L, Giles WR, Smith GL. Evidence of intercellular coupling between co-cultured adult rabbit ventricular myocytes and myofibroblasts. *J Physiol*. 2007;583:225-236

111. Camelliti P, Devlin GP, Matthews KG, Kohl P, Green CR. Spatially and temporally distinct expression of fibroblast connexins after sheep ventricular infarction. *Cardiovasc Res*. 2004;62:415-425

112. Follonier Castella L, Gabbiani G, McCulloch CA, Hinz B. Regulation of myofibroblast activities: Calcium pulls some strings behind the scene. *Exp Cell Res*. 2010;316:2390-2401

113. Kimura K, Ito M, Amano M, Chihara K, Fukata Y, Nakafuku M, Yamamori B, Feng J, Nakano T, Okawa K, Iwamatsu A, Kaibuchi K. Regulation of myosin phosphatase by rho and rho-associated kinase (rho-kinase). *Science*. 1996;273:245-248

114. Amano M, Fukata Y, Kaibuchi K. Regulation and functions of rho-associated kinase. *Exp Cell Res*. 2000;261:44-51

115. Schieffer B, Wirger A, Meybrunn M, Seitz S, Holtz J, Riede UN, Drexler H. Comparative effects of chronic angiotensin-converting enzyme inhibition and angiotensin ii type 1 receptor blockade on cardiac remodeling after myocardial infarction in the rat. *Circulation*. 1994;89:2273-2282

116. Hunter JJ, Chien KR. Signaling pathways for cardiac hypertrophy and failure. *N Engl J Med*. 1999;341:1276-1283

117. MacLellan WR, Schneider MD. Genetic dissection of cardiac growth control pathways. *Annu Rev Physiol*. 2000;62:289-319.:289-319

118. Roberts AB, McCune BK, Sporn MB. Tgf-beta: Regulation of extracellular matrix. *Kidney Int.* 1992;41:557-559

119. Ignotz RA, Massague J. Transforming growth factor-beta stimulates the expression of fibronectin and collagen and their incorporation into the extracellular matrix. *J Biol Chem*. 1986;261:4337-4345

120. Butt RP, Bishop JE. Mechanical load enhances the stimulatory effect of serum growth factors on cardiac fibroblast procollagen synthesis. *J Mol Cell Cardiol*. 1997;29:1141-1151

121. Roberts AB, Heine UI, Flanders KC, Sporn MB. Transforming growth factor-beta. Major role in regulation of extracellular matrix. *Ann N Y Acad Sci*. 1990;580:225-232

122. Wunsch M, Sharma HS, Markert T, Bernotat-Danielowski S, Schott RJ, Kremer P, Bleese N, Schaper W. In situ localization of transforming growth factor beta 1 in porcine heart: Enhanced expression after chronic coronary artery constriction. *J Mol Cell Cardiol*. 1991;23:1051-1062

123. Bujak M, Frangogiannis NG. The role of tgf-beta signaling in myocardial infarction and cardiac remodeling. *Cardiovasc Res*. 2007;74:184-195

124. Brand T, Schneider MD. Transforming growth factor-beta signal transduction. *Circ Res*. 1996;78:173-179

125. Brand T, Schneider MD. The tgf beta superfamily in myocardium: Ligands, receptors, transduction, and function. *J Mol Cell Cardiol*. 1995;27:5-18

126. Kingsley DM. The tgf-beta superfamily: New members, new receptors, and new genetic tests of function in different organisms. *Genes Dev.* 1994;8:133-146

127. Inagaki Y, Truter S, Ramirez F. Transforming growth factor-beta stimulates alpha 2(i) collagen gene expression through a cis-acting element that contains an sp1-binding site. *J Biol Chem*. 1994;269:14828-14834

128. Massague J. The tgf-beta family of growth and differentiation factors. *Cell*. 1987;49:437-438

129. Graycar JL, Miller DA, Arrick BA, Lyons RM, Moses HL, Derynck R. Human transforming growth factor-beta 3: Recombinant expression, purification, and biological activities in comparison with transforming growth factors-beta 1 and -beta 2. *Mol Endocrinol*. 1989;3:1977-1986

130. Pan H, Halper J. Cloning, expression, and characterization of chicken transforming growth factor beta 4. *Biochem Biophys Res Commun*. 2003;303:24-30

131. Kondaiah P, Sands MJ, Smith JM, Fields A, Roberts AB, Sporn MB, Melton DA. Identification of a novel transforming growth factor-beta (tgf-beta 5) mrna in xenopus laevis. *J Biol Chem*. 1990;265:1089-1093

132. Roberts AB. Molecular and cell biology of tgf-beta. *Miner Electrolyte Metab*. 1998;24:111-119

133. Annes JP, Munger JS, Rifkin DB. Making sense of latent tgfbeta activation. *J Cell Sci*. 2003;116:217-224

134. Wipff PJ, Hinz B. Integrins and the activation of latent transforming growth factor beta1 - an intimate relationship. *Eur J Cell Biol*. 2008;87:601-615

135. Ahamed J, Burg N, Yoshinaga K, Janczak CA, Rifkin DB, Coller BS. In vitro and in vivo evidence for shear-induced activation of latent transforming growth factor-beta1. *Blood*. 2008;112:3650-3660

136. Thompson NL, Flanders KC, Smith JM, Ellingsworth LR, Roberts AB, Sporn MB. Expression of transforming growth factor-beta 1 in specific cells and tissues of adult and neonatal mice. *J Cell Biol*. 1989;108:661-669

137. Kulkarni AB, Huh CG, Becker D, Geiser A, Lyght M, Flanders KC, Roberts AB, Sporn MB, Ward JM, Karlsson S. Transforming growth factor beta 1 null mutation in mice causes excessive inflammatory response and early death. *Proc Natl Acad Sci U S A*. 1993;90:770-774

138. Sanford LP, Ormsby I, Gittenberger-de Groot AC, Sariola H, Friedman R, Boivin GP, Cardell EL, Doetschman T. Tgfbeta2 knockout mice have multiple developmental defects that are non-overlapping with other tgfbeta knockout phenotypes. *Development*. 1997;124:2659-2670

139. Bartram U, Molin DG, Wisse LJ, Mohamad A, Sanford LP, Doetschman T, Speer CP, Poelmann RE, Gittenberger-de Groot AC. Double-outlet right ventricle and overriding tricuspid valve reflect disturbances of looping, myocardialization, endocardial cushion differentiation, and apoptosis in tgf-beta(2)-knockout mice. *Circulation*. 2001;103:2745-2752

140. Kaartinen V, Voncken JW, Shuler C, Warburton D, Bu D, Heisterkamp N, Groffen J. Abnormal lung development and cleft palate in mice lacking tgf-beta 3 indicates defects of epithelial-mesenchymal interaction. *Nat Genet*. 1995;11:415-421

141. Shah M, Foreman DM, Ferguson MW. Neutralisation of tgf-beta 1 and tgf-beta 2 or exogenous addition of tgf-beta 3 to cutaneous rat wounds reduces scarring. *J Cell Sci*. 1995;108 (Pt 3):985-1002

142. Jennings JC, Mohan S, Linkhart TA, Widstrom R, Baylink DJ. Comparison of the biological actions of tgf beta-1 and tgf beta-2: Differential activity in endothelial cells. *J Cell Physiol*. 1988;137:167-172

143. Merwin JR, Newman W, Beall LD, Tucker A, Madri J. Vascular cells respond differentially to transforming growth factors beta 1 and beta 2 in vitro. *Am J Pathol*. 1991;138:37-51

144. Sadoshima J, Izumo S. Molecular characterization of angiotensin ii--induced hypertrophy of cardiac myocytes and hyperplasia of cardiac fibroblasts. Critical role of the at1 receptor subtype. *Circ Res*. 1993;73:413-423

145. Ohta K, Kim S, Hamaguchi A, Yukimura T, Miura K, Takaori K, Iwao H. Role of angiotensin ii in extracellular matrix and transforming growth factor-beta 1 expression in hypertensive rats. *Eur J Pharmacol*. 1994;269:115-119

146. Brooks WW, Conrad CH. Myocardial fibrosis in transforming growth factor beta(1)heterozygous mice. *J Mol Cell Cardiol*. 2000;32:187-195

147. Loeys BL, Schwarze U, Holm T, Callewaert BL, Thomas GH, Pannu H, De Backer JF, Oswald GL, Symoens S, Manouvrier S, Roberts AE, Faravelli F, Greco MA, Pyeritz RE, Milewicz DM, Coucke PJ, Cameron DE, Braverman AC, Byers PH, De Paepe AM, Dietz HC. Aneurysm syndromes caused by mutations in the tgf-beta receptor. *N Engl J Med*. 2006;355:788-798

148. Massague J, Hata A, Liu F. Tgf-beta signalling through the smad pathway. *Trends Cell Biol.* 1997;7:187-192

149. Wrana J, Pawson T. Signal transduction. Mad about smads. *Nature*. 1997;388:28-29

150. Nakao A, Roijer E, Imamura T, Souchelnytskyi S, Stenman G, Heldin CH, ten Dijke P. Identification of smad2, a human mad-related protein in the transforming growth factor beta signaling pathway. *J Biol Chem*. 1997;272:2896-2900

151. Chen X, Rubock MJ, Whitman M. A transcriptional partner for mad proteins in tgf-beta signalling. *Nature*. 1996;383:691-696

152. Zhou S, Zawel L, Lengauer C, Kinzler KW, Vogelstein B. Characterization of human fast-1, a tgf beta and activin signal transducer. *Mol Cell*. 1998;2:121-127

153. Chen YG, Hata A, Lo RS, Wotton D, Shi Y, Pavletich N, Massague J. Determinants of specificity in tgf-beta signal transduction. *Genes Dev.* 1998;12:2144-2152

154. Derynck R, Zhang Y, Feng XH. Smads: Transcriptional activators of tgf-beta responses. *Cell*. 1998;95:737-740

155. Massague J. Tgf-beta signal transduction. *Annu Rev Biochem*. 1998;67:753-91:753-791

156. Wrana JL. Regulation of smad activity. *Cell*. 2000;100:189-192

157. Lee MK, Pardoux C, Hall MC, Lee PS, Warburton D, Qing J, Smith SM, Derynck R. Tgf-beta activates erk map kinase signalling through direct phosphorylation of shca. *Embo J*. 2007;26:3957-3967

158. Zavadil J, Bitzer M, Liang D, Yang YC, Massimi A, Kneitz S, Piek E, Bottinger EP. Genetic programs of epithelial cell plasticity directed by transforming growth factor-beta. *Proc Natl Acad Sci USA*. 2001;98:6686-6691

159. Davies M, Robinson M, Smith E, Huntley S, Prime S, Paterson I. Induction of an epithelial to mesenchymal transition in human immortal and malignant keratinocytes by tgf-beta1 involves mapk, smad and ap-1 signalling pathways. *J Cell Biochem*. 2005;95:918-931

160. Yamashita M, Fatyol K, Jin C, Wang X, Liu Z, Zhang YE. Traf6 mediates smad-independent activation of jnk and p38 by tgf-beta. *Molecular cell*. 2008;31:918-924

161. Atfi A, Djelloul S, Chastre E, Davis R, Gespach C. Evidence for a role of rho-like gtpases and stress-activated protein kinase/c-jun n-terminal kinase (sapk/jnk) in transforming growth factor beta-mediated signaling. *J.Biol.Chem.* 1997;272:1429-1432

162. Brown JD, DiChiara MR, Anderson KR, Gimbrone MA, Jr., Topper JN. Mekk-1, a component of the stress (stress-activated protein kinase/c-jun n-terminal kinase) pathway, can selectively activate smad2-mediated transcriptional activation in endothelial cells. *J.Biol.Chem.* 1999;274:8797-8805

163. Zhang L, Wang W, Hayashi Y, Jester JV, Birk DE, Gao M, Liu CY, Kao WW, Karin M, Xia Y. A role for mek kinase 1 in tgf-beta/activin-induced epithelium movement and embryonic eyelid closure. *Embo J*. 2003;22:4443-4454

164. Kim KY, Kim BC, Xu Z, Kim SJ. Mixed lineage kinase 3 (mlk3)-activated p38 map kinase mediates transforming growth factor-beta-induced apoptosis in hepatoma cells. *The Journal of biological chemistry*. 2004;279:29478-29484

165. Liao JH, Chen JS, Chai MQ, Zhao S, Song JG. The involvement of p38 mapk in transforming growth factor beta1-induced apoptosis in murine hepatocytes. *Cell Res*. 2001;11:89-94

166. Bhowmick NA, Ghiassi M, Bakin A, Aakre M, Lundquist CA, Engel ME, Arteaga CL, Moses HL. Transforming growth factor-beta1 mediates epithelial to mesenchymal transdifferentiation through a rhoa-dependent mechanism. *Molecular biology of the cell*. 2001;12:27-36

167. Wilkes MC, Mitchell H, Penheiter SG, Dore JJ, Suzuki K, Edens M, Sharma DK, Pagano RE, Leof EB. Transforming growth factor-beta activation of phosphatidylinositol 3-kinase is independent of smad2 and smad3 and regulates fibroblast responses via p21-activated kinase-2. *Cancer research*. 2005;65:10431-10440

168. Park SH. Fine tuning and cross-talking of tgf-beta signal by inhibitory smads. *J Biochem Mol Biol*. 2005;38:9-16

169. Xu W, Angelis K, Danielpour D, Haddad MM, Bischof O, Campisi J, Stavnezer E, Medrano EE. Ski acts as a co-repressor with smad2 and smad3 to regulate the response to type beta transforming growth factor. *Proc Natl Acad Sci USA*. 2000;97:5924-5929

170. Kokura K, Kim H, Shinagawa T, Khan MM, Nomura T, Ishii S. The ski-binding protein c184m negatively regulates tumor growth factor-beta signaling by

sequestering the smad proteins in the cytoplasm. *J Biol Chem*. 2003;278:20133-20139

171. Zhang Y, Feng X, We R, Derynck R. Receptor-associated mad homologues synergize as effectors of the tgf-beta response. *Nature*. 1996;383:168-172

172. Macias-Silva M, Abdollah S, Hoodless PA, Pirone R, Attisano L, Wrana JL. Madr2 is a substrate of the tgfbeta receptor and its phosphorylation is required for nuclear accumulation and signaling. *Cell*. 1996;87:1215-1224

173. Wrana JL, Attisano L, Wieser R, Ventura F, Massague J. Mechanism of activation of the tgf-beta receptor. *Nature*. 1994;370:341-347

174. Tsukazaki T, Chiang TA, Davison AF, Attisano L, Wrana JL. Sara, a fyve domain protein that recruits smad2 to the tgfbeta receptor. *Cell*. 1998;95:779-791

175. Miura S, Takeshita T, Asao H, Kimura Y, Murata K, Sasaki Y, Hanai JI, Beppu H, Tsukazaki T, Wrana JL, Miyazono K, Sugamura K. Hgs (hrs), a fyve domain protein, is involved in smad signaling through cooperation with sara. *Mol Cell Biol*. 2000;20:9346-9355

176. Wrana JL, Attisano L. The smad pathway. *Cytokine Growth Factor Rev*. 2000;11:5-13

177. Lagna G, Hata A, Hemmati-Brivanlou A, Massague J. Partnership between dpc4 and smad proteins in tgf-beta signalling pathways. *Nature*. 1996;383:832-836

178. Heldin CH, Miyazono K, ten Dijke P. Tgf-beta signalling from cell membrane to nucleus through smad proteins. *Nature*. 1997;390:465-471

179. Massague J, Wotton D. Transcriptional control by the tgf-beta/smad signaling system. *Embo J*. 2000;19:1745-1754

180. Ueki N, Hayman MJ. Direct interaction of ski with either smad3 or smad4 is necessary and sufficient for ski-mediated repression of transforming growth factor-beta signaling. *J Biol Chem*. 2003;278:32489-32492

181. Luo K, Stroschein SL, Wang W, Chen D, Martens E, Zhou S, Zhou Q. The ski oncoprotein interacts with the smad proteins to repress tgfbeta signaling. *Genes Dev.* 1999;13:2196-2206

182. Luo K. Ski and snon: Negative regulators of tgf-beta signaling. *Curr Opin Genet Dev*. 2004;14:65-70

183. Prunier C, Pessah M, Ferrand N, Seo SR, Howe P, Atfi A. The oncoprotein ski acts as an antagonist of transforming growth factor-beta signaling by suppressing smad2 phosphorylation. *J Biol Chem*. 2003;278:26249-26257

184. Dupont S, Mamidi A, Cordenonsi M, Montagner M, Zacchigna L, Adorno M, Martello G, Stinchfield MJ, Soligo S, Morsut L, Inui M, Moro S, Modena N, Argenton F, Newfeld SJ, Piccolo S. Fam/usp9x, a deubiquitinating enzyme essential for tgfbeta signaling, controls smad4 monoubiquitination. *Cell*. 2009;136:123-135

185. Vindevoghel L, Kon A, Lechleider RJ, Uitto J, Roberts AB, Mauviel A. Smad-dependent transcriptional activation of human type vii collagen gene (col7a1) promoter by transforming growth factor-beta. *J Biol Chem*. 1998;273:13053-13057

186. Vindevoghel L, Lechleider RJ, Kon A, de Caestecker MP, Uitto J, Roberts AB, Mauviel A. Smad3/4-dependent transcriptional activation of the human type vii

collagen gene (col7a1) promoter by transforming growth factor beta. *Proc Natl Acad Sci USA*. 1998;95:14769-14774

187. Zawel L, Dai JL, Buckhaults P, Zhou S, Kinzler KW, Vogelstein B, Kern SE. Human smad3 and smad4 are sequence-specific transcription activators. *Mol Cell*. 1998;1:611-617

188. Christian JL, Nakayama T. Can't get no smadisfaction: Smad proteins as positive and negative regulators of tgf-beta family signals. *Bioessays*. 1999;21:382-390

189. Hayashi H, Abdollah S, Qiu Y, Cai J, Xu YY, Grinnell BW, Richardson MA, Topper JN, Gimbrone MA, Jr., Wrana JL, Falb D. The mad-related protein smad7 associates with the tgfbeta receptor and functions as an antagonist of tgfbeta signaling. *Cell*. 1997;89:1165-1173

190. Imamura T, Takase M, Nishihara A, Oeda E, Hanai J, Kawabata M, Miyazono K. Smad6 inhibits signalling by the tgf-beta superfamily. *Nature*. 1997;389:622-626

191. Nakao A, Afrakhte M, Moren A, Nakayama T, Christian JL, Heuchel R, Itoh S, Kawabata M, Heldin NE, Heldin CH, ten Dijke P. Identification of smad7, a tgfbeta-inducible antagonist of tgf-beta signalling. *Nature*. 1997;389:631-635

192. Whitman M. Signal transduction. Feedback from inhibitory smads. *Nature*. 1997;389:549-551

193. Chong PA, Lin H, Wrana JL, Forman-Kay JD. An expanded ww domain recognition motif revealed by the interaction between smad7 and the e3 ubiquitin ligase smurf2. *J Biol Chem*. 2006;281:17069-17075

194. Kavsak P, Rasmussen RK, Causing CG, Bonni S, Zhu H, Thomsen GH, Wrana JL. Smad7 binds to smurf2 to form an e3 ubiquitin ligase that targets the tgf beta receptor for degradation. *Mol Cell*. 2000;6:1365-1375

195. Sutrave P, Hughes SH. Isolation and characterization of three distinct cdnas for the chicken c-ski gene. *Mol Cell Biol*. 1989;9:4046-4051

196. Grimes HL, Ambrose MR, Goodenow MM. C-ski transcripts with and without exon 2 are expressed in skeletal muscle and throughout chick embryogenesis. *Oncogene*. 1993;8:2863-2868

197. Grimes HL, Szente BE, Goodenow MM. C-ski cdnas are encoded by eight exons, six of which are closely linked within the chicken genome. *Nucleic Acids Res*. 1992;20:1511-1516

198. Nagase T, Mizuguchi G, Nomura N, Ishizaki R, Ueno Y, Ishii S. Requirement of protein co-factor for the DNA-binding function of the human ski proto-oncogene product. *Nucleic Acids Res*. 1990;18:337-343

199. Lyons GE, Micales BK, Herr MJ, Horrigan SK, Namciu S, Shardy D, Stavnezer E. Protooncogene c-ski is expressed in both proliferating and postmitotic neuronal populations. *Dev Dyn*. 1994;201:354-365

200. Soeta C, Suzuki M, Suzuki S, Naito K, Tachi C, Tojo H. Possible role for the c-ski gene in the proliferation of myogenic cells in regenerating skeletal muscles of rats. *Dev Growth Differ*. 2001;43:155-164

201. Colmenares C, Sutrave P, Hughes SH, Stavnezer E. Activation of the c-ski oncogene by overexpression. *J Virol*. 1991;65:4929-4935

202. Bruusgaard JC, Brack AS, Hughes SM, Gundersen K. Muscle hypertrophy induced by the ski protein: Cyto-architecture and ultrastructure. *Acta Physiol Scand.* 2005;185:141-149

203. Amaravadi LS, Neff AW, Sleeman JP, Smith RC. Autonomous neural axis formation by ectopic expression of the protooncogene c-ski. *Dev Biol*. 1997;192:392-404

204. Kaufman CD, Martinez-Rodriguez G, Hackett PB, Jr. Ectopic expression of c-ski disrupts gastrulation and neural patterning in zebrafish. *Mech Dev*. 2000;95:147-162

205. Shinagawa T, Nomura T, Colmenares C, Ohira M, Nakagawara A, Ishii S. Increased susceptibility to tumorigenesis of ski-deficient heterozygous mice. *Oncogene*. 2001;20:8100-8108

206. Colmenares C, Stavnezer E. Structure and activities of the ski oncogene. *Semin Cancer Biol*. 1990;1:383-387

207. Heyman HC, Stavnezer E. A carboxyl-terminal region of the ski oncoprotein mediates homodimerization as well as heterodimerization with the related protein snon. *J Biol Chem*. 1994;269:26996-27003

208. Marcelain K, Hayman MJ. The ski oncoprotein is upregulated and localized at the centrosomes and mitotic spindle during mitosis. *Oncogene.* 2005;24:4321-4329

209. Nagata M, Goto K, Ehata S, Kobayashi N, Saitoh M, Miyoshi H, Imamura T, Miyazawa K, Miyazono K. Nuclear and cytoplasmic c-ski differently modulate cellular functions. *Genes Cells*. 2006;11:1267-1280

210. Nagase T, Nomura N, Ishii S. Complex formation between proteins encoded by the ski gene family. *J Biol Chem*. 1993;268:13710-13716

211. Nicol R, Stavnezer E. Transcriptional repression by v-ski and c-ski mediated by a specific DNA binding site. *J Biol Chem*. 1998;273:3588-3597

212. Nomura T, Khan MM, Kaul SC, Dong HD, Wadhwa R, Colmenares C, Kohno I, Ishii S. Ski is a component of the histone deacetylase complex required for transcriptional repression by mad and thyroid hormone receptor. *Genes Dev*. 1999;13:412-423

213. Dahl R, Kieslinger M, Beug H, Hayman MJ. Transformation of hematopoietic cells by the ski oncoprotein involves repression of retinoic acid receptor signaling. *Proc Natl Acad Sci USA*. 1998;95:11187-11192

214. Kokura K, Kaul SC, Wadhwa R, Nomura T, Khan MM, Shinagawa T, Yasukawa T, Colmenares C, Ishii S. The ski protein family is required for mecp2-mediated transcriptional repression. *J Biol Chem*. 2001;276:34115-34121

215. Tokitou F, Nomura T, Khan MM, Kaul SC, Wadhwa R, Yasukawa T, Kohno I, Ishii S. Viral ski inhibits retinoblastoma protein (rb)-mediated transcriptional repression in a dominant negative fashion. *J Biol Chem*. 1999;274:4485-4488

216. Nicol R, Zheng G, Sutrave P, Foster DN, Stavnezer E. Association of specific DNA binding and transcriptional repression with the transforming and myogenic activities of c-ski. *Cell Growth Differ*. 1999;10:243-254

217. Tarapore P, Richmond C, Zheng G, Cohen SB, Kelder B, Kopchick J, Kruse U, Sippel AE, Colmenares C, Stavnezer E. DNA binding and transcriptional

activation by the ski oncoprotein mediated by interaction with nfi. *Nucleic Acids Res.* 1997;25:3895-3903

218. Liu X, Li P, Liu P, Xiong R, Zhang E, Chen X, Gu D, Zhao Y, Wang Z, Zhou Y. The essential role for c-ski in mediating tgf-beta1-induced bi-directional effects on skin fibroblast proliferation through a feedback loop. *Biochem J*. 2008;409:289-297

219. Sun Y, Liu X, Ng-Eaton E, Lodish HF, Weinberg RA. Snon and ski protooncoproteins are rapidly degraded in response to transforming growth factor beta signaling. *Proc Natl Acad Sci USA*. 1999;96:12442-12447

220. Nagano Y, Koinuma D, Miyazawa K, Miyazono K. Context-dependent regulation of the expression of c-ski protein by arkadia in human cancer cells. *J Biochem*. 2010;147:545-554

221. Macdonald M, Wan Y, Wang W, Roberts E, Cheung TH, Erickson R, Knuesel MT, Liu X. Control of cell cycle-dependent degradation of c-ski proto-oncoprotein by cdc34. *Oncogene.* 2004;23:5643-5653

222. Nagano Y, Mavrakis KJ, Lee KL, Fujii T, Koinuma D, Sase H, Yuki K, Isogaya K, Saitoh M, Imamura T, Episkopou V, Miyazono K, Miyazawa K. Arkadia induces degradation of snon and c-ski to enhance transforming growth factor-beta signaling. *J Biol Chem*. 2007;282:20492-20501

223. Le SE, Zhu Q, Wang L, Bandyopadhyay A, Javelaud D, Mauviel A, Sun L, Luo K. Transforming growth factor-beta suppresses the ability of ski to inhibit tumor metastasis by inducing its degradation. *Cancer Res.* 2008;68:3277-3285

224. Kim H, Yamanouchi K, Nishihara M. Expression of ski in the granulosa cells of atretic follicles in the rat ovary. *J Reprod Dev*. 2006;52:715-721

225. Liu X, Zhang E, Li P, Liu J, Zhou P, Gu DY, Chen X, Cheng T, Zhou Y. Expression and possible mechanism of c-ski, a novel tissue repair-related gene during normal and radiation-impaired wound healing. *Wound Repair Regen*. 2006;14:162-171

226. Liu X, Li P, Chen XY, Zhou YG. C-ski promotes skin fibroblast proliferation but decreases type i collagen: Implications for wound healing and scar formation. *Clin Exp Dermatol*. 2009

227. Wu JW, Krawitz AR, Chai J, Li W, Zhang F, Luo K, Shi Y. Structural mechanism of smad4 recognition by the nuclear oncoprotein ski: Insights on ski-mediated repression of tgf-beta signaling. *Cell.* 2002;111:357-367

228. Abate-Shen C. Deregulated homeobox gene expression in cancer: Cause or consequence? *Nat Rev Cancer*. 2002;2:777-785

229. Gehring WJ, Qian YQ, Billeter M, Furukubo-Tokunaga K, Schier AF, Resendez-Perez D, Affolter M, Otting G, Wuthrich K. Homeodomain-DNA recognition. *Cell*. 1994;78:211-223

230. Stocker RF, Edwards JS, Palka J, Schubiger G. Projection of sensory neurons from a homeotic mutant appendage, antennapedia, in drosophila melanogaster. *Dev Biol*. 1976;52:210-220

231. Garber RL, Kuroiwa A, Gehring WJ. Genomic and cdna clones of the homeotic locus antennapedia in drosophila. *Embo J*. 1983;2:2027-2036

232. Wu Z, Guo H, Chow N, Sallstrom J, Bell RD, Deane R, Brooks AI, Kanagala S, Rubio A, Sagare A, Liu D, Li F, Armstrong D, Gasiewicz T, Zidovetzki R, Song X, Hofman F, Zlokovic BV. Role of the meox2 homeobox gene in neurovascular dysfunction in alzheimer disease. *Nat Med*. 2005;11:959-965

233. Choi BJ, Kim CJ, Cho YG, Song JH, Kim SY, Nam SW, Lee SH, Yoo NJ, Lee JY, Park WS. Altered expression of cdx2 in colorectal cancers. *Apmis*. 2006;114:50-54

234. Candia AF, Hu J, Crosby J, Lalley PA, Noden D, Nadeau JH, Wright CV. Mox-1 and mox-2 define a novel homeobox gene subfamily and are differentially expressed during early mesodermal patterning in mouse embryos. *Development*. 1992;116:1123-1136

235. Mankoo BS, Skuntz S, Harrigan I, Grigorieva E, Candia A, Wright CV, Arnheiter H, Pachnis V. The concerted action of meox homeobox genes is required upstream of genetic pathways essential for the formation, patterning and differentiation of somites. *Development*. 2003;130:4655-4664

236. Futreal PA, Cochran C, Rosenthal J, Miki Y, Swenson J, Hobbs M, Bennett LM, Haugen-Strano A, Marks J, Barrett JC, et al. Isolation of a diverged homeobox gene, mox1, from the brca1 region on 17q21 by solution hybrid capture. *Hum Mol Genet*. 1994;3:1359-1364

237. Suh YA, Arnold RS, Lassegue B, Shi J, Xu X, Sorescu D, Chung AB, Griendling KK, Lambeth JD. Cell transformation by the superoxide-generating oxidase mox1. *Nature*. 1999;401:79-82

238. Gianakopoulos PJ, Skerjanc IS. Hedgehog signaling induces cardiomyogenesis in p19 cells. *J Biol Chem*. 2005;280:21022-21028

239. Kirilenko P, He G, Mankoo BS, Mallo M, Jones R, Bobola N. Transient activation of meox1 is an early component of the gene regulatory network downstream of hoxa2. *Mol Cell Biol*. 2011;31:1301-1308

240. Skopicki HA, Lyons GE, Schatteman G, Smith RC, Andres V, Schirm S, Isner J, Walsh K. Embryonic expression of the gax homeodomain protein in cardiac, smooth, and skeletal muscle. *Circ Res*. 1997;80:452-462

241. Gorski DH, LePage DF, Patel CV, Copeland NG, Jenkins NA, Walsh K. Molecular cloning of a diverged homeobox gene that is rapidly down-regulated during the g0/g1 transition in vascular smooth muscle cells. *Mol Cell Biol*. 1993;13:3722-3733

242. Weir L, Chen D, Pastore C, Isner JM, Walsh K. Expression of gax, a growth arrest homeobox gene, is rapidly down-regulated in the rat carotid artery during the proliferative response to balloon injury. *J Biol Chem*. 1995;270:5457-5461

243. Mankoo BS, Collins NS, Ashby P, Grigorieva E, Pevny LH, Candia A, Wright CV, Rigby PW, Pachnis V. Mox2 is a component of the genetic hierarchy controlling limb muscle development. *Nature*. 1999;400:69-73

244. Fisher SA, Siwik E, Branellec D, Walsh K, Watanabe M. Forced expression of the homeodomain protein gax inhibits cardiomyocyte proliferation and perturbs heart morphogenesis. *Development*. 1997;124:4405-4413

245. Smith RC, Branellec D, Gorski DH, Guo K, Perlman H, Dedieu JF, Pastore C, Mahfoudi A, Denefle P, Isner JM, Walsh K. P21cip1-mediated inhibition of cell

proliferation by overexpression of the gax homeodomain gene. *Genes Dev*. 1997;11:1674-1689

246. Gorski DH, Leal AJ. Inhibition of endothelial cell activation by the homeobox gene gax. *J Surg Res*. 2003;111:91-99

247. Perlman H, Sata M, Le Roux A, Sedlak TW, Branellec D, Walsh K. Bax-mediated cell death by the gax homeoprotein requires mitogen activation but is independent of cell cycle activity. *Embo J*. 1998;17:3576-3586

248. Witzenbichler B, Kureishi Y, Luo Z, Le Roux A, Branellec D, Walsh K. Regulation of smooth muscle cell migration and integrin expression by the gax transcription factor. *J Clin Invest*. 1999;104:1469-1480

249. Patel S, Leal AD, Gorski DH. The homeobox gene gax inhibits angiogenesis through inhibition of nuclear factor-kappab-dependent endothelial cell gene expression. *Cancer Res*. 2005;65:1414-1424

250. Liu P, Zhang C, Feng JB, Zhao YX, Wang XP, Yang JM, Zhang MX, Wang XL, Zhang Y. Cross talk among smad, mapk, and integrin signaling pathways enhances adventitial fibroblast functions activated by transforming growth factor-beta1 and inhibited by gax. *Arterioscler Thromb Vasc Biol*. 2008;28:725-731

251. Liu P, Zhang C, Zhao YX, Feng JB, Liu CX, Chen WQ, Yao GH, Zhang M, Wang XL, Zhang Y. Gax gene transfer inhibits vascular remodeling induced by adventitial inflammation in rabbits. *Atherosclerosis*. 2010;212:398-405

252. Valcourt U, Thuault S, Pardali K, Heldin CH, Moustakas A. Functional role of meox2 during the epithelial cytostatic response to tgf-beta. *Mol Oncol*. 2007;1:55-71

253. Larsson O, Diebold D, Fan D, Peterson M, Nho RS, Bitterman PB, Henke CA. Fibrotic myofibroblasts manifest genome-wide derangements of translational control. *PLoS One*. 2008;3:e3220

254. Chen Y, Banda M, Speyer CL, Smith JS, Rabson AB, Gorski DH. Regulation of the expression and activity of the antiangiogenic homeobox gene gax/meox2 by zeb2 and microrna-221. *Mol Cell Biol*. 2010;30:3902-3913

255. Comijn J, Berx G, Vermassen P, Verschueren K, van Grunsven L, Bruyneel E, Mareel M, Huylebroeck D, van Roy F. The two-handed e box binding zinc finger protein sip1 downregulates e-cadherin and induces invasion. *Mol Cell*. 2001;7:1267-1278

256. Vandewalle C, Comijn J, De Craene B, Vermassen P, Bruyneel E, Andersen H, Tulchinsky E, Van Roy F, Berx G. Sip1/zeb2 induces emt by repressing genes of different epithelial cell-cell junctions. *Nucleic Acids Res*. 2005;33:6566-6578

257. Ghavami S, Kerkhoff C, Chazin WJ, Kadkhoda K, Xiao W, Zuse A, Hashemi M, Eshraghi M, Schulze-Osthoff K, Klonisch T, Los M. S100a8/9 induces cell death via a novel, rage-independent pathway that involves selective release of smac/diablo and omi/htra2. *Biochim Biophys Acta*. 2008;1783:297-311

258. Hashemi M, Ghavami S, Eshraghi M, Booy EP, Los M. Cytotoxic effects of intra and extracellular zinc chelation on human breast cancer cells. *Eur J Pharmacol*. 2007;557:9-19

259. Wang B, Omar A, Angelovska T, Drobic V, Rattan SG, Jones SC, Dixon IM. Regulation of collagen synthesis by inhibitory smad7 in cardiac myofibroblasts. *Am J Physiol Heart Circ Physiol*. 2007;293:H1282-H1290

260. Montesano R, Orci L. Transforming growth factor beta stimulates collagen-matrix contraction by fibroblasts: Implications for wound healing. *Proc Natl Acad Sci U S A*. 1988;85:4894-4897

261. Desmouliere A, Geinoz A, Gabbiani F, Gabbiani G. Transforming growth factor-beta 1 induces alpha-smooth muscle actin expression in granulation tissue myofibroblasts and in quiescent and growing cultured fibroblasts. *J Cell Biol*. 1993;122:103-111

262. Petrov VV, Fagard RH, Lijnen PJ. Transforming growth factor-beta(1) induces angiotensin-converting enzyme synthesis in rat cardiac fibroblasts during their differentiation to myofibroblasts. *J Renin Angiotensin Aldosterone Syst*. 2000;1:342-352

263. Wang J, Chen H, Seth A, McCulloch CA. Mechanical force regulation of myofibroblast differentiation in cardiac fibroblasts. *Am J Physiol Heart Circ Physiol*. 2003;285:H1871-H1881

264. Dobaczewski M, Bujak M, Li N, Gonzalez-Quesada C, Mendoza LH, Wang XF, Frangogiannis NG. Smad3 signaling critically regulates fibroblast phenotype and function in healing myocardial infarction. *Circ Res*. 2010;107:418-428

265. Darby I, Skalli O, Gabbiani G. Alpha-smooth muscle actin is transiently expressed by myofibroblasts during experimental wound healing. *Lab Invest*. 1990;63:21-29

266. Serini G, Bochaton-Piallat ML, Ropraz P, Geinoz A, Borsi L, Zardi L, Gabbiani G. The fibronectin domain ed-a is crucial for myofibroblastic phenotype induction by transforming growth factor-beta1. *J Cell Biol*. 1998;142:873-881

267. Cunnington RH, Wang B, Ghavami S, Bathe KL, Rattan SG, Dixon IM. Antifibrotic properties of c-ski and its regulation of cardiac myofibroblast phenotype and contractility. *Am J Physiol Cell Physiol*. 2011;300:C176-186

268. Macias-Silva M, Li W, Leu JI, Crissey MA, Taub R. Up-regulated transcriptional repressors snon and ski bind smad proteins to antagonize transforming growth factor-beta signals during liver regeneration. *J Biol Chem*. 2002;277:28483-28490

269. Wrighton KH, Liang M, Bryan B, Luo K, Liu M, Feng XH, Lin X. Transforming growth factor-beta-independent regulation of myogenesis by snon sumoylation. *J Biol Chem*. 2007;282:6517-6524

270. Sutrave P, Kelly AM, Hughes SH. Ski can cause selective growth of skeletal muscle in transgenic mice. *Genes Dev.* 1990;4:1462-1472

271. van den Borne SW, Diez J, Blankesteijn WM, Verjans J, Hofstra L, Narula J. Myocardial remodeling after infarction: The role of myofibroblasts. *Nat Rev Cardiol*. 2010;7:30-37

272. Hinz B, Mastrangelo D, Iselin CE, Chaponnier C, Gabbiani G. Mechanical tension controls granulation tissue contractile activity and myofibroblast differentiation. *Am J Pathol*. 2001;159:1009-1020

273. Vaughan MB, Howard EW, Tomasek JJ. Transforming growth factor-beta1 promotes the morphological and functional differentiation of the myofibroblast. *Exp Cell Res*. 2000;257:180-189

274. Ronnov-Jessen L, Petersen OW. Induction of alpha-smooth muscle actin by transforming growth factor-beta 1 in quiescent human breast gland fibroblasts.

Implications for myofibroblast generation in breast neoplasia. *Lab Invest*. 1993;68:696-707

275. Frangogiannis NG, Michael LH, Entman ML. Myofibroblasts in reperfused myocardial infarcts express the embryonic form of smooth muscle myosin heavy chain (smemb). *Cardiovasc Res*. 2000;48:89-100

276. Gabbiani G, Ryan GB, Majne G. Presence of modified fibroblasts in granulation tissue and their possible role in wound contraction. *Experientia*. 1971;27:549-550

277. Amaravadi RK, Yu D, Lum JJ, Bui T, Christophorou MA, Evan GI, Thomas-Tikhonenko A, Thompson CB. Autophagy inhibition enhances therapy-induced apoptosis in a myc-induced model of lymphoma. *J Clin Invest*. 2007;117:326-336

278. Ghavami S, Eshragi M, Ande SR, Chazin WJ, Klonisch T, Halayko AJ, McNeill KD, Hashemi M, Kerkhoff C, Los M. S100a8/a9 induces autophagy and apoptosis via ros-mediated cross-talk between mitochondria and lysosomes that involves bnip3. *Cell Res*. 2010;20:314-331

279. Crighton D, Wilkinson S, Ryan KM. Dram links autophagy to p53 and programmed cell death. *Autophagy*. 2007;3:72-74